957
2005
002

Activation and localization of the emotional circuits in the brain: an fMRI study in patients with schizophrenia and healthy volunteers

Master thesis
Lieke van Balen (s1211013)
(October 26, 2005)

Internal supervisor: Dr. Fokie Cnossen
Artificial Intelligence
Rijksuniversiteit Groningen

External supervisor: Dr. Simone Reinders
Department of biological psychiatry
Rijksuniversiteit Groningen

September 1, 2004 – August 31, 2005

Artificial Intelligence
Rijksuniversiteit Groningen

Rijksuniversiteit Groningen
BIBLIOTHEEK
SOCIALE WETENSCHAPPEN

957

Abstract

The evolutionary survival of a species is dependent on individual organisms quickly detecting environmental threats and rapidly initiating defensive behavioral reactions. This graduation project investigated the perception of stimuli with different degrees of biological relevance, i.e. fearful faces (signalling an immediate threat), neutral faces (not signalling a threat), and houses (providing no information about either the presence or absence of environmental threats). Brain structures involved in the perception of these stimuli were investigated with functional magnetic resonance imaging (fMRI). In addition to healthy subjects, facial affect processing was examined in schizophrenia patients. Because it is believed that schizophrenia patients are impaired in facial affect recognition, it was investigated whether or not they would show differential brain activation (compared to healthy subjects) during the perception of fearful faces, neutral faces and houses. Subjects were presented with images of visual noise, from which a stimulus (fearful face, neutral face or house) gradually emerged. The moment of stimulus recognition was indicated with a button press. Brain activation during the task was measured with functional resonance imaging (fMRI).

Table of contents

Table of contents (detailed)

PART I

INTRODUCTION

Chapter 1: Introduction

1.1 Introduction

Emotion is one of those concepts that are hard to define, even though everyone knows what they mean. In everyday life, we experience emotion as the mood we are in and the feelings we have, and we observe emotion in others through body language and facial expressions. Our behavior is constantly guided by emotion, whether we like it or not. In addition, emotion is fundamentally involved in our daily social interaction.

On a basic level, emotion can be regarded as an important tool for evolutionary survival, driving behavior in such a way that an individual's chances of reproduction are increased. Fear, in this context, serves to increase the chances of survival by promoting behavior that minimizes exposure to danger. In addition, chances of survival are increased if an individual is capable of quickly detecting environmental threats and rapidly initiating defensive behavioral reactions. Stimuli that indicate such threats are therefore defined as biologically relevant information.

Both animal research and research with human subjects have indicated that the brain is capable of processing biologically relevant information faster and more robust than biologically irrelevant information. The amygdala, a brain structure in the temporal lobe, is believed to be involved in the perception of biologically relevant stimuli and the production of immediate defensive reactions to the threats these stimuli may indicate. This graduation project investigates the role of the amygdala in the perception of such stimuli, in both healthy subjects and patients with schizophrenia.

1.2. Outline of this thesis

This thesis consists of eight chapters, supplemented by three appendices. The chapters are divided over four parts. The current (first) part and chapter includes the introduction to the subject of this thesis and provides an overview of the contents of the thesis.

The second part, consisting of chapters 2, 3 and 4, contains the theoretical introduction to this graduation project. First, chapter 2 gives a short introduction into the theory of functional magnetic resonance imaging (fMRI), the neuroimaging technique that was used in this study to measure brain activation. Chapter 2 is followed by an overview of research on emotion and the amygdala in chapter 3. Then, in chapter 4, a description of research on facial affect processing in schizophrenia is given.

The third part of the thesis, consisting of chapters 5, 6, 7 and 8, describes the actual experiment. It starts with the hypotheses of the project in chapter 5, followed by the methods and materials in chapter 6. Chapter 7 describes the results of the experiment. Our interpretation of these results and the discussion are given in chapter 8.

Finally, the last part contains three appendices, which provide more detail on the methods and materials. Appendix A describes the selection procedure of the fearful and neutral face pictures that were used in the experiment. In appendix B, a description is given of how we turned these pictures into stimuli suitable for the experiment, and appendix C describes a technique to improve the temporal resolution of the paradigm, known as jittering.

PART II

THEORETICAL BACKGROUND

Chapter 2: fMRI

2.1. Introduction

Research in psychology and neuroscience has taken a giant leap forward since the introduction of neuroimaging techniques, which enable researchers to study the brain in a relatively non-invasive way. There are two types of neuroimaging: structural and functional neuroimaging. Structural neuroimaging techniques provide images of the structure of brain tissue and include computerized (axial) tomography (CT of CAT) and (structural) magnetic resonance imaging (MRI). Functional neuroimaging techniques, in contrast, provide information about brain activity, and are thus suitable for studying the function of different brain areas. Functional neuroimaging techniques include positron emission tomography (PET), electroencephalography (EEG), and functional magnetic resonance imaging (fMRI), the neuroimaging technique used in this study.

Every functional neuroimaging technique has its own spatial and temporal resolution. EEG, for example, which measures neuronal activity with electrodes on the scalp, has a high temporal resolution (in the order of milliseconds), but a low spatial resolution (not higher than several centimeters). Both the relatively new technique fMRI and the earlier available PET measure changes in local cerebral blood flow (CBF), which is an indirect measure of neural activity (see below). The temporal resolution of PET and fMRI is lower than the temporal resolution of EEG, but the spatial resolution of both techniques is much higher than that of EEG. Both the spatial resolution and temporal resolution of fMRI are higher than those of PET. In addition, fMRI (unlike PET) does not need radioactive tracers and is thus less invasive than PET.

It is beyond the scope of this thesis to give a detailed account of the theory of fMRI. For detailed reading material on fMRI, the reader is referred to Buxton (2002). Section 2.2 explains how neural activity is measured with fMRI, whereas section 2.3 describes the basic physics of MRI and what an MRI signal is.

2.2. fMRI

fMRI measures brain activity indirectly, by measuring changes in local cerebral blood flow (CBF). Since the brain influences all organs of the body, it can never be 'turned off'. For this reason, the body tries to ensure that the brain always receives enough oxygen and glucose. For example, if blood pressure falls, blood flow is decreased in all bodily tissues except the brain, to keep the brain functioning at a normal level. At normal blood pressure levels, if a certain brain area is highly active and consumes more oxygen, cerebral blood flow in that area increases as well. However, for reasons unknown, the increase in blood flow is several times higher than the increase in oxygen consumption. Thus, if a certain brain area is active, the blood oxygen level in that area *increases*.

A change in blood oxygen level can be measured with MRI because of the magnetic properties of hemoglobin (Hb). Hemoglobin, when bound to oxygen (oxyhemoglobin, or HbO), has different magnetic characteristics from when it is not bound to oxygen (deoxyhemoglobin, or dHb). The fMRI signal of HbO is stronger than that of dHb, causing an increase in the MR signal if the ratio HbO/dHb increases. In other words, if a certain brain area is active, the local increase in blood flow (which causes an increase in HbO and a decrease in dHb) causes a slight increase in the MR signal. The MR signal in functional MRI is therefore called the Blood Oxygen Level Dependent (BOLD) signal. A signal increase due to a specific event is referred to as a BOLD response. By measuring the BOLD signal, changes in brain activity in different regions of the brain can be investigated, providing a powerful tool to study cognitive processes.

2.3. The physics of MRI

2.3.1. Magnetic properties of atomic nuclei

Magnetic Resonance Imaging (MRI) makes use of the difference in magnetic characteristics between substances. The differences between substances arise from the fact that each substance consists of a different combination of atoms, which themselves are different combinations of protons, neutrons and electrons. All protons and neutrons have an intrinsic angular momentum called *spin*. This angular momentum always has the same magnitude (all protons and neutrons spin at the same speed); only the *axis* of spin can change. In the nucleus of an atom, protons and neutrons combine in pairs with oppositely oriented spins, so that a nucleus with an even number of protons and neutrons does not have net spin. A nucleus with an odd number of protons and neutrons (e.g. Hydrogen (H), which is the primary focus of MRI) does have a net spin. Such a nucleus is a magnetic dipole, with the magnetic axis as the axis of spin.

When a dipole nucleus is placed in a magnetic field, the field exerts a force on the axis of spin, causing the axis of spin to revolve around the axis of the magnetic field (see figure 2.1). This is similar to a spinning top that starts revolving around the axis of gravity, if its axis of spin is not exactly aligned with the direction of gravity. The speed at which the spin axis revolves around the axis of the magnetic field (the revolution speed) is called the frequency of magnetic resonance, and it is proportional to the strength of the magnetic field. However, the magnetic resonance frequency is different for the nuclei of different molecules. This difference in magnetic resonance frequency causes contrasts between different types of tissue in the MR image (see below), making it possible to construct an image of the brain.

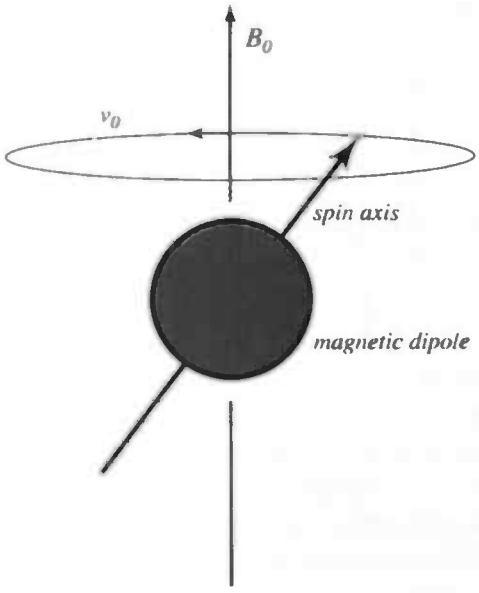

Figure 2.1: A magnetic dipole in a magnetic field B_0. The field exerts a force on the axis of spin, causing the axis of spin to revolve around the axis of the magnetic field with speed v_0. Adapted from Buxton (2002).

2.3.2. The MRI signal

In an MRI experiment, a sample is placed in a strong magnetic field (B_0), usually with a magnitude of 1.5 or 3 Tesla (as a comparison: the magnetic field of the earth is approximately 0.00005 Tesla). As explained in paragraph 2.3.1, the axes of spin of all atomic dipoles revolve around the axis of B_0. However, there is a slight tendency for the axis of spin to align with the direction of B_0. This results in a small net magnetization of the sample, called M_0 (M_0 is aligned with B_0, see figure 2.2).

An MRI experiment consists of several cycles of transmitting a signal and receiving a resonance signal. In the *transmit phase* of the experiment, an oscillating magnetic field (B_1) perpendicular to B_0 is created (see figure 2.2). B_1 is only applied for a relatively short time (a few milliseconds) and is therefore also referred to as a *pulse*. The oscillation frequency of B_1 is equal to the magnetic resonance frequency of the sample, causing the nuclei in the sample to resonate. In other words, the net magnetization is tipped over in the direction of B_1, and the new net magnetization M revolves around B_0 at an angle α (see figure 2.3). α is called the flip angle and depends on the state of the substance, the duration of the pulse and the strength of the pulse. The revolving net magnetization M is a changing magnetic field, which can be measured in the *receive phase* of the experiment. This is the MRI signal.

After the pulse is turned off, the net magnetization M slowly returns to the direction of B_0. Thus, after the pulse, the signal slowly decays. Since each substance has its own characteristic magnetic resonance frequency, the speed of decay is different for each substance. Therefore, if the MR signal is measured at a given time after the end of the pulse, the signal of one type of tissue (e.g. grey matter) may be weak, whereas that of an other (e.g. cerebrospinal fluid) may be strong. This difference in MRI signal strength is used to obtain contrasts between types of tissue in an MR image. Different images can be obtained depending on the pulse strength, duration, the frequency of the pulse, the time between pulses (repetition time, or TR), and the time between sending the pulse and measuring the signal. These parameters can be summarized as the *pulse sequence* of the MRI experiment. Many different pulse sequences are possible, yielding a wealth of applications for magnetic resonance imaging.

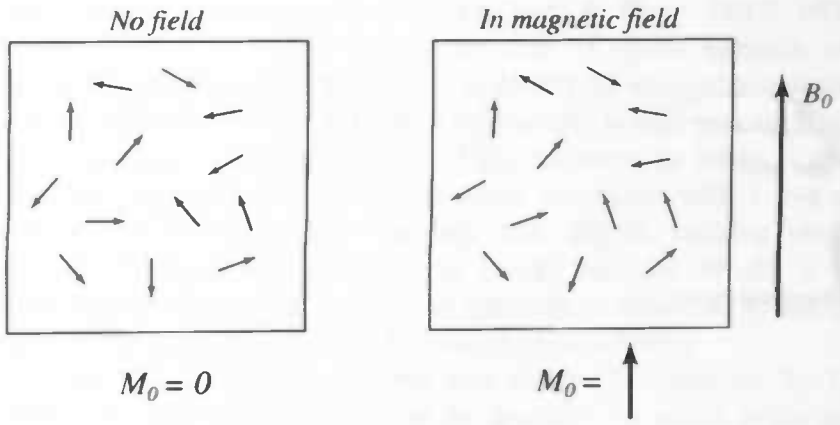

Figure 2.2: Although all atomic dipoles revolve around the axis of B_0, there is a slight tendency for the axis of spin to align with the direction of B_0. This results in a small net magnetization of the sample, called M_0. Adapted from Buxton (2002).

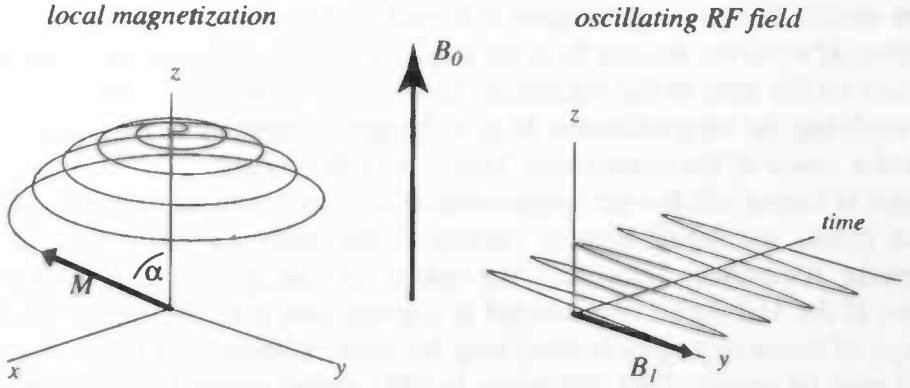

Figure 2.3: When an oscillating magnetic field B_1 perpendicular to B_0 is applied, the net magnetization is tipped over in the direction of B_1, and the new net magnetization M revolves around B_0 at an angle α. Adapted from Buxton (2002).

Chapter 3: The Amygdala

3.1. History of amygdala and emotion research

3.1.1. Introspection versus behaviorism

At the beginning of the 20th century, psychological experiences were studied through introspection. It was believed that complex conscious experiences such as emotions could be fully explained by careful examination of these experiences in one's own mind. However, the unreliability of these subjective observations eventually caused researchers to abandon the introspection method, because many "experimental" results could not be replicated.

As a reaction to introspectionism, the psychological movement known as behaviorism began to grow in popularity. Behaviorism holds that mental events can only be studied through objectively observable behavior. Behaviorists banned the introspective study of conscious experiences and focused on stimulus-response patterns as constructs for psychological theories. They were inspired by the experiments of Pavlov (1927/1960), who described a learning process now known as classical conditioning.

In his famous experiments, Pavlov simultaneously presented dogs with an unconditioned stimulus (food) and an initially neutral stimulus (a ringing bell). After several paired presentations, the unconditioned response to food (salivation) became conditioned to the sound of the ringing bell (which is therefore called the conditioned stimulus). In other words, salivation occurred after presentation of the sound alone, without presentation of food. This learning process could also be reversed: extinction of conditioning occurred if the conditioned stimulus was repeatedly presented without the unconditioned stimulus (i.e., after several presentations of the sound without food, salivation no longer occurred on presentation of the sound). The whole process of conditioning can be described completely in terms of objectively observable behavior to presented stimuli, and became one of the hallmarks of behaviorism.

3.1.2. Studying emotion

In the introspection movement, emotions were regarded as complex conscious experiences or feelings that constituted an essential part of the mind. In contrast, behaviorists were only interested in emotions as motivational factors that drove an individual's behavior. They studied emotion only if it was possible to do so with objective observation. Fear, for example, was studied with conditioning experiments in which an aversive stimulus (e.g. an electric shock) was used as the unconditioned stimulus (UCS). The unconditioned response (UR) of an animal in this case consists of fear behavior, such as increased blood pressure, increased heart rate and a freezing response. If the animal is repeatedly presented with a tone (the conditioned stimulus, or CS) just before the electric shock, the animal will after some time respond to the tone with a fear response, even in the absence of shock. This type of conditioning is called fear conditioning. A similar type of conditioning, known as avoidance conditioning, is also used to study fear. In avoidance conditioning, an animal learns to avoid a certain behavior, when this behavior results in an unpleasant experience (e.g. an electric shock). Fear conditioning and avoidance conditioning have been used extensively by researchers in the second half of the 20th century to study the neuro-anatomy of fear (see below).

3.1.3. History of amygdala research

In 1937 and 1938, Heinrich Klüver and Paul Bucy reported the behavior of a Rhesus monkey after bilateral temporal lobectomy (Klüver & Bucy 1937; 1938). They reported that the monkey seemed to suffer from some kind of visual agnosia, which they termed "psychic blindness": it seemed to have lost the ability to recognize objects by vision, although there were no sensory or motor deficits. The monkey would pick up any object, and inspect it orally (i.e., by putting it into its mouth, licking, chewing or biting it gently), regardless of whether the object was edible or not. Even when presented with a live snake or rat it would try to examine the animal orally, like any other object, without showing any fear. In fact, the monkey displayed no emotional or social behavior at all: it did not interact with other monkeys in any way, not even when attacked or mounted by another monkey. This pattern of behavior became known as the Klüver-Bucy syndrome.

The Klüver-Bucy syndrome was further investigated by Lawrence Weiskranz in the 1950s, who specifically addressed the question of which brain structure was responsible for the lack of emotion, or tameness, of animals with lesions to the temporal lobe (Weiskranz 1956). He reported that monkeys with lesions to the amygdala displayed the same fearless behavior as the monkey of Klüver & Bucy. In addition, the amygdala-lesioned monkeys were significantly slower in the acquisition of, and significantly faster in the extinction of avoidance conditioning.

The results of Klüver & Bucy (Klüver & Bucy 1937; 1938) and Weiskranz (1956) started a whole line of research on fear conditioning and the involvement of the amygdala in fear. Section 3.2 will summarize the results of animal research on the amygdala, followed by research on the human amygdala in section 3.3. Finally, section 3.4 will describe evidence of subconscious processing in the amygdala, in addition to conscious processing.

3.2. Recent animal research: the amygdala and fear conditioning

Recent animal research indicates that the learning process of fear conditioning takes place in the amygdala. Fear conditioning has been shown to alter neural responses to the conditioned stimulus in the amygdala (Rogan et al. 1997) and electrical stimulation of the amygdala can produce changes in heart rate, blood pressure and behavior very similar to those observed in a state of fear (Davis 1992). However, the exact type of amygdala responses depends on the state of the animal and the location of stimulation within the amygdala.

The amygdala consists of approximately 12 regions, of which the lateral (LA), basal (B), accessory basal (AB) and central (CE) nuclei are of most relevance to fear conditioning (for reviews, see LeDoux 1995; Maren & Fanselow 1996; LeDoux 2000; Maren 2001; LeDoux 2003). These regions and their connections are shown in figure 3.1 (LeDoux 2000). The lateral amygdaloid nucleus is thought to be the sensory interface of the amygdala (LeDoux et al. 1990). It receives input from sensory processing areas of both the thalamus and the cortex[1], and projects to B, AB and the central nucleus of the amygdala (LeDoux 1990; LeDoux et al. 1990; LeDoux 1995). Lesions to LA interfere with the acquisition and expression of fear conditioning (LeDoux et al. 1990; Campeau & Davis 1995a; Goosens & Maren 2001). In other words, if an animal is lesioned in LA before training, fear conditioning does not take place or is greatly reduced. If the animal is lesioned after fear conditioning, the learned relationship between the conditioned and unconditioned stimuli seems to be forgotten.

The B and AB nuclei receive input from both the LA and the hippocampus. The hippocampus is a brain structure involved in the formation of memories. During fear conditioning, the hippocampus seems to store memories of the environmental conditions under which fear conditioning has taken place: after the experiment, animals react with fear responses not only to the CS, but also to the environment in which the CS and the UCS were paired. This is called contextual fear conditioning and involves both the B and AB nuclei and the hippocampus (LeDoux 2000). Not surprisingly, lesions to B and AB interfere with contextual fear conditioning (Maren & Fanselow 1996).

Projections from LA, B and AB converge on the central nucleus (CE). The central nucleus, in turn, projects into a variety of hypothalamic and brainstem areas that are involved in the expression of several different fear responses (Davis 1992). For example, the CE projects into the lateral hypothalamus, an area responsible for regulation of sympathetic activation. Activation of this area by the amygdala may be responsible for the increased heart rate and elevated blood pressure observed in a state of fear. Similarly, the increased startle reflex and the freezing response may be caused by amygdala-mediated activation in the nucleus reticularis pontis caudalis (NRPC, which is involved in reflexive behavior), and regions in the central grey of the brainstem (which cause a cessation of behavior), respectively. The CE is therefore thought to be the general output system of the amygdala. Like the LA, lesions to CE interfere with both acquisition and expression of fear conditioning (LeDoux et al. 1990; Campeau & Davis 1995a; Goosens & Maren 2001). Figure 3.2 summarizes the roles of the different regions of the rat amygdala in fear conditioning.

[1] Most research on fear conditioning has focused on the auditory modality. The amygdala receives sensory input from the medial geniculate body of the thalamus and the primary auditory cortex. However, several tracing studies (for example, (Linke et al. 1999) suggest that the amygdala receives input from visual processing areas (and possibly other modalities) as well. Furthermore, recent lesion studies have shown that damage to the amygdala interferes with both auditory and visual fear conditioning (Campeau & Davis 1995a; 1995b).

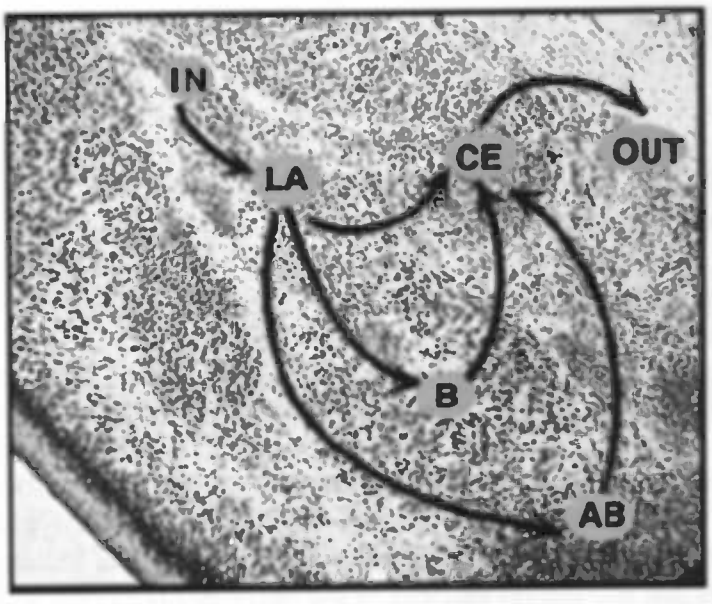

Figure 3.1: The amygdala of the rat, with the different subregions that are involved in fear conditioning: Lateral (LA), Basal (B), Accessory Basal (AB), and Central (CE) nuclei. The arrows indicate connections between these regions. Inputs (IN) arrive from the thalamus and cortex, and outputs (OUT) project to several brainstem and hypothalamic areas. Adapted from LeDoux (2000).

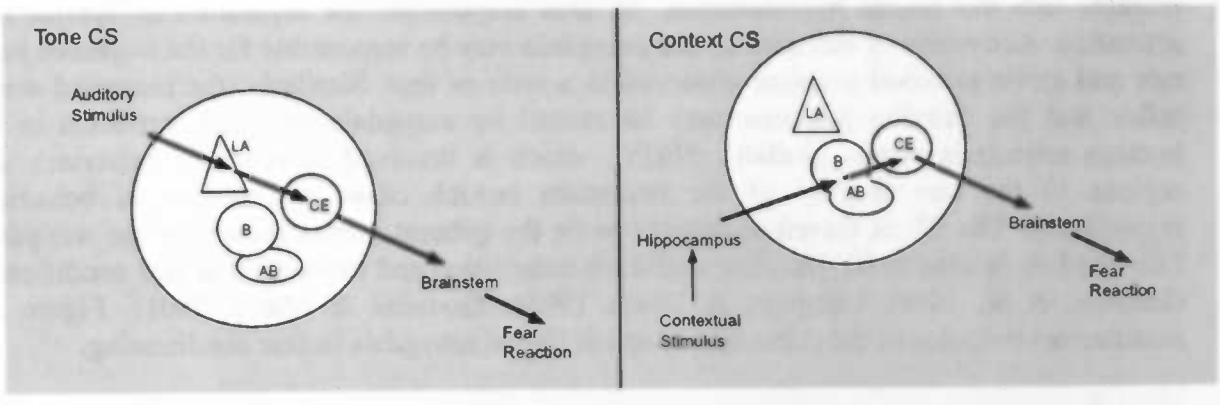

Figure 3.2: Two stimulus information pathways within the amygdala for fear conditioning. A simple auditory stimulus enters the amygdala through the lateral nucleus, whereas complex contextual information is retrieved from the hippocampus. Adapted from LeDoux (2000).

3.3. The human amygdala

The human amygdala is depicted in figure 3.3. As with animals, human patients suffering damage to the amygdala are impaired in fear conditioning (Bechara et al. 1995; LaBar et al. 1995). Furthermore, neuroimaging studies have shown that the amygdala is activated during both the acquisition and expression of conditioned fear (LaBar et al. 1998; Knight et al. 2005). The amygdala is active even when the conditioned stimulus (during acquisition) is presented for such a short duration that it is not consciously perceived, or, in other words, when fear conditioning occurs subconsciously (Morris et al. 2001). In addition, if subjects are *told* a shock will be administered only when a certain stimulus is presented, there is activation in the amygdala during presentation of that stimulus, even when no shock is administered at all (Phelps et al. 2001). Taken together, these results indicate that the amygdala is involved in fear conditioning in humans as well. The human amygdala may even be specifically involved in the perception of negative facial expressions, which will be explained in this section.

Fear conditioning, both in humans and animals, occurs throughout an individual's life. It enables the individual to avoid danger, because stimuli that coincide with an unpleasant or painful event are associated with that event, and are therefore avoided. For example, if a curious child gets bitten when it tries to pet a dog, the child will probably fear the dog and avoid it in the future, thus increasing its chance of survival.

In the course of evolution, the brain may have developed specialized (i.e. enhanced) fear conditioning to biologically relevant stimuli. In other words, stimuli that are more likely to signal a threat (e.g. fearful or angry facial expressions) may be conditioned easier than stimuli that are not likely to signal a threat (e.g. neutral or happy facial expressions). Indeed, several behavioral studies have found evidence for differential fear conditioning of biologically relevant and irrelevant stimuli (Esteves et al. 1994b; Regan & Howard 1995). For biologically relevant stimuli such as fearful or angry faces, the conditioned association between the CS and the UCS is much stronger than for biologically irrelevant stimuli, to the degree that relevant stimuli can even be conditioned subconsciously, whereas irrelevant stimuli can not (Esteves et al. 1994a; Esteves et al. 1994b; Wong et al. 1994; Regan & Howard 1995). This will be discussed further in section 3.4.

For humans, negative facial expressions (e.g. anger and fear) are biologically quite relevant. It would not be surprising, then, if the amygdala were involved in the perception of these stimuli. Indeed, a number of both neuroimaging and lesion studies indicate that the amygdala is involved in the processing of negative facial affect. Using PET, Morris and colleagues found significantly higher activation in the amygdala to fearful as opposed to happy faces (Morris et al. 1996; Morris et al. 1998). This activation was related to the intensity of the emotion: the neural response increased with increased fearfulness, and decreased with increased happiness. Activation of the amygdala during perception of fearful faces has also been found with fMRI, although the response to fearful faces habituated rapidly (Breiter et al. 1996; Reinders et al. 2005).

In addition, patients with damage to the amygdala are impaired in the recognition of negative facial expressions, particularly fear and anger (Adolphs et al. 1994; Calder et al. 1996; Young et al. 1996; Adolphs et al. 1999; Sato et al. 2002; Adolphs & Tranel 2003). This impairment caused patients to mistake fear and anger for happiness (Sato et al. 2002), to mistake a difference in expression for a difference in identity (Young et al. 1996), or to judge the intensity of negative emotions much lower than controls (Adolphs et al. 1994). Taken together, these studies provide further evidence that the amygdala is specifically involved in the perception of negative facial affect.

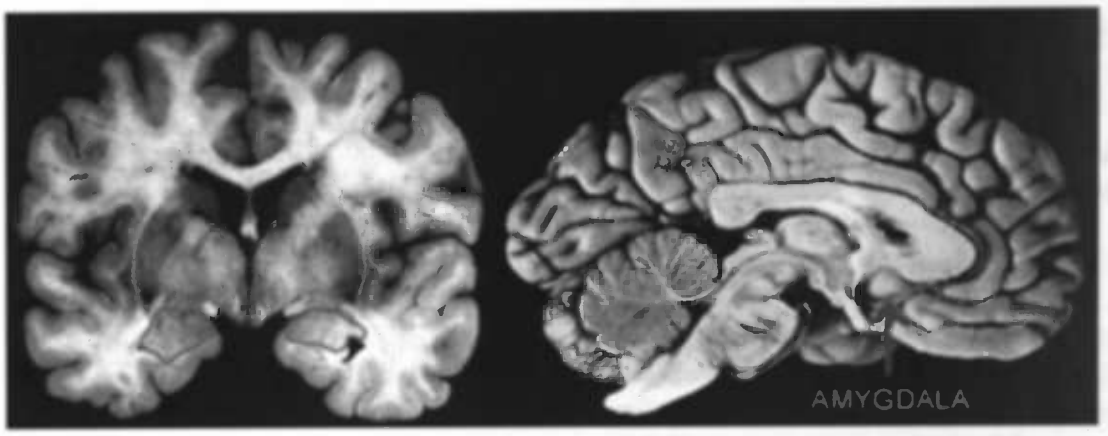

Figure 3.3: The human amygdala. The picture on the left is a coronal slice of an fMRI scan, with the amygdala encircled in red. The picture on the right is a medial saggittal view of the left hemisphere, in which the amygdala is indicated by the blue arrow.

3.4. Different pathways to the amygdala

As stated before, the amygdala receives inputs from the sensory cortex and the thalamus. Although inputs from both these areas are capable of mediating fear conditioning in rats, the inputs from the sensory cortex are slower and do not seem to be crucial to fear conditioning (see LeDoux 2000; 2003). This has led LeDoux and colleagues to propose that sensory information mediates fear conditioning through two distinct pathways: the direct thalamic (i.e. subcortical) pathway and the thalamo-cortical (i.e. cortical) pathway.

The subcortical pathway is shorter and faster, but also more capacity-limited, because it contains fewer neurons (Bordi & LeDoux 1994a; 1994b). It probably provides coarse stimulus information (Vuilleumier et al. 2003) that is suitable for generating fast, life saving responses to simple stimuli that may signal a threat. The cortical pathway, in contrast, provides detailed information which is also suitable for processing complex stimulus patterns, but the cortical pathway is slower than the subcortical pathway (LeDoux 2000; 2003).

Research on the human amygdala supports the idea of a subcortical processing pathway providing crude sensory information about biologically relevant stimuli. Morris et al (2001) presented pictures of fearful and happy faces to a patient with damage to the primary visual (i.e. striate) cortex. Although these pictures were presented in the patient's cortically blind field and the patient denied perceiving the faces, significant amygdala activation was found during presentation of fearful faces. In a second experiment, after conditioning to one fearful face (the CS) but not another (the control condition), a greater amygdala response was found during (blind field) presentation of the conditioned fearful face compared to the presentation of the unconditioned fearful face. Given the patient's lesion, information mediating the amygdala responses must have accessed the amygdala through a pathway bypassing the striate cortex. In an additional analysis, the amygdala responses to the fearful faces from the first experiment and to the conditioned face from the second experiment (but not to the other face stimuli from either experiment) were found to covary with neural activity in the posterior thalamus and superior colliculus, supporting the theory of a direct thalamic pathway mediating amygdala activity (Morris et al. 2001). Since the patient denied perception of faces in his blind field, the subcortical pathway must have processed the information subconsciously.

Studies with healthy subjects have offered similar conclusions. Using backward masking procedures to prevent conscious perception of the stimuli, Whalen et al. (1998) have found amygdala activation in healthy subjects during presentation of fearful faces. In a similar paradigm, Morris and colleagues (1998) measured neural activity in subjects who were presented with two backward masked angry faces, one of which was previously used as the conditioned stimulus in fear conditioning. The conditioned masked face elicited a response in the right amygdala while the unconditioned face did not. None of the masked faces were perceived consciously, indicating subconscious processing by way of the subcortical amygdala pathway. This was confirmed by a follow-up study, which showed increased connections between the right amygdala, pulvinar, and superior colliculus during presentation of subconsciously processed conditioned faces, but not during presentation of consciously processed conditioned faces (Morris et al. 1999).

The subcortical (subconscious) pathway may be specialized for biologically relevant stimuli. This theory is supported by the fact that, in the study of Whalen et al. (1998), unseen happy faces did not elicit increased amygdala responses. Furthermore, in a series of subconscious fear conditioning experiments (using backward masked stimuli) Esteves and colleagues (1994b) showed that a conditioned angry face elicited an increased skin conductance response (a measure of autonomic arousal frequently used in fear conditioning

paradigms), whereas a conditioned happy face did not. In other words, if backward masking is used to prevent conscious perception of the stimuli, fear conditioning occurred only when the conditioned stimulus was an angry face. This supports the idea that the subcortical amygdala pathway is specialized for biologically relevant stimuli, providing fast processing of stimuli signaling potential threats.

Chapter 4: Schizophrenia

4.1. Introduction

In chapter 3, it was explained that the amygdala is a brain structure specialized for processing biologically relevant information, including emotional facial expressions. Schizophrenia is a complex, disabling brain disease that may affect facial affect processing in addition to many other aspects of the mind, as will be explained in the current chapter. The first section gives an introduction to schizophrenia, followed by a discussion on facial affect processing and the role of the amygdala in schizophrenia, in sections 4.2 and 4.3.

Schizophrenia is a brain disease characterized by symptoms such as disorganized thinking, hallucinations and delusions. So far, the exact cause of schizophrenia is unknown, although some genetic factors appear to be involved, since family members of a schizophrenia patient are more likely to develop schizophrenia than other individuals. Usually, the onset of the disease is in early adulthood between 15 and 30 years of age.

The onset of schizophrenia may be gradual or acute. In most patients, the course of the disease is characterized by one or more acute psychotic episodes. During psychosis, a patient experiences disorganized thoughts and loses contact with reality. Thoughts become confused and conversation and sentences don't make sense. The patient may suffer from hallucinations: he or she perceives things that are not actually there. Many patients report hearing voices that comment on their activities or give them commands. In addition, patients often hold strong but false beliefs known as delusions. For example, a patient may be convinced that he or she is being monitored by a government agency through the television antenna. A psychotic episode is usually followed by an intermittent episode of relatively few and stable symptoms.

The psychotic symptoms mentioned above, although most common and well-known, are not the only symptoms of schizophrenia. Other symptoms[2] include catatonia (complex involuntary movements, such as unusual postures, automatic repetition of actions, mannerisms, etc.), emotional disturbances (such as flattening of affect, loss of feeling or heightened feeling, and loss of motivation), cognitive deficits (e.g. impaired attention, lack of initiative, and intellectual decline), and impaired social functioning. Schizophrenia is a complex disorder, with different patients exhibiting different symptoms.

The symptoms of schizophrenia are usually classified into positive and negative symptoms. Positive symptoms are phenomena that are present in patients but absent in healthy individuals, such as hallucinations, delusions, disorganized thinking and catatonia. Negative symptoms, in contrast, are phenomena that are present in healthy individuals but absent in patients. Negative symptoms are mainly emotional disturbances and include for example apathy, flattening of affect and loss of feeling. In addition, sometimes a third category, cognitive impairment, is used to classify symptoms such as impaired memory and executive function (impaired attention and lack of initiative).

[2] Not all phenomena observed in schizophrenia are symptoms (i.e. subjective experiences that the patient can feel and therefore complain about); some are signs (phenomena that are observed by others, but not mentioned by the patient himself). For simplicity, however, in this text the term 'symptoms' is used for both symptoms and signs.

4.2. Schizophrenia and facial affect processing

The emotional disturbances in schizophrenia have led many researchers to investigate affect recognition in schizophrenia patients. To date, a large body of literature has accumulated that indicates that patients with schizophrenia are impaired in facial affect recognition (for reviews, see Mandal et al. 1998; Edwards et al. 2002). However, the exact nature of this deficit is wrought with controversy. Firstly, it is unclear whether the facial affect recognition deficit is related to the negative symptoms of schizophrenia. Secondly, there is an ongoing debate on whether impaired facial affect recognition is part of a generalized performance deficit in schizophrenia, or whether schizophrenia patients have a differential (i.e. specific) deficit in facial emotion recognition.

The first issue concerns the relationship between negative symptoms and disturbed facial affect recognition. Two studies have found poorer performance in emotion discrimination to correlate with severity of negative symptoms in schizophrenia (Schneider et al. 1995; Sachs et al. 2004). It has been suggested that impaired emotion recognition is the cause of affective flattening in schizophrenia patients (Shaw et al. 1999). However, the results of other studies do not support this notion. Although patients exhibit flattened affect, their subjective experience of affect may be comparable to that of controls (Blanchard & Panzarella 1998). In other words, there may not always be convergence between the outward expression of emotion and the patient's subjective emotional experience. In addition, four recent studies that addressed the issue of a relationship between negative symptoms and impaired facial affect recognition directly have not found any correlation between them (Lewis & Garver 1995; Addington & Addington 1998; Shaw et al. 1999; Silver & Shlomo 2001). Moreover, emotion perception was found to correlate with attention (Addington & Addington 1998) and with early perceptional processing (Kee et al. 1998), suggesting that impaired facial affect recognition may be related to cognitive impairment in schizophrenia. Finally, Kohler and colleagues (2000) report that facial emotion recognition correlates with cognitive abilities as well as positive and negative symptoms. Therefore, the role of the facial emotion perception deficit in the symptomatology of schizophrenia is as yet unknown.

The second issue of debate concerns the generalized versus specific deficit in facial affect processing. Although there is consensus that patients with schizophrenia are impaired in facial affect perception (Mandal et al. 1998; Edwards et al. 2002), it is unclear whether this deficit is specific for facial affect. Kerr and Neale (1993) argue that, while many studies have found an emotion perception deficit, only a few have used an adequate control task suited for a differential deficit design. When such a control task is used, most studies report a generalized deficit that encompasses not only facial affect perception, but face recognition as well (Kerr & Neale 1993; Mueser et al. 1996; Kohler et al. 2000; Sachs et al. 2004). An exception is a study by Penn and colleagues (Penn et al. 2000), who did find a specific deficit in emotion perception relative to face perception, but only in acutely ill schizophrenia patients. Since the chronic patients in their study did not exhibit a differential deficit, they proposed that active symptoms may have an important role in specifically disrupting emotion perception in schizophrenia.

Regardless of whether the emotion perception deficit is specific and whether or not it is related to negative symptoms, this deficit does affect the lives of schizophrenia patients. Several studies have shown that impaired facial emotion recognition is related to social functioning in schizophrenia (Mueser et al. 1996; Penn et al. 1996; Ihnen et al. 1998; Hooker & Park 2002). Therefore, it is important to further investigate the nature of this deficit and the neural pathology that underlies it.

4.3. Schizophrenia and the amygdala

Since the symptomatology of schizophrenia is so diverse, it is probably not caused by an abnormality or dysfunction of a single brain area. Anatomical neuroimaging studies have found that cerebral volume is reduced in patients with schizophrenia, whereas ventricular volume is greater than that of normal controls (Wright et al. 2000). Furthermore, many studies have found structural abnormalities in the prefrontal and temporal lobes (e.g. Sanfilipo et al. 2000; Sigmundsson et al. 2001; Wible et al. 2001).

Given the impairment in facial affect recognition in schizophrenia patients, it is interesting to investigate the role of the amygdala in schizophrenia. Neuroimaging studies investigating the structure of the amygdala in schizophrenia patients have produced inconsistent results. Although many studies have found that amygdala volume is bilaterally reduced in schizophrenia patients (Wright et al. 2000; Steel et al. 2002; Kucharska-Pietura et al. 2003; Exner et al. 2004), some studies have reported different findings. Gur et al. (2000) report decreased amygdala volume in men but increased amygdala volume in women. Moreover, Narr and colleagues (2001) report a volume increase in the right amygdala, while Hulshoff Pol et al. (2001) found a grey matter density reduction only in the left amygdala.

At this point, few functional neuroimaging studies have been published that investigated the role of the amygdala in facial affect processing in schizophrenia. However, the few studies published do indicate amygdala involvement. That is, activation in the amygdala of schizophrenia patients is lower than that of healthy controls during perception of emotional faces, even if behavioral performance on a facial emotion discrimination task is at a normal level (Phillips et al. 1999; Gur et al. 2002; Takahashi et al. 2004). Thus, impaired facial affect recognition in schizophrenia may at least in part be due to failure to activate the amygdala.

In addition, two behavioral studies have shown that schizophrenia patients are impaired in aversive avoidance conditioning (Kosmidis et al. 1999; Hofer et al. 2001). In the study of Hofer et al., one type of stimulus (a green light) was followed by an aversive event (an air puff to the cornea), while another type of stimulus (a red light) was not. After several paired presentations of the green light with the air puff, healthy subjects developed an automatic conditioned response (i.e. reflexive eyelid closure) to the green light, but patients with schizophrenia did not. The study of Kosmidis et al. used a similar paradigm in which the aversive event, the sound of a buzzer, could be avoided by pressing a button. Schizophrenia patients needed significantly more trials to learn to avoid the sound than healthy controls. These studies indicate that patients with schizophrenia are impaired in avoidance conditioning. Since avoidance conditioning is believed to take place in the amygdala (see chapter 3), the avoidance conditioning deficit observed in schizophrenia may be caused by amygdala dysfunction. Taken together, these studies indicate that amygdala dysfunction may be involved in the emotion perception deficit in schizophrenia.

PART III

THE EXPERIMENT

Chapter 5: The Paradigm

5.1. Introduction

As discussed in chapter 3, the amygdala may be part of a threat detection circuit specialized for processing biologically relevant information. This circuit was further investigated in a recent fMRI study, in which Reinders et al. (2005) studied the robustness of perception using degraded stimulus information in a stimulus detection task. They presented healthy subjects with a grayscale image of visual noise from which a stimulus slowly emerged (a fearful face, a neutral face or a house). Subjects were to indicate the moment of recognition (i.e., the moment at which the stimulus "popped out" from the noise) with a button press (one button regardless of stimulus type). Activation in the amygdala during the pop-out of the face stimuli was found, with more activation for fearful faces than for neutral faces. Moreover, fearful faces were perceived earlier (i.e. with more noise still present in the image) than neutral faces, and neutral faces were perceived earlier than houses. In a follow-up analysis, amygdala activation was also found before the moment of pop-out, further supporting the idea that the amygdala processes possibly threatful visual information through a subcortical pathway even before it enters conscious awareness.

In the present study, we used the paradigm of Reinders et al. (2005) to study the threat detection circuit and facial affect processing role of the amygdala in both healthy volunteers and patients with schizophrenia. The paradigm was improved (1) by measuring and using simple reaction time to obtain a better estimate of the moment of pop-out, and (2) by using color images instead of grayscale images, to create more realistic stimuli.

We constructed an experiment in which healthy subjects were presented with a color image of visual noise from which a stimulus slowly emerged. Each trial consisted of a sequence of 100 pictures presented in rapid succession, in which the amount of stimulus information increased with each picture. Three stimulus types with different degrees of biological relevance were used: fearful faces (high relevance), neutral faces (intermediate relevance) and houses (low relevance). Subjects indicated the moment of stimulus recognition (referred to in the rest of the text as the moment of pop-out) with a button press.

To examine which brain structures were involved in processing the different types of stimuli, brain activation was continually measured with fMRI during both the detection and perception of the stimuli. The two stimulus types (faces and houses) have been found to activate different specific areas of the brain (for review, see Grill-Spector 2003). The ventral visual pathway (which extends from the occipital lobe into the ventral and lateral temporal lobe) has been reported to be involved in specialized processing of certain stimulus types, such as houses, faces or other objects. Houses have been reported to activate an area in the parahippocampal gyrus known as the parahippocampal place area (PPA, see Epstein & Kanwisher 1998; Epstein et al. 1999), while faces have been reported to activate an area in the fusiform gyrus, the so-called fusiform face area (FFA, see Kanwisher et al. 1997; Kanwisher et al. 1999). Brain activation in one of these specific brain areas would therefore indicate processing of the stimulus type associated with that brain area.

5.2. Hypotheses

5.2.1 Healthy subjects

We hypothesized that the amygdala is part of a fast, subconscious threat detection circuit specialized in processing biologically relevant information, to enable an individual to detect environmental threats quickly and initiate immediate behavioral reactions. Since a fearful face is a biologically relevant stimulus (i.e., it signals a possible threat), it was hypothesized to be processed by the fast, subconscious amygdala pathway. Therefore, we hypothesized that healthy subjects would detect a fearful face earlier (i.e., with more noise) than a neutral face or a house. We also expected that faces, both fearful and neutral, would be detected earlier than houses because faces, regardless of expression, are biologically more relevant than houses. Concerning the localization of brain activation, we hypothesized that during the moment of stimulus detection and/or during full perception of the stimuli, face stimuli would cause activation in the fusiform gyrus and/or the amygdala, and that house stimuli would activate the parahippocampal gyrus.

We also hypothesized that fearful faces would cause more activation in the amygdala than neutral faces, because fearful faces are biologically more relevant than neutral faces. Finally, since the hypothesized subconscious amygdala pathway includes the thalamus as a relay station for visual and other sensory information, we expected activation in the lateral geniculate nucleus of the thalamus during all trials of all conditions (i.e., all times in the experiment during which a stimulus (noise, house or face) was perceived).

5.2.2 Patients with schizophrenia

The second aim of the experiment was to examine facial affect processing of patients with schizophrenia. We hypothesized that, due to a deficit in facial affect processing, schizophrenia patients would not detect fearful faces significantly earlier than neutral faces.

As with the healthy controls, we expected brain activation in the parahippocampal gyrus (i.e. the PPA) due to the perception of houses, and brain activation in the fusiform gyrus (i.e. the FFA) due to the perception of faces. We also expected brain activation in the lateral geniculate nucleus of the thalamus for all conditions in the experiment. However, due to the proposed involvement of the amygdala in the facial affect processing deficit observed in schizophrenia patients (see chapter 4), we expected that the face-dependent brain activation patterns of the amygdala in schizophrenia patients would deviate from those in healthy controls.

Chapter 6: Methods and Materials

6.1. Subjects

A total of 30 subjects (including pilot studies) participated in the experiment. The experiment was approved by the local ethics committee, and all participants gave their written informed consent to participate in the experiment. Two of the participants were schizophrenia patients, the other 28 participants were healthy controls. The control group consisted of 14 males and 14 females, between 18 and 37 years old, with a mean age of 25.

The patients participated with the consent of their attending psychiatrist. The first patient was male, 36 years old, and had been diagnosed with schizophrenia 8 years prior to the experiment. Three days before the experiment, the severity of positive and negative symptoms was assessed with the Positive and Negative Syndrome Scale[3] (PANSS). The patient scored an average value of 2.29 on the positive scale and an average value of 1 on the negative scale. The second patient was male, 30 years old, and had been diagnosed with schizophrenia one year prior to the experiment. His PANSS scores (also taken three days before the experiment) were 1.43 on the positive scale and 1.57 on the negative scale. Both patients were on anti-psychotic medication (aripiprazol 15 mg for both patients). In addition, patient number 2 also used an anti-depressant (citalopram 20 mg).

6.2. Stimuli

6.2.1 Stimulus selection

Front view color images of neutral and fearful faces were drawn from the Karolinska Directed Emotional Faces set (Lundqvist et al. 1998). The selection was made on the basis of extensive rating of the neutral and fearful expression of all front view pictures in the set (described in detail in appendix A), which resulted in 20 neutral faces (10 male, 10 female), and 20 fearful faces (10 male, 10 female). Ten color house pictures were used, which were pictures of standard European houses of light color. The pictures were adjusted to remove any information other then the house itself (see also Reinders et al. 2005).

[3] The Positive and Negative Syndrome Scale (PANSS) for schizophrenia was developed in 1986 to create a standardized instrument for classifying positive and negative symptoms in schizophrenia. The PANSS test consists of a semi-structured interview in which a total of 30 psychopathological symptoms (including 7 positive, 7 negative and 16 general psychopathological symptoms) are scored on a scale from 1 (not present) to 7 (extremely severe).

6.2.2 Stimulus development

For each of the 50 stimuli (20 neutral faces, 20 fearful faces and 10 houses), 110 pictures with increasing stimulus information were created, so that the first picture consisted of 100 % noise and the last picture consisted of 100% stimulus information. The pictures were created using frequency domain methods (see also Rainer et al. 2001; Reinders et al. 2005), which involves applying the discrete Fourier transform to the pictures to manipulate them in the frequency domain (described in appendix B). Both the amplitude spectra and the phase spectra of the images were manipulated in the frequency domain. To ensure that all images had the same brightness and contrast, the same averaged amplitude spectrum was used for all images. The different noise levels in the pictures were obtained by linear interpolation of the original phase spectrum of the pictures and a completely random phase spectrum (see appendix B).

The amount of stimulus information (i.e., the phase coherence, or the fraction of the original phase spectrum) was increased according to the following exponential function (see also appendix B):

$$\text{fraction of original phase} = \frac{(e^{0,0033 \cdot p} - 1)}{(e^{0,0033 \cdot (N-1)} - 1)} \qquad p \in [0, N-1]$$

where N is the number of pictures to be created, in this case 110. This function was chosen to ensure that the moment of pop-out is approximately halfway in the stimulus sequence, for an optimal timing of the BOLD response (explained in the next section). For the actual experiment, a subset of only 100 pictures of the 110 pictures originally created was used for each stimulus sequence. In this way, the moment of pop-out was jittered slightly, improving the temporal resolution of the fMRI signal and making the timing of the experiment less predictable (see appendix C for more details).

The stimuli were presented with a screen resolution of 1024x768 pixels. The images were resized in such a way that they were presented within visual focus of 5 degrees (see also section B.4.1 in appendix B, and Rainer et al. 2001). Finally, the edges of the pictures were smoothed into the background, by presenting a frame of 60 pixel width as a foreground to the images (see figures B.7, B.8 and B.10 in appendix B, and Rainer et al. 2001). The frame contained both transparent pixels and pixels with the same (grey) color as the background. The number of grey pixels increased linearly over the 60 pixels from the inside to the outside of the frame, resulting in a smooth transition from picture to background. This minimizes any neural activation due to the contrast between the outer edges of the images and the background. The color of the background was equal to the average color of the first and 110th pictures of all stimuli, to further minimize the contrast between images and background.

6.3. Experimental procedure

6.3.1 Time course of the experiment

Before the experiment, each subject received verbal instructions of the task, and performed a practice task (with pictures not used in the pop-out task) until (s)he understood the instructions. The subject was then placed into the scanner for the actual fMRI-experiment. First, pictures of neutral faces, fearful faces, and houses were shown to the subject in order to localize the specific brain activation areas for these stimulus categories in the subject's brain[4].

After the localizer pictures, the subject performed the pop-out task, where the stimulus (a face or a house) emerged from visual noise, and the subject was to press a button at the moment of stimulus recognition (i.e., the moment of pop-out). Finally, when the subject was out of the scanner, a reaction time task (with conditions similar to those of the pop-out task) was performed by the subject, for a more accurate assessment of the moment of pop-out (see section 6.3.3). The subjects were debriefed both verbally and by filling in a questionnaire, about their well-being in the scanner, their concentration during the task, and how well they thought they had done on the task.

6.3.2 The pop-out task

The stimuli were presented using Presentation (http://nbs.neuro-bs.com/presentation). The pop-out task consisted of five sessions of ten trials each, with a short break between sessions. The total of 50 stimuli were pseudo-randomly distributed over the sessions, in such a way that there were two houses, four neutral faces and four fearful faces in each session. The stimuli within each session were presented in random order, with a blank grey screen presented between trials.

Each trial consisted of a sequence of 100 pictures in which the stimulus (a fearful face, a neutral face or a house) gradually emerged from visual noise. Every picture in the sequence was presented for 200 ms, so the sequence took 20 seconds to complete. The moment of pop-out was expected to be approximately halfway in the sequence, with conscious stimulus perception giving rise to a BOLD response in the brain from the moment of the button press to the end of the stimulus sequence (see also section 6.5.2). Timing the perception of the stimulus in this manner allows the BOLD response to subside after the end of the stimulus sequence, approaching its baseline level during presentation of the blank screen between two trials (10 seconds) and the first half of the next stimulus sequence, before the next pop-out (approximately 10 seconds, making a total of approximately 20 seconds between two BOLD responses).

During each stimulus sequence, the subject had to perform two tasks. While the image gradually changed from noise to original image, a fixation dot was presented in the centre of the screen. The fixation dot was either blue or red and changed color randomly every few seconds (between 2 and 4 seconds). The subjects were to press a button with the index finger of their dominant hand every time the dot changed color. In this manner, the attention of the subject was kept in the centre of the screen, and the motor activation in the brain due to the button presses was kept constant throughout the stimulus sequence. At the same time, the

[4] The face pictures that were used for this localizer task were pictures of the same faces as those used for the pop-out task, but with interchanged neutral and fearful expressions. That is, if in the pop-out task the picture of face X was a neutral face, then the picture of face X in the localizer task was a fearful face, and vice versa. In this way, activation found in the pop-out task cannot be due to novelty of the stimulus, while at the same time the subjects are not biased by the localizer stimuli, since they haven't seen the actual pictures of the pop-out task.

subjects had to press a button with the middle finger of their dominant hand when they recognized the stimulus (i.e., at the moment of pop-out). This button press was simply to indicate the moment of pop-out, not the specific type of stimulus (subjects were to press the same button regardless of stimulus type).

6.3.3 The reaction-time task

During the pop-out task, the actual moment of pop-out is slightly earlier than the time of the button-press, because of the time needed for response preparation (the reaction time). To estimate the reaction times in the scanner, subjects had to perform a separate reaction time task after the fMRI-experiment. The task was similar to the task in the scanner, with the exception that the stimulus did not appear gradually, as in the pop-out task, but suddenly.

The task contained 15 trials, consisting of five houses, five neutral faces and five fearful faces presented in random order. In each trial, a noise picture was shown for a few seconds (a random number of seconds between 5 and 9), followed by a stimulus (house, neutral face or fearful face). As in the pop-out task, a fixation dot was presented in the centre of the screen, which continuously changed color (from red to blue and back) after a random number of seconds between 2 and 4. Subjects were to press a button with their index finger when the dot changed color. Concurrently, they were to press a button with their middle finger as soon as the stimulus appeared. As in the pop-out task, there was only one button for all three stimuli: the subjects were to indicate the recognition of the stimulus regardless of stimulus type.

6.4. fMRI parameters

The neural activation during the task was measured using functional magnetic resonance imaging (fMRI). Magnetic resonance was performed on a 3 Tesla MRI scanner (Philips). An echo planar imaging (EPI), T2* weighted pulse sequence was used to acquire the scans (TR = 1.24 s, TE = 25 ms, flip angle = 74 degrees). For each subject 5 sessions were obtained, with each session consisting of 255 scans (23 axial slices (interleaved), slice thickness 3 mm, no gap). The first 5 scans of each session were discarded to allow for T1 equilibration effects.

The scanner settings were based on the subcortical fear perception pathway (see LeDoux 1995) and the ventral object perception pathway, to include the parahippocampal place area (PPA, see Epstein & Kanwisher 1998; Epstein et al. 1999) and the fusiform face area (FFA, see Kanwisher et al. 1997; Kanwisher et al. 1999).The brain areas scanned included the thalami, amygdalae, visual cortices (including the primary visual cortex and the dorsal extrastriate cortex), parahippocampal gyri and fusiform gyri of both hemispheres.

6.5. Statistical analysis

6.5.1. Behavioral data

The data from the simple reaction time task were analyzed first. For each subject, the mean and standard deviation of the reaction times were computed. Outliers, defined as values that differed from the mean by more than two standard deviations, were excluded from further analysis for the subject under consideration. The new mean reaction time (i.e., the mean reaction time of the data set without the outliers) was used as an indication for the reaction time during the actual fMRI experiment, i.e. the time between conscious perception of the stimulus and the actual button press. This reaction time was subtracted from all response times of the pop-out task to obtain a better estimation of the moment of conscious pop-out.

The response times of the pop-out task needed to be adjusted for the jittering that was introduced by manipulating the amount of stimulus information of the first picture in the sequence (see appendix C). For each stimulus, a series of 110 pictures had originally been created, with the first picture containing 100% noise and the 110^{th} picture containing 100% stimulus information. A subset containing 100 of the 110 pictures was used in the actual experiment, varying from the set of pictures 1 through 100 to the set of pictures 10 through 109 (see appendix C). In other words, each trial started with picture number n ($n \in [1,10]$) of the original set of 110 pictures, and the pictures 1 through $(n-1)$ were omitted. Therefore, we added $0.2 \cdot (n-1)$ seconds to the response time of each trial (since each picture was presented for 0.2 seconds). In this way, the response times were adjusted for jittering (i.e., all trials were matched for the amount of stimulus information in each consecutive picture).

The response times of the pop-out task were then analyzed using SPSS 11.5 (www.spss.com). Absolute z-scores of all response times were computed to detect outliers (defined as values that differed from the mean by more than 1.96 standard deviations, in other words values with an absolute z-score greater than 1.96). By this definition, data from two subjects were marked as outliers and therefore excluded from further data analysis. The data from the remaining 28 subjects (2 patients and 26 controls) were analyzed with a repeated measures ANOVA, with the response times for fearful faces, neutral faces and houses (corrected for reaction time and jittering) as within-subject variables. Degrees of freedom were corrected for violation of the sphericity assumption using Greenhouse-Geisser estimates of sphericity, and significance levels were adjusted with Bonferroni-tests for multiple comparisons.

6.5.2. fMRI data

At the time of writing, the fMRI data of three controls and two patients had been analyzed with single subject analyses. For each control subject, data from all five sessions were analyzed, while for the patients, due to a software problem in the first session, only four of the five sessions were suitable for fMRI data analysis.

Statistical parametric mapping (SPM2, www.fil.ion.ucl.ac.uk/spm/spm2.html) was used for both data pre-processing and statistical analysis. First, the data were checked for artefacts using tsdiffana (www.mrc-cbu.cam.ac.uk/Imaging/Common/diagnostics.shtml). Then, the fMRI images were realigned to the mean, which corrects for within-subject head movement during the experiment. The scans were spatially normalized (i.e. transformed) into the standard stereo-taxic Montreal neurological institute (MNI) space (Friston et al. 1995) using 7x8x7 non-linear basis functions and heavy regularization. Finally, noise was suppressed by spatially smoothing the images with an isotropic Gaussian kernel of 7 mm.

In SPM2, the statistical analysis consisted of multiple linear regression analysis of task-related, voxel-specific differences in blood oxygenation level dependent (BOLD) responses. For each subject, a general linear model (GLM) was constructed with seven regressors reflecting the different events and conditions of the pop-out task. These regressors were subdivided into 3 groups: (1) full perception, (2) pop-out, and (3) visual stimulation.

(1) Three regressors were used to model full (i.e. conscious) perception of the stimuli from the three experimental conditions (fearful faces, neutral faces and houses). These regressors modeled an elevated BOLD response with a prolonged hemodynamic response function (HRF) from the moment of the button press until the end of the stimulus sequence (see figure 6.1, part (c)). The duration of these regressors was variable, i.e. depending on the time of the pop-out button press.

(2) Brain activation due to the pop-out event was modeled by a simple canonical hemodynamic response function, (HRF) producing three additional regressors, one for each condition (see figure 6.1, part (b)). These pop-out regressors were time-locked to the moment of pop-out (i.e. the time of the button press minus simple reaction time).

(3) The seventh regressor modeled variance due to visual perception in general and repeated button presses during the trial, resulting in a regressor modeled by an prolonged HRF that started at the beginning of the trial (i.e. the first picture of the sequence) and ended at the end of the trial (i.e. the last picture of the sequence). This regressor is depicted in figure 6.1, part (d). In sum, the GLM consisted of seven regressors: six condition-dependent regressors that modeled brain activation due to full perception of the stimuli and pop-out effects, and one regressor for each trial that modeled brain activation due to button presses and visual stimulation.

Brain activation (as measured by the BOLD response) due to the perception of faces (fearful and neutral faces taken together) was compared to brain activation due to the perception of houses, for both full perception of the stimuli and the moment of pop-out. In addition, brain activation due to fearful faces was compared to brain activation due to neutral faces. Based on our hypotheses (see chapter 5), seven different contrast images were constructed to test for differences in brain activation patterns due to the condition-dependent pop-out and the condition-dependent full perception. The contrast definitions are shown in table 6.1.

The single subject contrast images were investigated for *a priori* hypothesis-based brain regions, i.e. the fusiform gyrus, the parahippocampal gyrus, the amygdala and the lateral geniculate nucleus of the thalamus (see section 5.2). Contrast images were viewed at the statistical level of $p < 0.001$ uncorrected for multiple comparisons. Correction for multiple comparisons was performed within the volume of interest (a sphere with a radius of 9 mm for the fusiform gyrus and parahippocampal area, and a sphere with a radius of 7mm for the amygdala, based on the approximate size of these regions as indicated by Talairach & Tournoux (1988)). For the remaining brain areas, for which we had no *a priori* hypotheses, multiple comparison correction was performed for the entire brain volume analyzed. Therefore, unless indicated differently, all statistical values reported are significant at the $p < 0.05$ corrected level.

Event:	Conditions:		
Full perception	houses > faces	faces > houses	fearful faces > neutral faces
Pop-out	houses > faces	faces > houses	fearful faces > neutral faces
Visual stimulation	all conditions (fearful faces, neutral faces and houses)		

Table 6.1: Seven contrast images were constructed for the different events and hypotheses of the experiment (see text). "houses > faces" = testing for a larger BOLD response in reaction to houses as compared to faces.

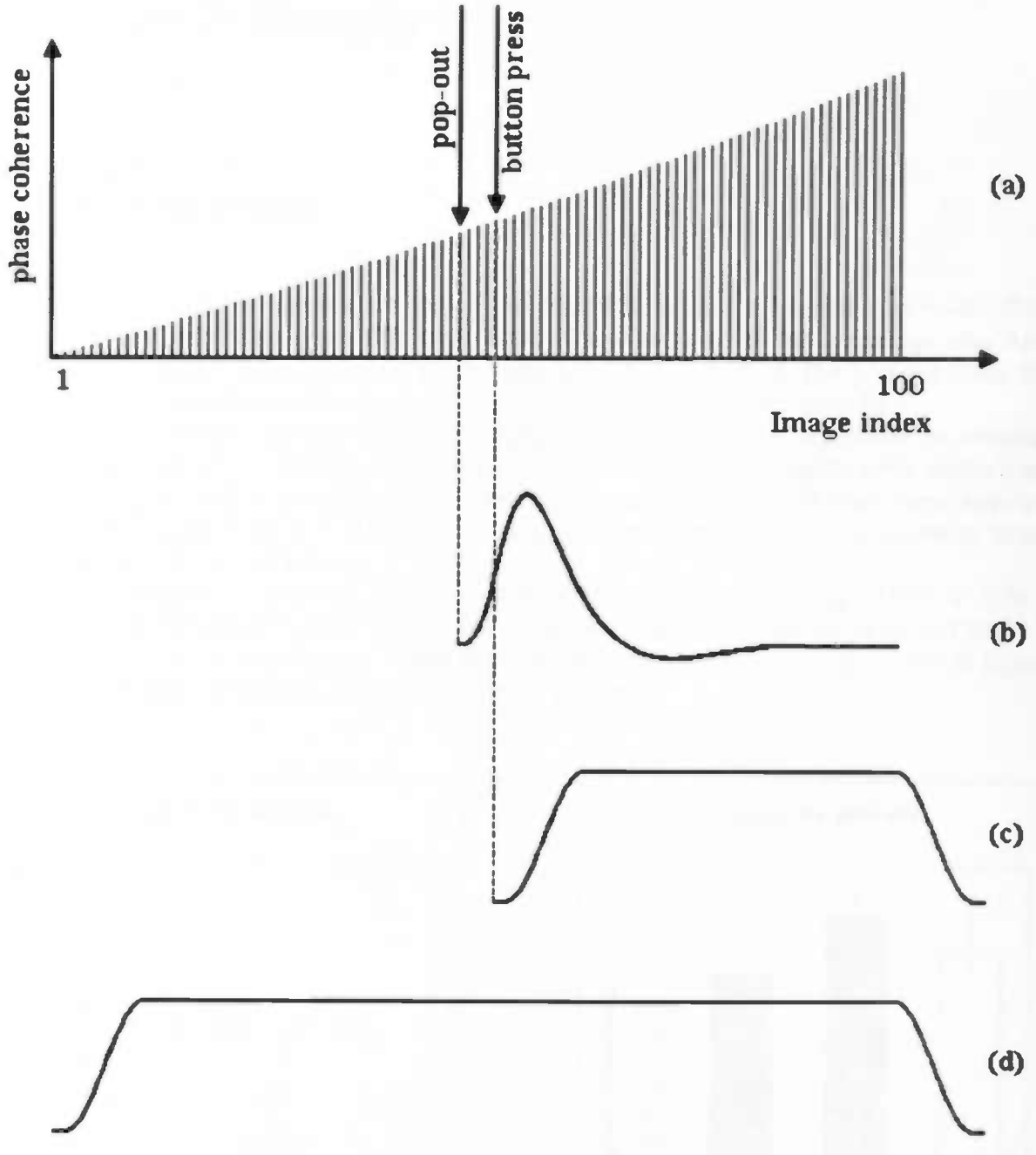

Figure 6.1: The general linear model (GLM) was estimated with three types of regressors. Part (a) of the figure shows the time course of one stimulus sequence. During presentation of the sequence, the amount of stimulus information (i.e. the phase coherence) increases from 0% to 100%. The moment of conscious pop-out and the time of the pop-out button press (which is some time after the moment of pop-out due to the subject's reaction time) are indicated by the two arrows. Condition-dependent brain activation due to the pop-out is modeled with a standard canonical hemodynamic response function (HRF), depicted in part (b). Condition-dependent brain activation during full perception of the stimulus, depicted in part (c), is modeled by a prolonged HRF of variable duration, starting at the pop-out button press and ending at the end of the stimulus sequence. Finally, the regressor shown in part (d) is a prolonged HRF starting at the first and ending at the last picture in the sequence, which models brain activation due to visual stimulation or button presses. Adapted from Reinders et al. (2004).

Chapter 7: Results

7.1. Behavioral data

For healthy controls, the moment of pop-out for fearful faces was on average after 9.40 ± 0.22 s (mean + s.e.m.) from the start of the trial. Neutral faces were perceived on average after 9.60 ± 0.19 s, and houses were perceived on average after 9.33 ± 0.17 s). The pop-out times for fearful faces, neutral faces and houses are depicted in the left panel of figure 7.1.

The moment of pop-out for healthy subjects was significantly dependent on stimulus type, $F(1.475, 36.869) = 5.299$, $p < 0.05$. Fearful faces were detected significantly earlier than neutral faces ($p < 0.05$), although the difference was small (200 ms). Houses were detected earlier than neutral faces ($p < 0.01$). There was no significant difference in response times between fearful faces and houses.

The moment of pop-out for schizophrenia patients was on average 10.21 ± 0.26 s (mean + s.e.m.) for fearful faces, 10.42 ± 0.11 s (mean + s.e.m.) for neutral faces, and 10.30 ± 0.19 s (mean + s.e.m.) for houses. These pop-out times are shown in the right panel of figure 7.1. No significant differences were found for the patients.

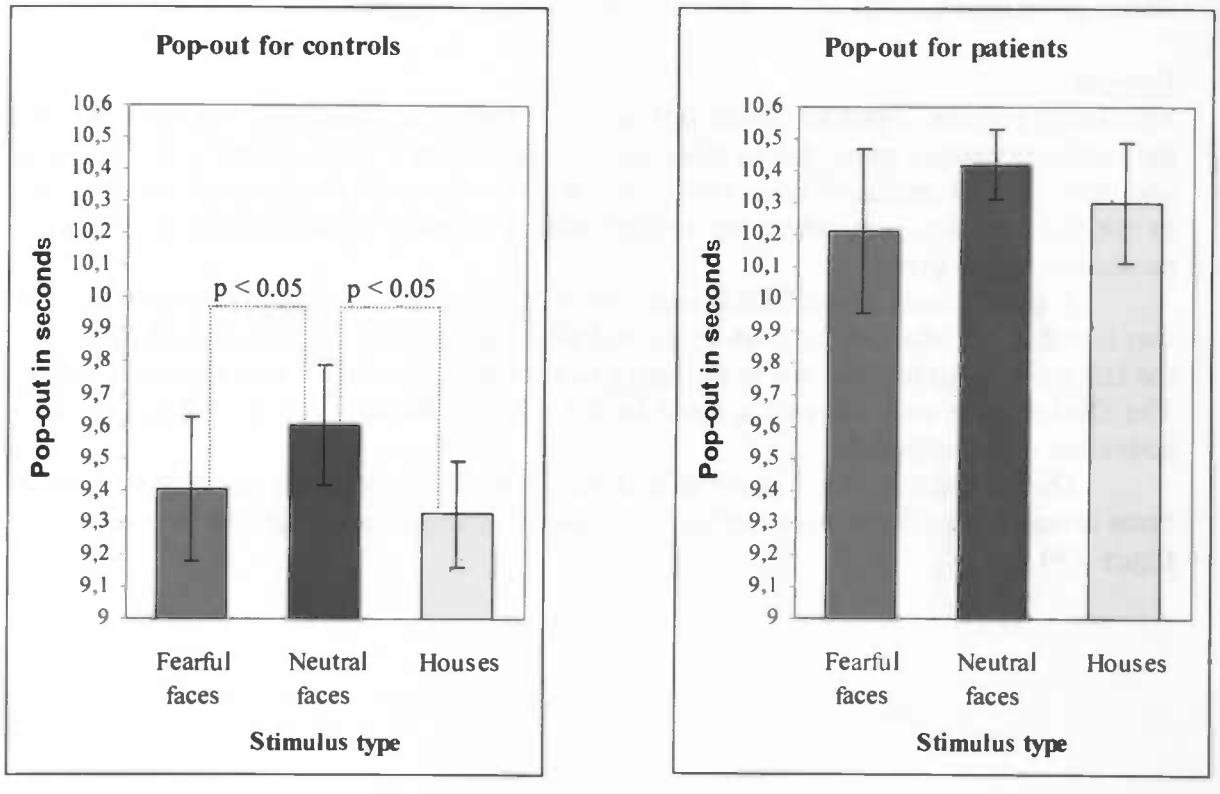

Figure 7.1: The average moment of pop-out (in seconds) for controls (left panel) and patients (right panel). Healthy controls perceived both fearful faces and houses significantly earlier than neutral faces, but there was no significant difference between the pop-out times for fearful faces and houses. Differences between patients and healthy controls, as well as between pop-out times within patients, did not reach significance.

7.2. fMRI data

7.2.1. Healthy controls

Full perception

Results of the fMRI data for healthy controls are summarized in table 7.1 (see page 50). The statistical parametric map (spm) testing for a larger BOLD response for the full perception of houses as compared to the full perception of faces revealed significant brain activation of the parahippocampal gyrus in all three control subjects (see figure 7.2). For subjects one and three, this brain activation was bilateral, whereas for the second subject, the parahippocampal gyrus was activated only in the left hemisphere.

Upon testing for a larger BOLD response for the full perception of faces as compared to houses, brain activation in the fusiform gyrus and amygdala was found in all three subjects (see table 7.1 and figures 7.3 and 7.4). Both the amygdala and the fusiform gyrus were activated bilaterally in two subjects and unilaterally in one subject (the left amygdala and the right fusiform gyrus).

The spm testing for a larger BOLD response for the full perception of fearful faces as compared to neutral faces revealed significant brain activation in the left amygdala of only one of the three subjects (see figure 7.5). For the second subject, no amygdala activation was found for this condition, and in the third subject a trend was found in the left amygdala ($p = 0.133$).

Finally, upon testing for a significant BOLD response during visual stimulation, or in other words, from the beginning to the end of each trial, no significant brain activation in the lateral geniculate nucleus of the thalamus could be determined.

Pop-out

Significant pop-out dependent brain activation for houses as compared to faces was found in the parahippocampal gyrus for all three subjects (see table 7.1 and figure 7.6). Subjects one and three showed unilateral brain activation (subject one in the left hemisphere, subject three in the right hemisphere), while the second subject showed bilateral brain activation in the parahippocampal gyrus.

A significantly larger BOLD response for the pop-out of faces as compared to houses was found in the bilateral fusiform gyrus and bilateral amygdala for the second subject and in the left fusiform gyrus (but not in the amygdala) of the first subject (see figures 7.7 and 7.8). The third subject only showed a trend in the right fusiform gyrus ($p = 0.1$) and no brain activation in the amygdala.

The spm testing for a larger BOLD response for fearful faces as compared to neutral faces revealed significant brain activation in the left amygdala of subjects two and three (see figure 7.9).

7.2.2 Patients with schizophrenia

Results of the fMRI data for schizophrenia patients are summarized in table 7.2 (see page 51). The contrast image of a larger BOLD response for the full perception of houses as compared to the full perception of faces revealed significant brain activation in the right parahippocampal gyrus for patient 1, and in the bilateral parahippocampal gyrus of patient 2 (see figure 7.10). Upon testing for a larger BOLD response for the full perception of faces as compared to the full perception of houses, significant brain activation of the bilateral fusiform gyrus was found in both patients (see figure 7.11), while no brain activation was found in the amygdala of either patient for this condition (unlike healthy controls).

For the pop-out event, patient 1 showed significant brain activation only for the pop-out of houses as compared to the pop-out of faces, in the right parahippocampal gyrus (see figure 7.12). For patient 2, significant brain activation was found in the bilateral parahippocampal gyrus for the pop-out of houses as compared to the pop-out of faces (see figure 7.12). For the pop-out of faces as compared to the pop-out of houses, we found significant brain activation in the right fusiform gyrus (see figure 7.13). Upon testing for pop-out dependent brain activation for fearful faces as compared to pop-out dependent brain activation for neutral faces, significant brain activation of the bilateral amygdala was found (see figure 7.14). Finally, equal to the controls, upon testing for a significant BOLD response during visual stimulation no significant brain activation in the lateral geniculate nucleus of the thalamus was revealed.

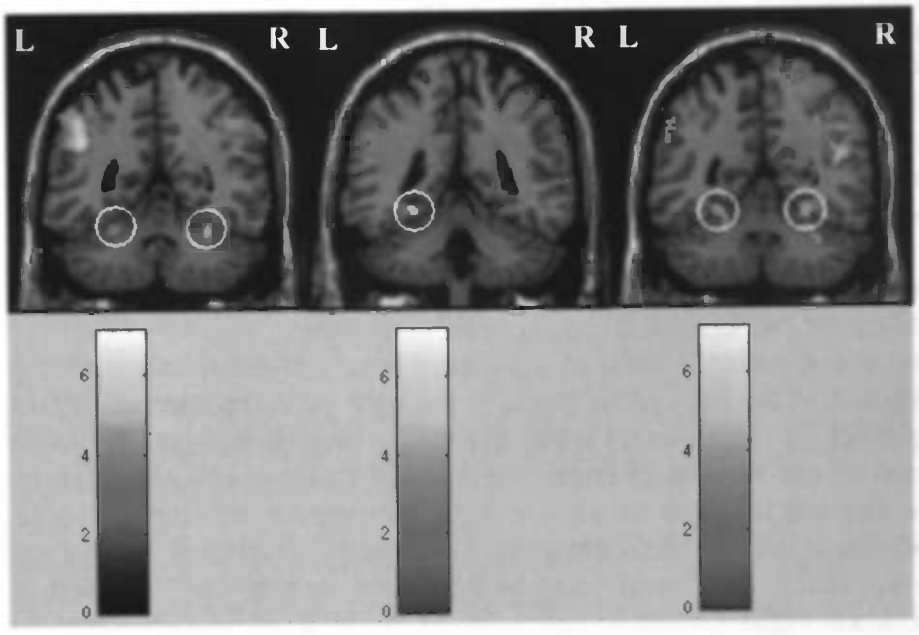

Figure 7.2: Brain activation in the parahippocampal gyrus due to the full perception of houses as compared to the full perception of faces, for subject 1 (left panel), subject 2 (middle panel) and subject 3 (right panel). Brain activation is shown on coronal slices with y = -50, -44 and -51, respectively. *t* values for each picture are indicated by the color bars.

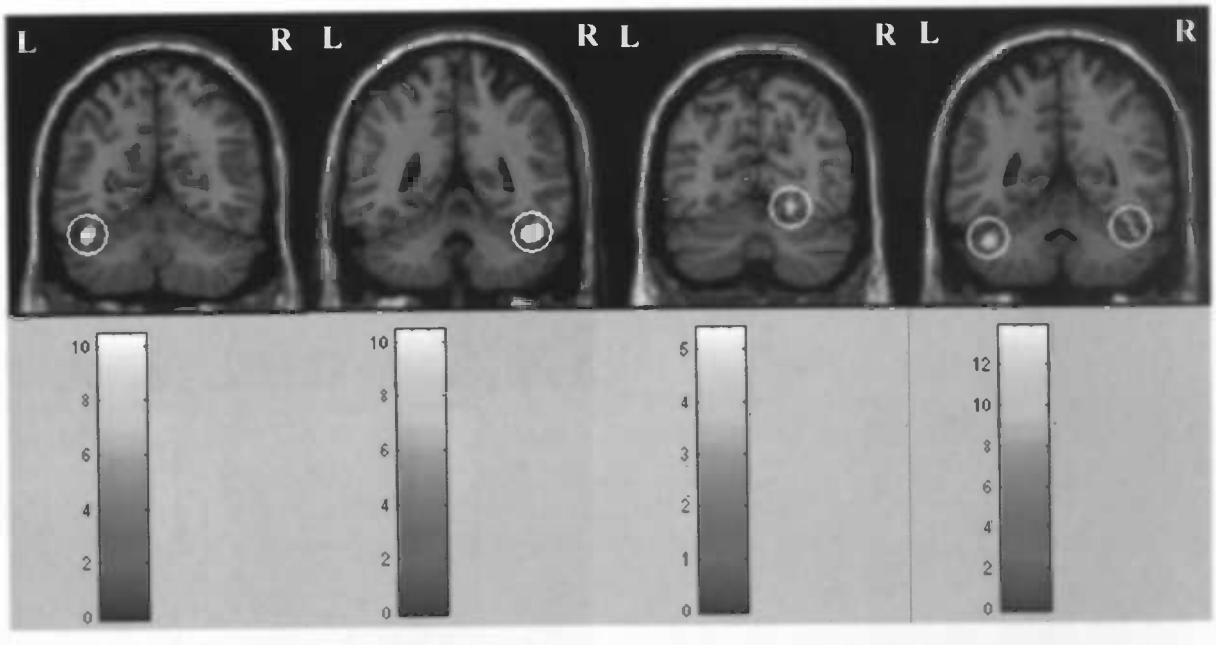

Figure 7.3: Brain activation in the fusiform gyrus due to the full perception of faces as compared to the full perception of houses, for subject 1 (left and middle left panel), subject 2 (middle right panel) and subject 3 (right panel). Brain activation is shown on coronal slices with y = -57, -46, -68 and -49, respectively. Brain activation for subject 1 in the left hemisphere is slightly posterior to brain activation in the right hemisphere, resulting in two coronal slices with different y-coordinates for subject 1. *t* values for each picture are indicated by the color bars.

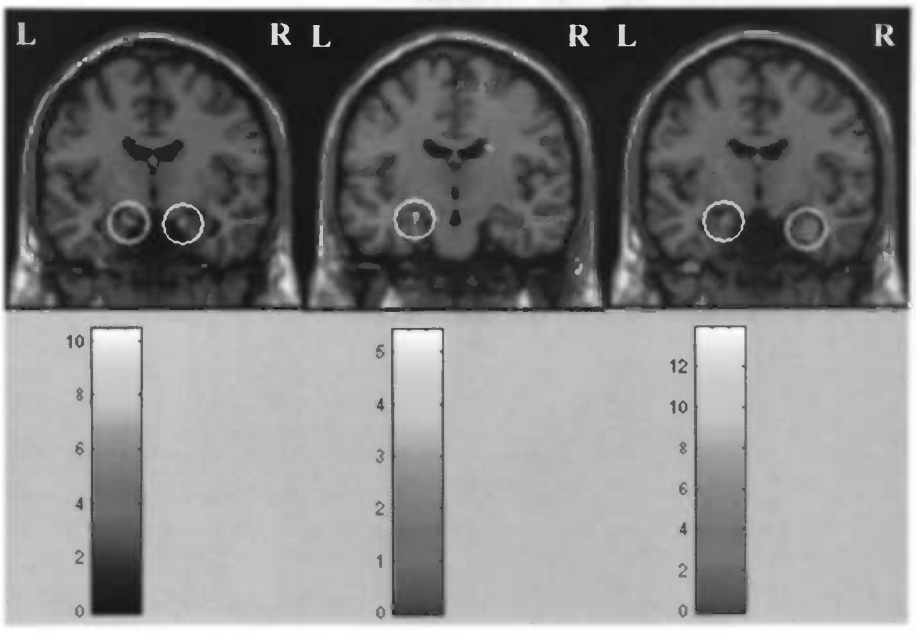

Figure 7.4: Brain activation in the amygdala due to the full perception of faces as compared to the full perception of houses, for subject 1 (left panel), subject 2 (middle panel) and subject 3 (right panel). Brain activation is shown on coronal slices with y = -8, -13, -8, respectively. *t* values for each picture are indicated by the color bars.

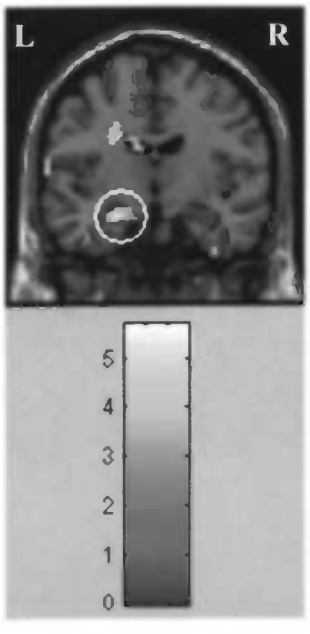

Figure 7.5: Brain activation in the amygdala due to the full perception of fearful faces as compared to the full perception of neutral faces, for subject 1. Brain activation is shown on a coronal slice with y = -10. *t* values are indicated by the color bar.

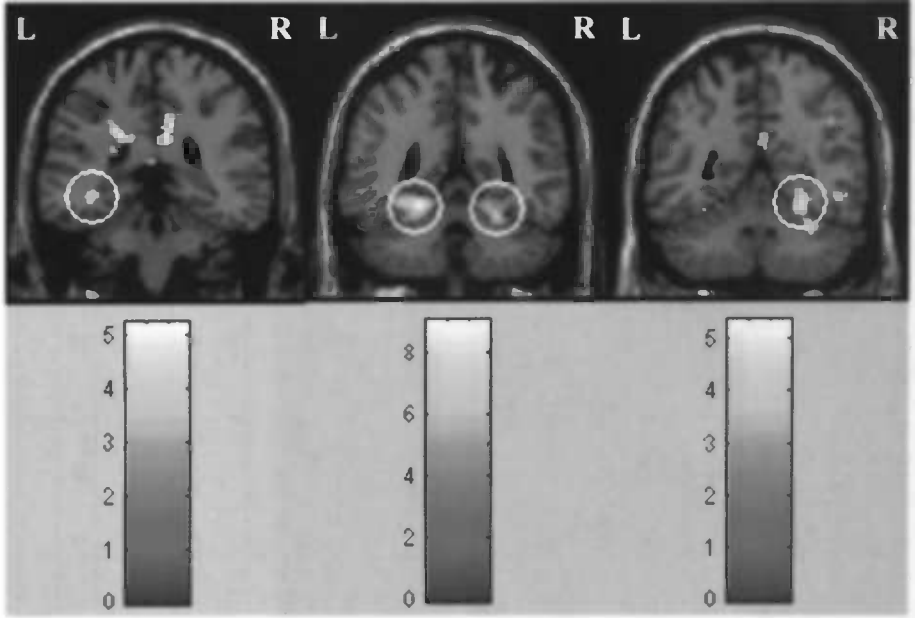

Figure 7.6: Brain activation in the parahippocampal gyrus due to the detection (pop-out) of houses as compared to the detection of faces, for subject 1 (left panel), subject 2 (middle panel) and subject 3 (right panel). Brain activation is shown on coronal slices with y = -36, -46 and -52, respectively. *t* values for each picture are indicated by the color bars.

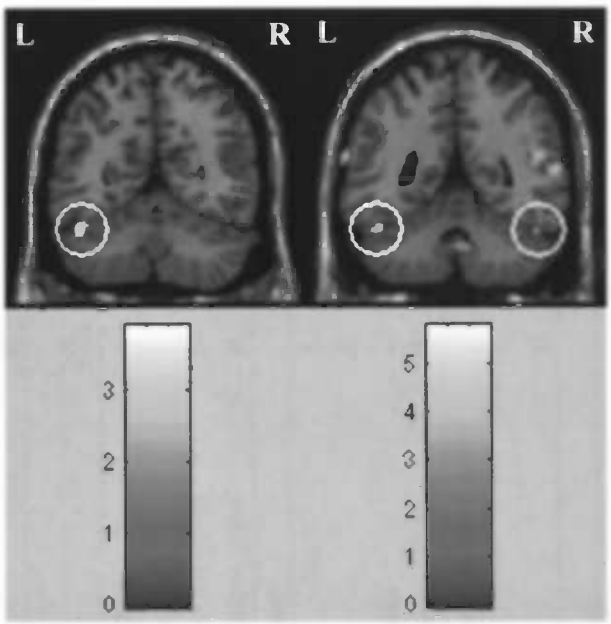

Figure 7.7: Brain activation in the fusiform gyrus due to the detection (pop-out) of faces as compared to the detection of houses, for subject 1 (left panel) and subject 2 (right panel). Brain activation is shown on coronal slices with y = -58 and -49 respectively. *t* values for each picture are indicated by the color bars.

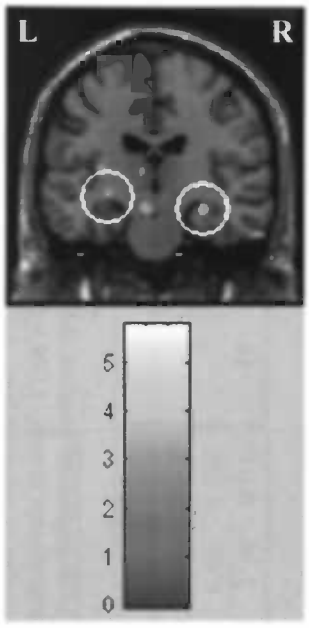

Figure 7.8: Brain activation in the amygdala due to the detection (pop-out) of faces as compared to the detection of houses for subject 2. Brain activation is shown on a coronal slice with y = -18. *t* values are indicated by the color bar.

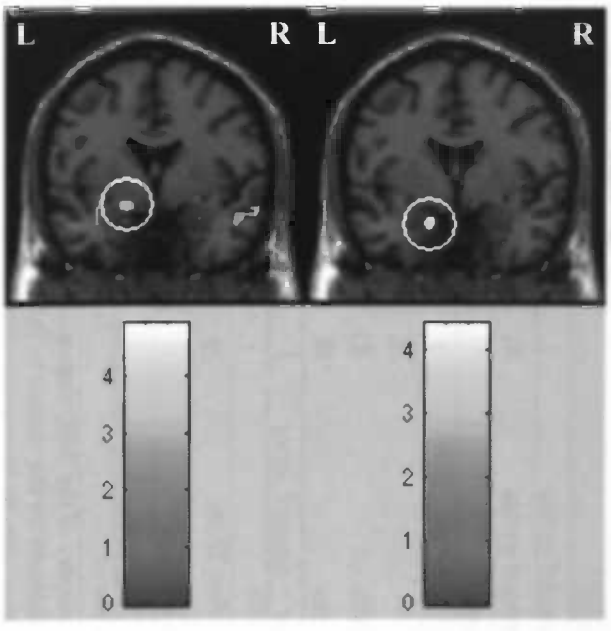

Figure 7.9: Brain activation in the amygdala due to the detection (pop-out) of fearful faces as compared to the detection of neutral faces for subject 2 and subject 3. Brain activation is shown on two coronal slices with y = 0. *t* values for each picture are indicated by the color bars.

		Subject 1					Subject 2					Subject 3				
Brain area	**L/R**	**x**	**y**	**z**	***t***	p_{corr}	**x**	**y**	**z**	**t**	p_{corr}	**x**	**y**	**z**	***t***	p_{corr}
Full perception																
Houses > faces																
Parahippocampal gyrus	L	-28	-50	-24	3.76	0.000	-30	-42	-12	6.13	0.000	-26	-56	-16	4.97	0.000
Parahippocampal gyrus	R	30	-46	-24	5.81	0.015			n.s.			24	-48	-18	5.26	0.000
Faces > houses																
Amygdala	L	-16	-4	-18	6.16	0.000	-24	-12	-16	3.26	0.045	-20	-8	-20	3.28	0.046
Amygdala	R	18	-10	-20	5.39	0.005			n.s.			32	-8	-26	5.06	0.035
Fusiform gyrus	L	-42	-58	-24	9.91	0.000			n.s.			-44	-50	-34	10.28	0.000
Fusiform gyrus	R	48	-46	-26	10.44	0.000	18	-68	-10	3.66	0.000	44	-50	-26	7.23	0.000
Fearful faces > neutral faces																
Amygdala	L	-22	-12	-18	5.03	0.000			n.s.			-16	-4	-14	2.84	0.133
Amygdala	R			n.s.					n.s.					n.s.		
Pop-out																
Houses > faces																
Parahippocampal gyrus	L	-38	-36	-8	4.12	0.004	-22	-46	-14	9.06	0.000			n.s.		
Parahippocampal gyrus	R			n.s.			20	-44	-15	5.65	0.000	28	-52	-10	4.81	0.000
Faces > houses																
Amygdala	L			n.s.			-28	-18	-6	3.31	0.040			n.s.		
Amygdala	R			n.s.			30	-16	-14	4.18	0.002			n.s.		
Fusiform gyrus	L	-44	-58	-24	3.58	0.025	-48	-48	-26	4.02	0.008			n.s.		
Fusiform gyrus	R			n.s.			50	-48	-26	2.59	0.191	20	-62	-14	3.21	0.100
Fearful faces > neutral faces																
Amygdala	L			n.s.			-18	0	-10	3.36	0.035	-16	0	-24	4.43	0.001
Amygdala	R			n.s.					n.s.					n.s.		
General perception																
LGN of the thalamus				n.s.					n.s.					n.s.		

Table 7.1: Summary of the fMRI data results, with coordinates presented in MNI space. t values are presented under 1190 degrees of freedom. All p values are corrected for multiple comparisons for the volume of interest (p_{corr}, see section 6.7). L/R = left or right hemisphere; (x,y,z) = MNI coordinates in mm; LGN = Lateral geniculate nucleus; * = not significant after multiple comparisons correction, only reported because of significant (controlateral) brain activation in other subjects. n.s. = not significant.

		Patient 1					Patient 2				
Brain area	**L/R**	**x**	**y**	**z**	***t***	p_{corr}	**x**	**y**	**z**	**t**	p_{corr}
Full perception											
Houses > faces											
Parahippocampal gyrus	L			n.s.			-28	-52	-6	9.04	0.000
Parahippocampal gyrus	R	22	-56	-12	7.35	0.000	32	-60	-6	6.60	0.000
Faces > houses											
Amygdala	L			n.s.					n.s.		
Amygdala	R			n.s.					n.s.		
Fusiform gyrus	L	-42	-64	-26	10.10	0.000	-44	-58	-24	12.48	0.000
Fusiform gyrus	R	42	-66	-22	9.68	0.000	40	-46	-30	7.91	0.000
Fearful faces > neutral faces											
Amygdala	L			n.s.					n.s.		
Amygdala	R			n.s.					n.s.		
Pop-out											
Houses > faces											
Parahippocampal gyrus	L			n.s.			-26	-40	-8	7.49	0.000
Parahippocampal gyrus	R	24	-58	-12	5.22	0.015	28	-42	-6	6.76	0.000
Faces > houses											
Amygdala	L			n.s.					n.s.		
Amygdala	R			n.s.					n.s.		
Fusiform gyrus	L			n.s.					n.s.		
Fusiform gyrus	R			n.s.			36	-52	-20	6.98	0.000
Fearful faces > neutral faces											
Amygdala	L			n.s.			-14	-6	-14	4.16	0.003
Amygdala	R			n.s.			14	-10	-16	3.63	0.016
General perception											
LGN of the thalamus				n.s.					n.s.		

Table 7.2: Summary of the fMRI data results, with coordinates presented in MNI space. t values are presented under 1190 degrees of freedom. All p values are corrected for multiple comparisons for the volume of interest (p_{corr}, see section 6.7). L/R = left or right hemisphere; (x,y,z) = MNI coordinates in mm; LGN = Lateral geniculate nucleus; * = not significant after multiple comparisons correction, only reported because of significant (controlateral) brain activation in other subjects.

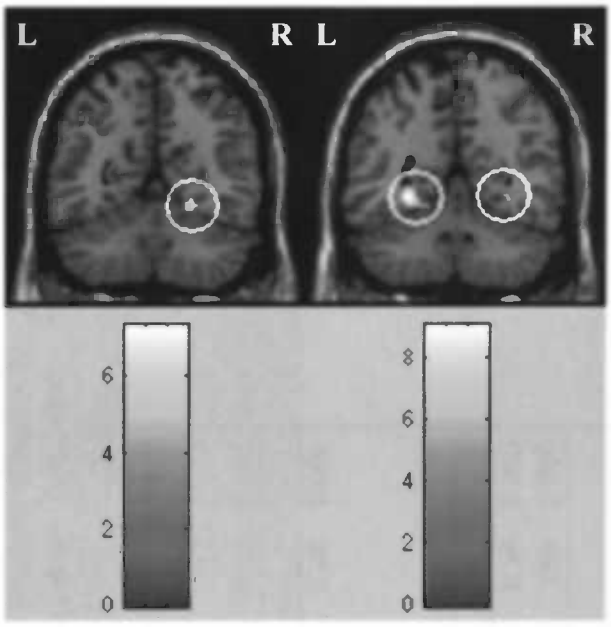

Figure 7.10: Brain activation in the parahippocampal gyrus due to the full perception of houses as compared to the full perception of faces, for patient 1 (left panel) and patient 2 (right panel). Brain activation is shown on coronal slices with y = -56, and -52, respectively. *t* values for each picture are indicated by the color bars.

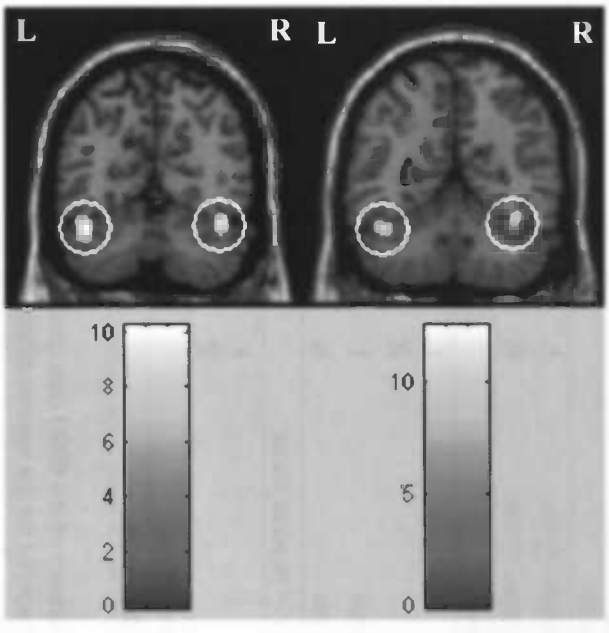

Figure 7.11: Brain activation in the fusiform gyrus due to the full perception of faces as compared to the full perception of houses, for patient 1 (left panel) and patient 2 (right panel). Brain activation is shown on coronal slices with y = -64 and -55, respectively. *t* values for each picture are indicated by the color bars.

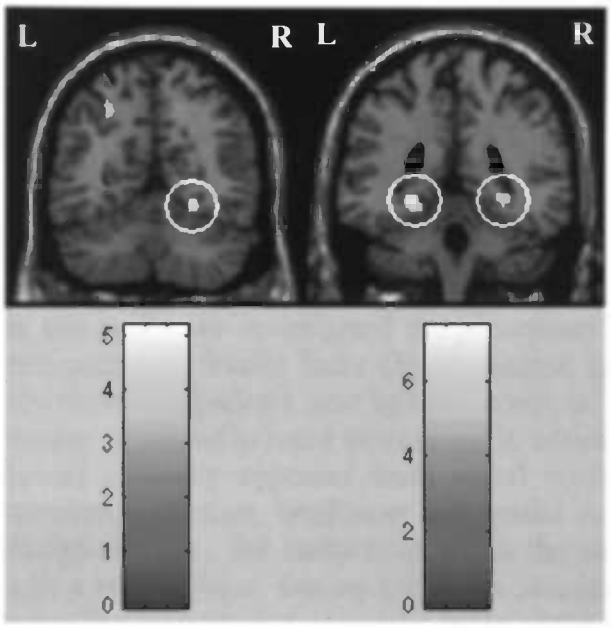

Figure 7.12: Brain activation in the parahippocampal gyrus due to the detection (pop-out) of houses as compared to the detection of faces, for patient 1 (left panel) and patient 2 (right panel). Brain activation is shown on coronal slices with y = -58 and -40, respectively. *t* values for each picture are indicated by the color bars.

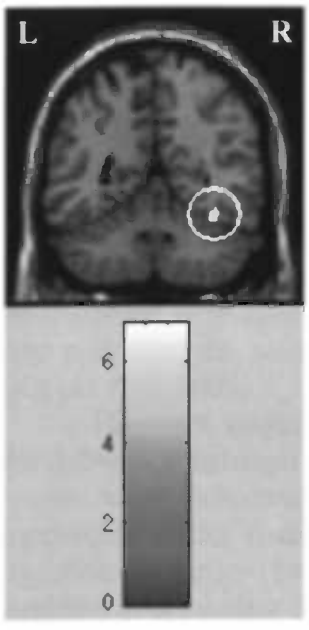

Figure 7.13: Brain activation in the fusiform gyrus due to the detection (pop-out) of faces as compared to the detection of houses for patient 2. Brain activation is shown on a coronal slice with y = -52. *t* values are indicated by the color bar.

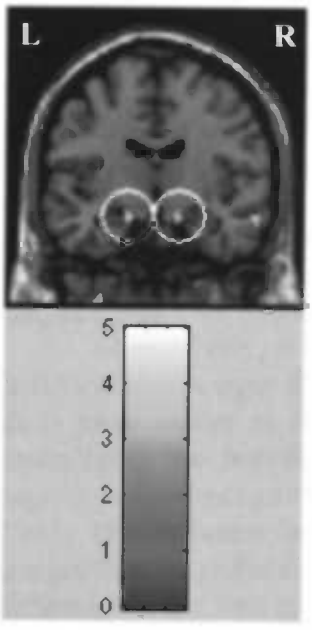

Figure 7.14: Brain activation in the amygdala due to the detection (pop-out) of fearful faces as compared to the detection of neutral faces for patient 2. Brain activation is shown on a coronal slice with y = -10. *t* values are indicated by the color bar.

Chapter 8: Discussion

8.1. Introduction

In this study, we investigated the perception of stimuli with different degrees of biological relevance, i.e. fearful faces (high), neutral faces (intermediate) and houses (low), in both schizophrenia patients and healthy controls. Subjects were presented with a sequence of images presented in rapid succession, in which the stimulus (a fearful face, a neutral face or a house) gradually appeared from visual noise. All stimuli were color images matched or luminance, contrast, brightness and spatial frequency information. The moment of stimulus recognition (i.e., the moment at which the stimulus "pops out" of the noise) was indicated with a button press. During the entire stimulus sequence, a fixation dot that changed color every few seconds was presented in the centre of the screen. Subjects were instructed to focus on the fixation dot during the pop-out task and press a button every time the dot changed color, in order to keep the subjects' attention in the centre of the screen.

The times of the pop-out button presses were adjusted for reaction time (see chapter 6), to obtain a more accurate estimate of the moment of pop-out. We examined condition-dependent brain activation patterns during both the moment of pop-out (i.e. the response time adjusted for reaction time) and full perception (i.e. the time from the pop-out button press until the end of the stimulus sequence).

8.2. The amygdala as part of a robust threat-detection circuit

8.2.1 Behavioral data

In accordance with our hypothesis, the behavioral data show that fearful faces are perceived earlier than neutral faces. Fearful faces were perceived 200 ms earlier than neutral faces, which is in agreement with the results of Reinders et al. (2005), who found a difference in response times of 240 ms between fearful faces and neutral faces. This finding supports the notion of a fast, subcortical amygdala pathway in which information concerning the environment is relayed through the thalamus directly to the amygdala (Morris et al. 1999), thus providing the possibility to initiate rapid behavioral responses to environmental threats (Knight et al. 2005).

However, contrary to our hypothesis, houses were perceived earlier than faces. While the difference between the detection times of fearful faces and houses was not significant, houses were perceived significantly earlier (270 ms) than neutral faces. This finding contradicts earlier findings of Reinders et al (2005), who found that faces were perceived significantly earlier (240 ms) than houses. Since we used the same paradigm as the study of Reinders et al., except for the fact that we used different face stimuli and color images instead of grayscale images, the difference in results is probably due to differences between the stimuli used in the two studies. Two possible scenarios may explain the present findings.

First, the change from grayscale to color images may have benefited house recognition more than face recognition. House stimuli activate the parahippocampal gyrus (i.e. the parahippocampal place area, or PPA) that is believed to be involved in visual processing of scenes and spatial layout, but not objects (Epstein & Kanwisher 1998; Epstein et al. 1999). Houses may therefore not be experienced as objects, but as landmarks that help define the spatial layout of a scene (Epstein & Kanwisher 1998; Epstein et al. 1999). Color images of scenes are recognized faster than grayscale images (Gegenfurtner & Rieger 2000; Steeves et al. 2004). Thus, since houses and faces are processed in distinctly different ways, it is possible that recognition of houses benefits more from color images than recognition of faces.

Alternatively, it is possible that both house and face stimuli are generally recognized faster in color images than in grayscale images, but that the face stimuli used for the current study were harder to recognize than those from the study of Reinders et al. (2005), thus neutralizing the beneficial color effect for our face stimuli. Usually, when stimuli are degraded, face recognition is better in color images than in grayscale images (Yip & Sinha 2002). This indicates that faces, as well as houses, can be recognized with more noise in color images than in grayscale images. Therefore, it is more likely that our findings are caused by a difference in the face stimuli, e.g. less artificial, more life-like and including hair.

Whatever the cause, the results indicate that there are more factors influencing the robustness of stimulus recognition than just the amount of stimulus information in the image. Although faces may be emotionally more salient (because they are biologically more relevant) than houses, houses may be more salient in another dimension, for example shape (i.e., sharp corners may cause more salient contrasts with the background than an oval shape, and this difference may be more pronounced in color images than in grayscale images). This means that the hypothesis that biologically relevant information can be detected more robustly than biologically irrelevant information can only be tested with stimuli that are matched for salience in other dimensions, such as simple shape. However, it would be preferable to use a control stimulus that activates a specific area of the brain distinct from the fusiform face area (like the parahippocampal gyrus for houses), because stimulus-specific brain activation gives an objective control measure for stimulus recognition (apart from the button press, which is not stimulus-specific). This is an interesting challenge for future research.

8.2.2 fMRI data

Although more data need to be analyzed to reach a more solid conclusion, the fMRI data analyzed so far do seem to support our hypotheses. The data show stimulus-dependent brain activation patterns consistent with previous studies. For both the moment of pop-out and full perception, house stimuli caused brain activation in the parahippocampal gyrus (Epstein & Kanwisher 1998; Epstein et al. 1999). Face-specific brain activation during both the pop-out and full perception was found in the fusiform gyrus (Kanwisher et al. 1997; Kanwisher et al. 1999) and the amygdala (Breiter et al. 1996; Morris et al. 1998; Reinders et al. 2005). Furthermore, brain activation in the amygdala was found for both the pop-out and full perception comparisons of fearful faces to neutral faces (Morris et al. 1996; Morris et al. 1998; Reinders et al. 2005).

We did not find significant brain activation in the lateral geniculate nucleus of the thalamus during the trials. This might be explained by the fact that this nucleus is quite small and does not easily yield significant results. Alternatively, it may very well be that this nucleus is activated at all times when an individual perceives the environment, which implies that it was activated during the entire experiment, including the breaks between trials. Further analysis of the data may resolve this question. Nevertheless, the behavioral and fMRI data do support the hypothesized subcortical amygdala pathway. Fearful faces caused stronger

activation in the amygdala and were recognized with more noise than neutral faces, indicating that the amygdala is capable of robust processing of biologically relevant stimuli such as fearful faces (Morris et al. 1996; Morris et al. 1998). In sum, since all but one of the brain areas for which we had *a priori* hypotheses were activated by the stimuli in the way we expected, we conclude that the data analyzed are in support of our hypotheses. We expect that a group analysis of the data of the remaining subjects will counterbalance individual differences in support of our hypotheses.

8.3. The amygdala in schizophrenia

The first point of attention when looking at the behavioral data of the schizophrenia patients is that patients were generally slower to respond, even after the response times had been corrected for reaction time. This may point to impaired attention or impaired executive function that is more pronounced in tasks requiring sustained attention (for more than several seconds, such as the pop-out task). Executive function and attention are associated with the prefrontal lobes (Andrewes 2001), and patients with schizophrenia have been found to have structural abnormalities in the prefrontal lobe (Sanfilipo et al. 2000; Sigmundsson et al. 2001; Wible et al. 2001). A recent study investigating selective attention and executive function in schizophrenia showed that schizophrenia patients were initially able to attend to auditory stimuli but failed to sustain selective attention (Mathalon et al. 2004), which may account for the present findings.

Apart from the slower responses, the behavioral data of the schizophrenia patients show a trend comparable with the pattern of pop-out times as that of healthy controls, although little data are available to reach solid conclusions. Given that patients with schizophrenia are capable of perceiving fearful faces earlier than neutral faces, like healthy controls, it seems that the function of the subcortical amygdala pathway seems to be normal. However, the fMRI data does not support this conclusion. Patient 1 did not show any amygdala activation for any condition, while patient 2 did have brain activation in the amygdala, but only during the pop-out of fearful faces when compared to the pop-out of neutral faces. In other words, the behavioral data seem to be in accordance with normal amygdala functioning while the fMRI data might indicate deviant functioning of the amygdala.

When looking at the individual differences between the two patients, the discrepancy seems to be resolved. The first patient, who did not show any amygdala activation, perceived fearful faces on average after 10,47 seconds, neutral faces on average after 10,53 seconds, and houses on average after 10,49 seconds. In other words, this patient did not perceive fearful faces earlier than neutral faces, and did not activate the amygdala. In contrast, the second patient perceived fearful faces on average after 9,96 seconds, neutral faces on average after 10,31 seconds, and houses on average after 10,11 seconds. This patient did show bilateral amygdala activation during the pop-out of fearful faces as compared to the pop-out of neutral faces, as well as faster detection of fearful faces than neutral faces.

These findings indicate that schizophrenia patients may be differentially impaired in their amygdala function. This may explain the inconsistent findings of neuroimaging studies investigating the role of the amygdala in schizophrenia (Gur et al. 2000; Wright et al. 2000; Hulshoff Pol et al. 2001; Narr et al. 2001; Steel et al. 2002; Kucharska-Pietura et al. 2003; Exner et al. 2004, see also section 4.3). In addition, in a review of both structural and

functional neuroimaging studies investigating temporal lobe structures (including the amygdala) in schizophrenia, Zakzanis and colleagues suggest that there may be differential impairment of temporal function for different subtypes of schizophrenia (Zakzanis et al. 2000).

Since the amygdala has been associated with facial affect processing, it is likely that the same theory holds for facial affect recognition in schizophrenia. For example, chronicity of illness has been found to be correlated to impaired facial affect recognition (Mueser et al. 1996), and paranoid schizophrenia patients are reported to perform better on facial affect recognition tasks than nonparanoid schizophrenia patients (Lewis & Garver 1995). Unfortunately, we did not test the performance of the participating patients on a facial affect recognition task. To resolve the issue of the role of the amygdala in facial affect recognition in schizophrenia, patients should also be tested for their performance on facial affect recognition. If the facial affect recognition deficit in schizophrenia patients is related to impaired functioning of the amygdala, there may be considerable individual differences for facial affect recognition as well.

In conclusion, the deficit of facial affect recognition observed in patients with schizophrenia may be related to abnormal functioning of the amygdala, but there may be considerable differences between individuals exhibiting different characteristics of the disease. Data from more patients are needed to test this hypothesis.

8.4. Conclusion

Evidence was found in both the behavioral data and the fMRI data for the hypothesized fast subcortical amygdala pathway that provides the amygdala with coarse information of the environment in order to rapidly detect environmental threats. In addition, the behavioral data indicated that the amygdala may process biologically relevant information more robustly than biologically irrelevant information, through a subcortical pathway that enables immediate behavioral reactions to environmental threats.

From the data of the schizophrenia patients, we conclude that there may be a relationship between facial affect recognition and deviant functioning of the amygdala. However, since one of the patients seemed to exhibit deviant amygdala function while the other did not, or at least not severely, it seems likely that there are considerable differences in facial affect recognition and amygdala function between individuals exhibiting different characteristics of the disease. These issues provide interesting objectives for further research.

PART IV

APPENDICES

Appendix A: Stimulus Selection

A.1. Introduction

For the fMRI experiment, pictures of houses, neutral faces and fearful faces were needed. The house pictures were taken from European houses of light color (see also Reinders et al. 2005), whereas the face pictures were drawn from the Karolinska Directed Emotional Faces set (Lundqvist et al. 1998).

Many studies on facial affect recognition use stimuli from the pictures of facial affect (Ekman & Friesen 1976), for example (Adolphs et al. 1994; Young et al. 1996; Morris et al. 1998; Whalen et al. 1998; Morris et al. 1999; Reinders et al. 2005). The pictures of this set have been validated by extensive research (Ekman et al. 1972; Ekman & Friesen 1975), and have been the standard set of pictures for research on facial affect ever since. However, there are some drawbacks to using these pictures. Firstly, the pictures are grayscale, while color images would be more realistic. Secondly, because the set of Ekman and Friesen is the standard, these pictures have been used for an overwhelming amount of studies. At some point, even though the pictures have been validated extensively, it becomes questionable whether the conclusions of all of those studies can be generalized to theories on facial affect, since they all used the same data set.

For these two reasons, we chose not to use the set of Ekman and Friesen. An alternative set of facial affect pictures was the KDEF set, which is also used by Vuilleumier and colleagues (Vuilleumier et al. 2003). This set contains color pictures of 70 individuals (35 male, 35 female), each displaying seven different emotions. The expressions were photographed from five different angles: full left profile, half left profile, front view, half right profile and full right profile. Each emotion was displayed and photographed twice, resulting in two series of five pictures of each expression. In total, the set contains 4900 pictures.

Although these pictures have been used for other studies (Vuilleumier et al. 2003), no validation (i.e., rating) study of these pictures has been published as yet. Therefore, we rated the front view pictures of neutral, fearful and happy faces of the set, in order to select the best pictures for our experiment. The happy faces were rated as a reserve, although eventually they were not used in the fMRI experiment. For the experiment, 40 (20 neutral, 20 fearful) front view face pictures were needed, approximately half male, half female.

In order to select the best face pictures from the set, two rating sessions were held, in which subjects had to rate the expressions of the neutral, fearful and happy faces. In the first session, the two front view pictures of each face were presented to the subjects simultaneously, and the subjects were to choose which of them displayed the expression best. The pictures that were rated highest in this session were used for the second session, where only one face picture was presented at a time. In the second session, the subjects were to rate the intensity and genuineness of the displayed emotion.

A.2. Session 1

A.2.1. Stimulus presentation procedure

The procedure was carried out in one session, with a group of 25 subjects (10 male, 15 female) between 21 and 55 years of age. Subjects were not allowed to deliberate during the session. The subjects were shown a slideshow of the face pictures, with on each slide the two front view pictures of one face displaying the same emotion. An example is shown in figure A.1. The faces were presented in three blocks: one for neutral faces, one for fearful faces and one for happy faces (in that order). Neutral faces were presented first, so that subjects could use these as a reference when rating the intensity of the emotional faces.

Happy faces were presented last because they were considered to be the easiest (based on pilot rating sessions) and would suffer the least from fatigue. For each block, subjects were given a form on which they could note their answers. Instructions were both printed on the forms and given verbally before each block.

The order of the faces within blocks was randomized for each block. Each slide was presented for approximately 30 seconds, or until all subjects indicated they had finished. For each slide, subjects had to indicate which of the two face pictures depicted the emotion (or lack of emotion, in the case of neutral faces) best, by marking their choice on the form and writing down why they thought the chosen face was better (see figure A.2).

A.2.2. Analysis and results

For each pair of the faces of each emotion, the subjects' answers on the forms were scored on a scale from one to five, where "A++" (see figure A.2) was scored as one and "B++" was scored as five. The mean and standard deviation of these scores were then computed in order to select the better of the two pictures of each face. Since the standard deviations of all scores were within a normal range, only the average scores were used to select the better of the two faces. For faces with an average score lower than 3, face A was chosen, and for faces with an average score higher than 3, face B was chosen. If the score was 3.0, the face that had fewer negative and/or more positive remarks was chosen.

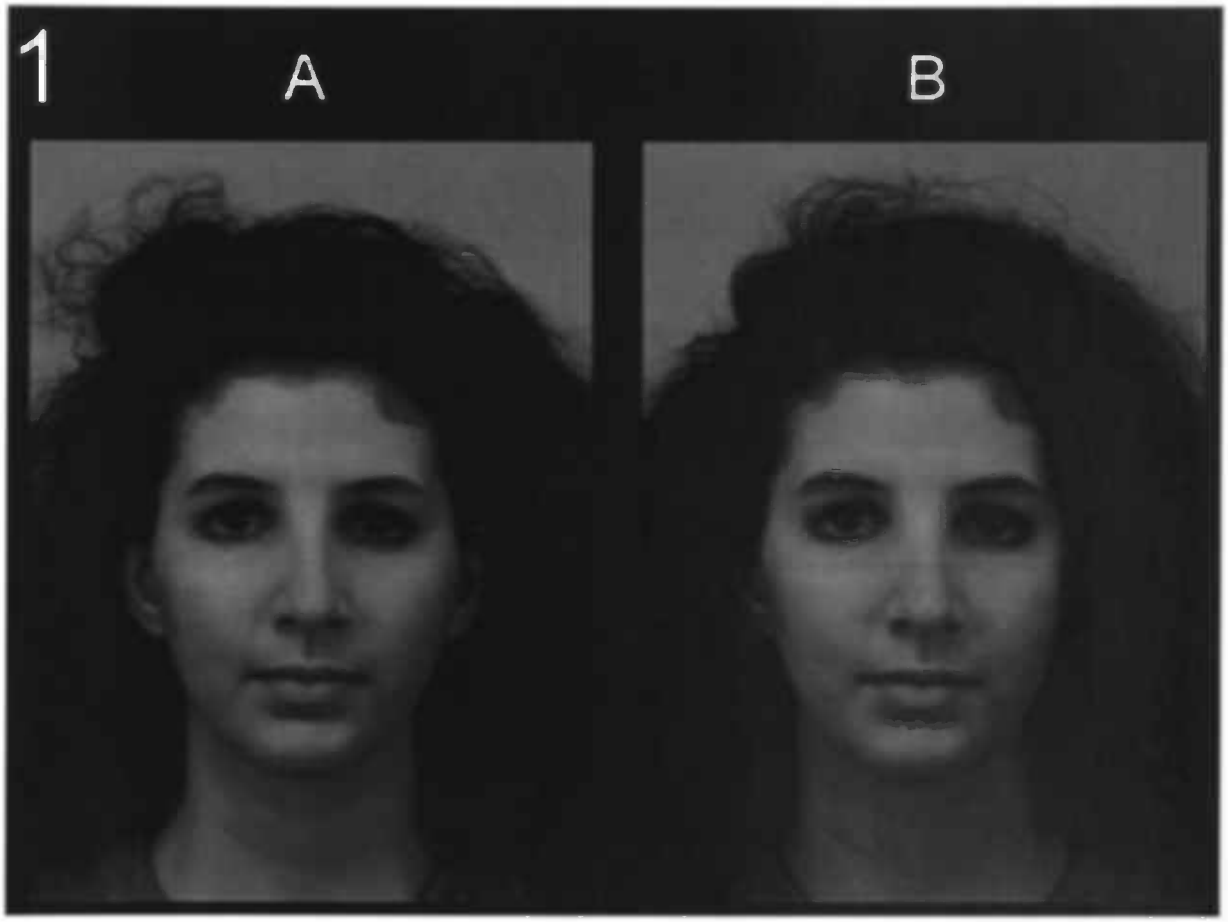

Figure A.1: An example of the stimuli used in session 1. Subjects had to indicate which one of the two faces (A, B or both/neither) depicted the emotion (in this case a neutral face) best.

Geef van elke dia aan welk van de 2 gezichten het beste een neutrale gezichtsuitdrukking weergeeft
door middel van het plaatsen van een kruisje in 1 van de volgende 5 kolommen

A++ = gezicht A is veel neutraler dan gezicht B
A+ = gezicht A is enigszins neutraler dan gezicht B
0 = beide gezichten zijn even neutraal
B+ = gezicht B is enigzins neutraler dan gezicht A
B++ = gezicht B is veel neutraler dan gezicht A

Geef daarnaast aan waarom je het gekozen gezicht neutraler vindt: welke emotie(s) zie je in het andere gezicht?

	A ++	A +	0	B +	B ++	waarom?
1						
2						
3						
4						
5						

Geef van elke dia aan welk van de 2 gezichten de emotie Angst het beste weergeeft,
door middel van het plaatsen van een kruisje in 1 van de volgende 5 kolommen
A++ = gezicht A geeft de emotie Angst veel beter weer dan gezicht B
A+ = gezicht A geeft de emotie Angst enigszins beter weer dan gezicht B
0 = beide gezichten geven de emotie Angst even goed weer
B+ = gezicht B geeft de emotie Angst enigszins beter weer dan gezicht A
B++ = gezicht B geeft de emotie Angst veel beter weer dan gezicht A

Geef daarnaast aan waarom je het gekozen gezicht beter vindt,
met een kruisje in **één of meerdere** van de volgende kolommen:
In de kolom **intensiteit** als je de Angst van het gekozen gezicht intenser vindt
In de kolom **echtheid** als je de Angst van het gekozen gezicht echter vindt,
d.w.z. minder gespeeld / nep dan bij het andere gezicht
In de kolom **anders**, namelijk.. eventuele andere redenen voor je keuze:
zie je bijvoorbeeld andere emoties dan Angst?

	A ++	A +	0	B +	B ++	waarom? intensiteit	echtheid	anders, namelijk...
1								
2								
3								
4								
5								

Geef van elke dia aan welk van de 2 gezichten de emotie Blijdschap het beste weergeeft,
door middel van het plaatsen van een kruisje in 1 van de volgende 5 kolommen
A++ = gezicht A geeft de emotie blijdschap **veel beter** weer dan gezicht B
A+ = gezicht A geeft de emotie blijdschap **enigszins beter** weer dan gezicht B
0 = beide gezichten geven de emotie blijdschap **even goed** weer
B+ = gezicht B geeft de emotie blijdschap **enigszins beter** weer dan gezicht A
B++ = gezicht B geeft de emotie blijdschap **veel beter** weer dan gezicht A

Geef daarnaast aan waarom je het gekozen gezicht beter vindt,
met een kruisje in **één of meerdere** van de volgende kolommen:
In de kolom **intensiteit** als je de blijdschap van het gekozen gezicht intenser vindt
In de kolom **echtheid** als je de blijdschap van het gekozen gezicht echter vindt,
d.w.z. minder gespeeld / nep dan bij het andere gezicht
In de kolom **anders**, namelijk.. eventuele andere redenen voor je keuze:
zie je bijvoorbeeld andere emoties dan blijdschap?

	A ++	A +	0	B +	B ++	waarom? intensiteit	echtheid	anders, namelijk...
1								
2								
3								
4								
5								

Figure A.2: The forms used in session 1 (in Dutch), for neutral (top panel), fearful (middle panel) and happy faces (bottom panel).

A.3. Session 2

A.3.1. Stimulus presentation procedure

The resulting faces of the first session were used for the second session. Again, the procedure was carried out in one session, this time with a group of 28 subjects (12 male, 17 female) between 21 and 55 years old. Subjects were not allowed to deliberate during the session. As in the first session, the subjects were shown a slideshow, but this time each slide depicted only the face that was chosen in the first session. The faces were again presented in three blocks, in the same order as was used in session 1 (neutral faces, fearful faces, happy faces). The order of the slides within blocks was randomized for each block. Each slide was presented until all subjects indicated they had finished.

For neutral faces, subjects were to mark on their form the amount (none, slightly or a lot) of happiness, surprise, fear, anger, disgust, sadness and boredom they saw in each face (see the top panel of figure A.3). They were instructed to write down any (other) characteristic of the face that influenced their opinion of the face (compared to their mental image of a normal, average, neutral face). For fearful and happy faces, subjects were to rate both the intensity of the emotion and the degree to which they thought the emotion was genuine (see the bottom panel of figure A.3). In addition, like with the neutral faces, they were instructed to write down any (other) characteristic of the face that influenced their opinion of the face (compared to their mental image of a fearful/happy face).

Ziet u emoties in dit gezicht? Zo ja, welke en hoeveel?

1	Blijdschap Happiness	Verbazing Surprise	Angst Fear	Boosheid Anger	Walging Disgust	Verdriet Sadness	Verveling Boredom
Niet / Not							
Enigszins / Slightly							
Veel / a lot							
Overige opmerkingen:							

2	Blijdschap Happiness	Verbazing Surprise	Angst Fear	Boosheid Anger	Walging Disgust	Verdriet Sadness	Verveling Boredom
Niet / Not							
Enigszins / Slightly							
Veel / a lot							
Overige opmerkingen:							

	niet intens/ not intense 1	2	3	4	5	6	zeer intens/ very intense 7	niet echt/ not real	twijfelgeval/ doubtful	echt/ real	opmerkingen
1											
2											
3											
4											
5											
6											
7											
8											
9											
10											

Figure A.3: The forms that were used in session 2 (in Dutch), for neutral (top panel) and happy/fearful faces (bottom panel).

A.3.2. Analysis and results: neutral faces

The neutrality of the faces was determined by computing average scores on the amount of rated emotion and the remarks. In relation to whether of not the face was a "good" neutral face, each remark was assigned a value. The values assigned were -2 (negative), -1 (slightly negative), 0 (neutral), 1 (slightly positive) or 2 (positive). That is, a remark such as "arrogant face" was scored as -2 (negative), whereas a remark such as "good neutral face" was scored as 2 (positive). Remarks concerning the appearance and general impression of the face were also scored as either negative or positive, because the required face pictures were to be as inconspicuous as possible, in the sense that they had to match the subjects' mental image of a normal, neutral face. Remarks that did not concern either emotion or appearance of the face (e.g. "bright picture") were scored as 0 (neutral).

The values that were obtained from the remarks were averaged, yielding a more or less quantitative measure of the total number of positive and negative remarks. For both the female and male face pictures, two rankings were made: one based on the average amount of rated emotion in each face, and one based on the average scores on the remarks (see table A.1). These two rankings were then visually inspected to determine the weight factors for computing the average, final score for each face (⅓ the amount of emotion and ⅔ remarks). The final rankings are also shown in figure A.3. Of the ten best male neutral faces, two were overexposed and therefore replaced by the 11^{th} and 12^{th} pictures in the final ranking (pictures 10 and 1). The score of the 10^{th} female and the 12^{th} male neutral face were comparable (0.779 vs. 0.778, where lower is better), which therefore validates the removal of the two pictures. The selection of the 20 best neutral faces is shown in figure A.4.

A.3.3. Analysis and results: fearful and happy faces

The selection of the faces was based on 1) the intensity of the expression, 2) the genuineness of the expression, and 3) further remarks. For each face, the average intensity and genuineness of the emotions were computed and rescaled to values between zero and one. Remarks were scored in the same way as those of neutral faces.

Rankings of the faces based on intensity, genuineness and remarks were compared to determine the weight factors for computing the average, final scores (¼ intensity, ½ genuineness and ¼ remarks). These rankings, as well as the final ranking, are depicted in table A.2 (fearful faces) and table A.3 (happy faces). Since the final score of the tenth male fearful face was equal to the score of the 10^{th} female fearful face, the ten best fearful face pictures of each sex were selected. These pictures are shown in figure A.5.

Female Neutral Faces		Faces sorted by their score on:		
Face no.	Total score	Total	Intensity	Remarks
1	0,7799672	33	19	1
2	0,8259442	19	33	6
3	0,8243021	6	25	34
4	0,8341544	21	27	3
5	0,7684729	34	24	33
6	0,7454844	25	21	21
7	0,7783251	5	6	12
8	0,7881773	27	5	2
9	0,8243021	7	11	19
10	0,8243021	12	16	5
11	0,7799672	1	7	7
12	0,7799672	11	17	17
13	0,8308703	17	18	18
14	0,8850575	18	31	8
15	0,7914614	8	34	15
16	0,7914614	15	13	28
17	0,7816092	16	8	35
18	0,7816092	31	22	4
19	0,7323481	28	12	29
20	0,8292282	22	15	11
21	0,7536946	35	26	31
22	0,7996716	24	28	22
23	0,8768473	32	9	20
24	0,816092	3	10	32
25	0,7651888	9	35	25
26	0,8949097	10	32	27
27	0,7750411	2	1	16
28	0,7947455	20	20	9
29	0,8505747	13	23	10
30	0,8899836	4	4	14
31	0,7931034	29	2	13
32	0,8173235	23	30	23
33	0,7307061	14	3	30
34	0,7619048	30	29	24
35	0,8045977	26	14	26

Male Neutral Faces		Faces sorted by their score on:		
Face no.	Total score	Total	Intensity	Remarks
1	0,7766631	25	32	25
2	0,909688	32	25	9
3	0,8292282	9	9	12
4	0,9310345	12	35	22
5	0,8078818	22	10	8
6	0,7799672	8	26	19
7	0,7651888	19	5	32
8	0,7487685	7	12	6
9	0,7224959	20	1	27
10	0,7783251	35	7	3
11	0,8702791	1	22	7
12	0,7389163	10	20	20
13	0,816092	6	29	31
14	0,9622332	27	8	28
15	0,8226601	29	13	1
16	0,8571429	31	17	35
17	0,8308703	33	18	10
18	0,8768473	5	19	29
19	0,7619048	23	33	33
20	0,7684729	26	15	23
21	0,8817734	13	23	34
22	0,7422003	28	6	16
23	0,8111658	15	27	24
24	0,8669951	3	30	13
25	0,6715928	17	31	15
26	0,816092	30	11	21
27	0,7832512	34	2	5
28	0,817734	16	28	17
29	0,7914614	24	34	30
30	0,8407225	11	16	26
31	0,7980296	18	3	11
32	0,7077176	21	24	14
33	0,8078818	2	21	4
34	0,8538588	4	4	18
35	0,771757	14	14	2

Table A.1: Results of the rating session for all female (left panel) and male (right panel) neutral faces. The first column shows the face numbers, followed by the rating scores in the second column. The third, fourth and fifth columns shows the face numbers from the first column sorted by their total score, the scores on the intensity of rated emotion and the scores on the remarks, respectively. The total scores shown in the second column were obtained by averaging the scores on the intensity of rated emotion and remarks. The weight factors for this average (⅓ the amount of emotion and ⅔ remarks) were determined by inspecting the rankings shown in column four and five, resulting in the final ranking shown in the third column. The selection of the 10 best faces of each panel is shown in blue.

Female Fearful Faces		Faces sorted by their score on:			
Face no.	Total score	Total	Intensity	Genuineness	Remarks
1	0,3270833	29	21	9	25
2	0,3943452	14	28	29	16
3	0,1946429	21	6	27	28
4	0,0622024	16	31	14	6
5	0,3776786	31	16	20	27
6	0,2440476	9	14	21	11
7	0,3625	20	29	2	29
8	0,2991071	27	19	31	14
9	0,4925595	28	7	16	31
10	0,2291667	26	13	26	5
11	0,3845238	2	17	5	1
12	0,0863095	11	20	17	20
13	0,2321429	5	10	22	7
14	0,5116071	17	9	11	22
15	0,2666667	22	33	8	21
16	0,5029762	7	18	25	9
17	0,375	25	30	30	2
18	0,2875	30	24	3	24
19	0,2229167	1	26	32	26
20	0,4696429	33	3	7	35
21	0,5089286	24	11	33	33
22	0,3744048	32	8	1	30
23	0,1190476	8	15	28	18
24	0,3080357	18	32	24	32
25	0,3625	15	22	15	15
26	0,403869	35	27	4	17
27	0,4619048	6	1	18	8
28	0,4270833	13	35	23	13
29	0,5235119	10	2	19	10
30	0,3276786	19	25	35	19
31	0,4982143	3	12	34	34
32	0,2994048	23	23	12	23
33	0,3241071	34	34	13	12
34	0,1183292	12	4	10	3
35	0,2565476	4	5	6	4

Male Fearful Faces		Faces sorted by their score on:			
Face no.	Total score	Total	Intensity	Genuineness	Remarks
1	0,445238	17	8	17	17
2	0,11369	5	17	13	11
3	0,26994	13	5	11	35
4	0,418155	11	19	22	22
5	0,49881	22	16	5	10
6	0,387798	1	18	1	9
7	0,192857	35	24	20	31
8	0,331548	4	3	10	13
9	0,383036	10	4	35	24
10	0,403274	24	12	6	8
11	0,472619	6	27	4	34
12	0,317262	9	13	9	5
13	0,484821	34	1	34	1
14	0,322917	16	23	23	27
15	0,136012	20	35	14	23
16	0,368155	23	11	16	6
17	0,564881	8	20	24	19
18	0,330952	18	32	25	4
19	0,252381	14	6	12	14
20	0,366964	12	34	32	25
21	-0,013988	27	14	7	16
22	0,453869	25	22	30	18
23	0,364019	3	29	18	26
24	0,4	19	15	3	30
25	0,302083	29	25	29	12
26	0,091369	32	9	28	29
27	0,308333	30	28	27	20
28	0,126488	31	7	2	3
29	0,244345	7	26	8	15
30	0,233333	15	31	15	2
31	0,2	28	10	31	32
32	0,24375	2	30	21	7
33	-0,071726	26	2	19	28
34	0,377679	21	33	26	33
35	0,440476	33	21	33	21

Table A.2: Results of the rating session for all female (left panel) and male (right panel) fearful faces. The first column shows the face numbers, followed by the rating scores in the second column. Columns three through six show the face numbers from the first column sorted by their total score and the scores on the intensity of fear, the genuineness of fear, and remarks, respectively. The total scores shown in the second column were obtained by averaging the scores on intensity, genuineness and remarks. The weight factors for this average (¼ intensity, ½ genuineness and ¼ remarks) were determined by inspecting the rankings shown in column four, five and six, resulting in the final ranking shown in the third column. The selection of the 10 best faces of each panel is shown in blue.

Female Happy Faces		Faces sorted by their score on:			
Face no.	Total score	Total	Intensity	Genuineness	Remarks
1	0,6279762	23	23	17	11
2	0,5089286	17	17	1	23
3	0,2782738	12	12	12	17
4	0,6160714	1	34	4	12
5	0,4047619	11	11	23	1
6	0,4047619	4	13	21	21
7	0,5267857	21	31	11	4
8	0,5744048	8	21	8	13
9	0,4717262	13	18	20	8
10	0,5044643	14	1	14	31
11	0,6205357	20	4	13	7
12	0,6369048	7	7	10	14
13	0,5714286	31	8	19	34
14	0,5401786	2	32	2	20
15	0,4360119	10	3	9	33
16	0,3363095	33	24	7	2
17	0,6458333	35	26	33	35
18	0,4583333	34	5	35	18
19	0,4747024	19	35	31	10
20	0,53125	9	15	34	24
21	0,6130952	18	33	25	15
22	0,3526786	24	14	6	9
23	0,6547619	15	2	24	19
24	0,4479167	25	27	15	27
25	0,4255952	27	25	18	6
26	0,3720238	5	20	5	16
27	0,4136905	6	22	27	25
28	0,3169643	26	10	26	22
29	0,172619	22	30	16	28
30	0,202381	32	9	22	5
31	0,516369	16	6	28	32
32	0,3407738	28	19	32	30
33	0,5044643	3	29	3	26
34	0,4955357	30	28	29	3
35	0,4985119	29	16	30	29

Male Happy Faces		Faces sorted by their score on:			
Face no.	Total score	Total	Intensity	Genuineness	Remarks
1	0,4627976	33	13	33	33
2	0,4345238	9	27	3	9
3	0,5625	15	33	15	15
4	0,4925595	3	34	9	13
5	0,4553571	22	15	22	3
6	0,5133929	13	28	34	22
7	0,5133929	18	16	14	18
8	0,2767857	34	29	18	24
9	0,5922619	24	11	24	30
10	0,1592262	14	18	30	14
11	0,4940476	30	5	7	6
12	0,4360119	6	9	35	7
13	0,5416667	7	6	16	11
14	0,5282738	16	24	6	28
15	0,578869	35	30	4	4
16	0,5	11	22	20	35
17	0,2901786	4	7	13	20
18	0,5357143	28	2	1	5
19	0,3511905	20	14	11	1
20	0,4866071	27	4	12	21
21	0,4330357	1	3	28	12
22	0,5535714	5	20	21	26
23	0,3050595	12	35	2	25
24	0,5282738	2	8	32	19
25	0,3407738	21	1	27	8
26	0,4166667	26	26	5	17
27	0,4642857	31	25	26	31
28	0,4880952	19	21	31	34
29	0,3199405	32	32	19	16
30	0,5267857	25	31	25	27
31	0,3705357	29	23	23	2
32	0,3511905	23	12	17	29
33	0,6502976	17	17	29	23
34	0,5342262	8	10	8	10
35	0,4985119	10	19	10	32

Table A.3: Results of the rating session for all female (left panel) and male (right panel) happy faces. The first column shows the face numbers, followed by the rating scores in the second column. Columns three through six show the face numbers from the first column sorted by their total score and the scores on the intensity of happiness, the genuineness of happiness, and remarks, respectively. The total scores shown in the second column were obtained by averaging the scores on intensity, genuineness and remarks. The weight factors for this average (¼ intensity, ½ genuineness and ¼ remarks) were determined by inspecting the rankings shown in column four, five and six, resulting in the final ranking shown in the third column. The selection of the 10 best faces of each panel is shown in blue.

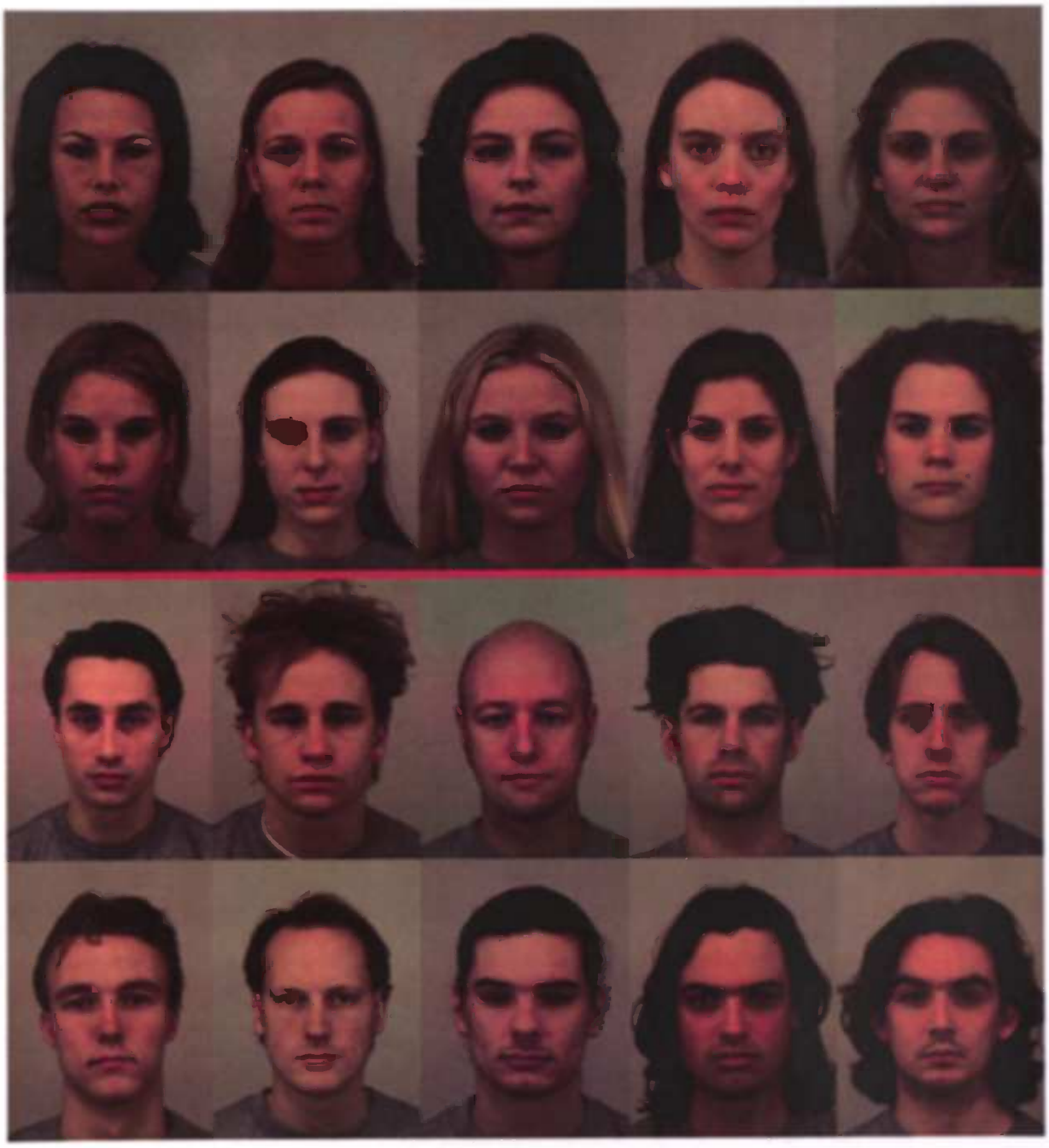

Figure A.4: The final selection of neutral faces. Female faces are shown in the top panel, male faces are shown in the bottom panel. For each sex, faces are sorted by their total score (from left to right and from top to bottom, so that the face in upper left corner is the face with the highest score).

Figure A.5: The final selection of fearful faces. Female faces are shown in the top panel, male faces are shown in the bottom panel. For each sex, faces are sorted by their total score (from left to right and from top to bottom, so that the face in upper left corner is the face with the highest score).

Appendix B: Stimulus Development

B.1. Introduction

In any experiment, there are many independent variables that influence the quantities that are measured. Therefore, if we want to measure the effect of a single variable X on the quantity Y, the variable X has to be quantitatively controlled, while all other variables are kept constant. For the fMRI-experiment, visual stimuli were presented to the subjects. In this case the independent variable X was the amount of stimulus information in the images that were presented to the subjects. The amount of stimulus information in an image had to be quantitatively controlled, whereas all other aspects of the image, such as brightness and contrast, had to be held constant. For this reason, the stimuli were created using the discrete Fourier transform. The discrete Fourier transform is a mathematical tool providing the possibility to manipulate properties of images that would otherwise be very hard to manipulate, such as the amount of stimulus information in the image.

In the next section, a general theoretical outline of the discrete Fourier transform and its properties is given. The discrete Fourier transform is used mostly for digital signal processing, such as the processing of sound signals. A signal is nothing but a quantity that changes with time. Digital simply means that the signal is described in discrete steps of time, in contrast to a real-time signal, which is a continuous function.

In the third section, the Fourier theory concentrates on the specific case of digital images and how the Fourier transform can be used to manipulate these images. This section explains that an image is just like a digital signal, except that the "quantity" in this case (the color intensity in the picture) depends on the position in the picture, not time.

Finally, the last section describes the process of the actual stimulus development, which includes manipulating images in the frequency domain with the Fourier transform.

B.2. Fourier theory

Fourier theory incorporates that any periodic function or signal can be represented by a summation of a series of sine and cosine terms of different frequencies. This means that a periodic function can be described in two different domains: the time domain and the frequency domain. In the time domain, a periodic function, say $y = f(t)$, is a description of how the values of y (e.g. the intensity of a signal) depend on the values of t (e.g. time). In the frequency domain, the same function is described by a summation of sinusoidal waves of different frequencies. The Fourier transform is used to transform the signal from the time domain to the frequency domain, or, in other words, it describes the sinusoidal waves in the frequency domain that, together, constitute the original signal in the time domain.

B.2.1. The discrete Fourier transform

The Fourier transform has been defined for both continuous and discrete signals. Continuous signals and Fourier transforms are not suitable for computer calculations, because they consist of an infinite number of values. The discrete Fourier transform is a special case of the continuous Fourier transform, in which both the signal and its Fourier transform function have been sampled and truncated so that they can be described by a finite number of samples. In other words, in the discrete case both the signal and its Fourier transform consist of a finite number, say N, of equally spaced sample values. A detailed account of the relationship between the continuous and discrete Fourier transforms is given by Brigham (1974).

The discrete Fourier transform is given by:

$$S(k) = \sum_{n=0}^{N-1} s[n] \cdot e^{\frac{-i2\pi nk}{N}} \tag{1}$$

in which n denotes time (in discrete steps), and $s[n]$ is the signal in the time domain. $S(k)$ is the Fourier transform function, in which k denotes frequency. N is the number of samples that completely describes $s[n]$.

The *inverse* discrete Fourier transform transforms $S(k)$ back from the frequency domain to the time domain and yields the original signal $s[n]$:

$$s[n] = \frac{1}{N} \sum_{k=0}^{N-1} S(k) \cdot e^{\frac{i2\pi nk}{N}} \tag{2}$$

In this way, $s[n]$ is defined as a series of sinusoidal waves of different frequencies (this will be considered in more detail in a later section). A signal can be manipulated in both the time and frequency domain, using the Fourier transform (and the inverse transform) to switch between the domains.

B.2.2. The amplitude and phase spectra of a signal

Even though the signal $s[n]$ may be real, its Fourier transform $S(k)$ is usually complex. If so, $S(k)$ is basically a vector of N complex numbers z: $S(k)=[z_0,z_1,z_2,\ldots,z_{N-1}]$.

Any complex number z can be decomposed into a real part, x, and an imaginary part, y, in such a way that $z=x+iy$. Real numbers are a subset of the complex numbers, namely the subset of numbers for which the imaginary part is zero, thus $z=x$. Another special kind of complex number is the conjugate of z, z^*. The conjugate of a complex number $z=x+iy$ is defined as $z^*=x-iy$. Thus, z^* has the same real part as z, but the imaginary part is multiplied by -1.

In a so-called Argand diagram, which is shown in figure B.1, the complex number z is plotted in a real-imaginary plane at position (x,y). The real part of z, x, is measured at the real axis, whereas the imaginary part of z, y, is measured at the imaginary axis.

The coordinates (x,y) of z are called Cartesian coordinates of z. From figure B.1, it can be seen that z can also be defined by its polar coordinates, the radius $|z|$ and angle θ. The distance of z to the origin, $|z|$, is called the *amplitude* of z, and is given by $|z|=\sqrt{x^2+y^2}=z\cdot z^*$. The argument of z, arg(z), is called the *phase* of z, and is given by the angle θ. The complex number z is then defined as $z=|z|\cdot e^{i\theta}$ (for definition, see equation (3))

The same holds for the complex Fourier transform $S(k)$. The vector $S(k)$ can be decomposed into a vector of the real parts of $S(k)$, $S_r(k)$, and a vector of the imaginary parts of $S(k)$, $S_i(k)$. $S(k)$ can then be defined as $|S(k)|\cdot e^{i\theta(k)}$. The vector $|S(k)|$ is called the *amplitude spectrum* of $S(k)$, and is given by $|S(k)|=\sqrt{S_r(k)^2+S_i(k)^2}$. The vector $\theta(k)$ is called the *phase spectrum* of $S(k)$.

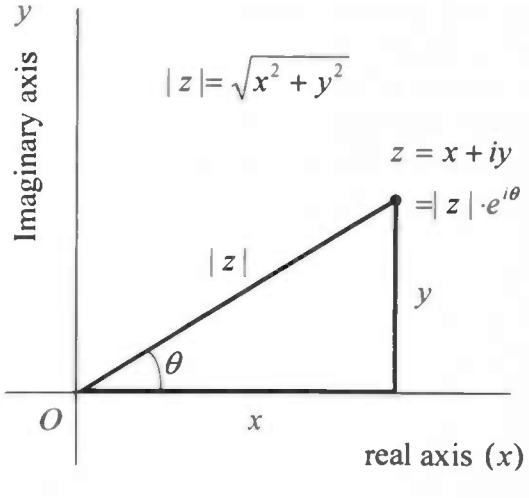

Figure B.1: an Argand diagram of complex numbers $z=|z|\cdot e^{i\theta}$

B.2.3. The Fourier transform as a series of sinusoidal waves

From the definition of the discrete Fourier transform, it may not be apparent at first glance that the Fourier transform is a superposition of sinusoidal waves of different frequencies. This may be clarified by figure B.2. Figure B.2 depicts a special case of the Argand diagram, in which z lies on the *unit circle*. In this case, $|z| = \sqrt{x^2 + y^2} = 1$, thus $0 \le x \le 1$, $0 \le y \le 1$ and $z = e^{i\theta}$. The conjugate of $z = e^{i\theta}$, $z^* = e^{-i\theta}$, is also shown in the figure. Figure B.2 shows the relationship between complex exponentials and sine and cosine functions, the so-called Euler formula:

(3) $$e^{i\theta} = \cos\theta + i\sin\theta$$

From these mathematical definitions it is shown that a complex exponential is basically a sinusoidal wave. Since the Fourier transform is a summation of complex exponentials, it is basically a summation of sinusoidal waves.

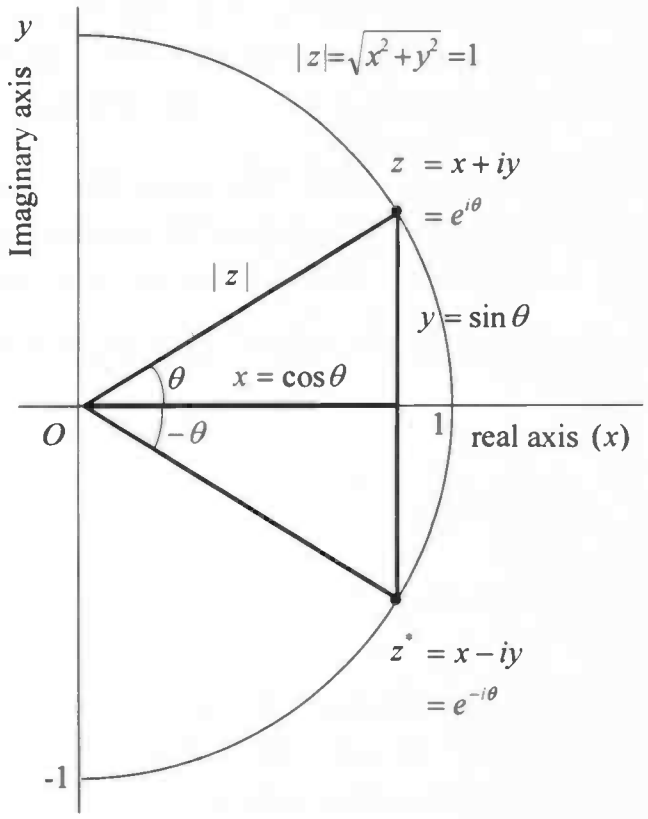

Figure B.2: the Argand diagram of complex numbers $z = e^{i\theta}$, for which $|z| = 1$

B.2.4 Properties of the discrete Fourier transform

The discrete Fourier transform has several properties that are useful for shortening computation time. This section describes two of these properties, which were used in the process of stimulus development: periodicity and symmetry.

Periodicity

Both the signal $s[n]$ and its discrete Fourier transform function $S(k)$ are periodic functions, with N sample values in one period. To show this, take $k = p$, in which p is an arbitrary integer. Equation (1) then becomes:

$$S(p) = \sum_{n=0}^{N-1} s[n] \cdot e^{\frac{-i2\pi np}{N}} \tag{4}$$

Then let $k = p + N$. Equation (1) becomes:

$$\begin{aligned} S(p+N) &= \sum_{n=0}^{N-1} s[n] \cdot e^{\frac{-i2\pi n(p+N)}{N}} \\ &= \sum_{n=0}^{N-1} s[n] \cdot e^{\frac{-i2\pi np}{N}} \cdot e^{-i2\pi n} \\ &= \sum_{n=0}^{N-1} s[n] \cdot e^{\frac{-i2\pi np}{N}} \\ &= S(p) \end{aligned} \tag{5}$$

Thus, $S(k)$ is periodic with N samples per period. The same reasoning can be applied to the definition of $s[n]$, proving that $s[n]$, as well as $S(k)$, is a periodic function with N samples in one period. This means that both a signal and its Fourier transform are completely described by the N samples in one period, as stated earlier. This can be used to our advantage. If we have a periodic signal $u[n]$, we can compute the Fourier transform of $u[n]$ over one period of $u[n]$ and simply discard the rest of the signal. On the other hand, if we have a digital signal $v[n]$ that is defined by a finite number of samples, N, but that is not periodic, we can simply pretend that it *is* periodic (with N samples in one period) and compute its discrete Fourier transform. In other words, any digital signal that is defined by a finite number of samples can be seen as one period of a periodic signal, of which the discrete Fourier transform can be computed. This is exactly what is done in the stimulus development, and it is explained in more detail in the third section.

Symmetry

As indicated earlier, the Fourier transform is generally complex, consisting of a real part $S_r(k)$ and an imaginary part $S_i(k)$: $S(k) = S_r(k) + i \cdot S_i(k)$ (see also equation (3). The signal $s[n]$ may also be complex, $s[n] = s_r[n] + i \cdot s_i[n]$. The Fourier transform of $s[n]$ then becomes:

(6)
$$\begin{aligned} S(k) &= \sum_{n=0}^{N-1} (s_r[n] + i \cdot s_i[n]) \cdot e^{\frac{-i2\pi nk}{N}} \\ &= \sum_{n=0}^{N-1} (s_r[n] + i \cdot s_i[n])(\cos\tfrac{2\pi nk}{N} - i\sin\tfrac{2\pi nk}{N}) \\ &= \sum_{n=0}^{N-1} (s_r[n]\cos\tfrac{2\pi nk}{N} + s_i[n]\sin\tfrac{2\pi nk}{N}) + i\sum_{n=0}^{N-1} (s_i[n]\cos\tfrac{2\pi nk}{N} - s_r[n]\sin\tfrac{2\pi nk}{N}) \\ &= S_r(k) + i \cdot S_i(k) \end{aligned}$$

With equation (6), $S_r(k)$ and $S_i(k)$ are defined as:

(7)
$$S_r(k) = \sum_{n=0}^{N-1} (s_r[n]\cos\tfrac{2\pi nk}{N} + s_i[n]\sin\tfrac{2\pi nk}{N})$$

(8)
$$S_i(k) = \sum_{n=0}^{N-1} (s_i[n]\cos\tfrac{2\pi nk}{N} - s_r[n]\sin\tfrac{2\pi nk}{N})$$

If the signal is real, $s_i[n] = 0$, yielding $s[n] = s_r[n]$. Substituting this in equations (7) and (8) yields:

(9)
$$S_r(k) = \sum_{n=0}^{N-1} s_r[n]\cos\tfrac{2\pi nk}{N}$$

(10)
$$S_i(k) = -i\sum_{n=0}^{N-1} s_r[n]\sin\tfrac{2\pi nk}{N}$$

Since $\cos(t)$ is an even function ($\cos(t) = \cos(-t)$), the real part of $S(k)$, $S_r(k)$, is an even function as well: $S_r(k) = S_r(-k)$. The imaginary part of $S(k)$, $S_i(k)$, is an odd function ($S_i(k) = -S_i(-k)$), since $\sin(t) = -\sin(-t)$. In other words, for a real signal $s[n]$, the Fourier transform $S(k)$ is equal to its complex conjugate: $S(k) = S^*(k)$. This means that the amplitude spectrum $|S(k)|$ is an even function as well. The amplitude spectrum, as specified in the previous section, is defined as $|S(k)| = \sqrt{S_r(k)^2 + S_i(k)^2}$. If $S_r(k) = S_r(-k)$ and $S_i(k) = -S_i(-k)$, then

(11)
$$|S(-k)| = \sqrt{S_r(-k)^2 + S_i(-k)^2} = \sqrt{S_r(k)^2 + S_i(k)^2} = |S(k)|$$

Thus, for a real signal $s[n]$, the amplitude spectrum is symmetric. This is a useful property that can be used to shorten computation time considerably.

B.3. The discrete Fourier transform of digital images

The discrete Fourier transform can be applied to digital images as well. In this section, it is explained how we can transform an image into the frequency domain using the discrete Fourier transform, by viewing the image as a two-dimensional periodic digital signal. As stated before, a digital signal is generally a quantity that changes with discrete steps of time. However, time does not necessarily have to be the independent variable. In the case of a picture, the independent variable is the position in space (think of yourself standing on a giant picture: the color of the ground under your feet depends on where you stand). Therefore, the time domain is in this case referred to as image space and the frequency domain is referred to as Fourier space.

B.3.1. Grayscale and color images

A digital grayscale image that is w pixels wide and h pixels high consists of a matrix of $w \times h$ grey-intensity values. That is, a digital grayscale image is nothing but a matrix of numbers, where the number at position (x, y) in the matrix denotes the brightness of the pixel at position (x, y) in the picture. Usually, the numbers in the matrix vary from zero, which is black, to 255, which is white, but many image processing programs can use other scales as well. Thus, the "color" of a pixel in a grayscale image is denoted by the value of one number.

In contrast, the color of a pixel in a color image is denoted by the values of three independent numbers, one for each color Red, Green and Blue (i.e. the RGB values). A color image, therefore, consists of three matrices of color intensity values. The numbers in the "red" matrix denote the amount of red in the image pixels, those of the "blue" matrix denote the amount of blue, and those of "green" the amount of green in the image pixels. Since these three matrices consist of intensity values in the same way as the matrix of a grayscale image, a color image can be treated as three separate grayscale images. Therefore, although the text in the next section concerns the matrix of a grayscale image, it applies to color images as well.

B.3.2. A digital image as a two-dimensional signal

For each pixel at position (x, y) in a grayscale image, we can look up its intensity value in the pixel matrix at position (x, y). In this way, the matrix can be seen as a function $f(x, y)$ of two variables, x and y, where $x, y \in N$, $1 \leq x \leq w$ and $1 \leq y \leq h$. If we think of the picture as a tile in an endlessly repeating pattern, the function $f(x, y)$ is periodic, with a period the size of the picture. Thus, an image can be seen as a periodic two-dimensional signal, to which the discrete Fourier transform can be applied. Since the image is two-dimensional, applying the discrete Fourier transform results in a two-dimensional *matrix* of complex numbers, instead of a vector, as is the case with a one-dimensional Fourier transform. The number of frequencies in the Fourier matrix (one period of the Fourier transform) is equal to the number of pixels, or sample values, of the image (one period of the signal).

Each element in the Fourier matrix represents a sinusoidal wave of a certain frequency. Therefore, the element at position (x, y) in the matrix will be defined as the Fourier coefficient of frequency (x, y). Each Fourier coefficient $F(x, y)$, as in the one-dimensional Fourier transform, has the following characteristics:

1. The amplitude of $F(x,y)$, $|F(x,y)| = \sqrt{F_r(x,y)^2 + F_i(x,y)^2}$
2. The phase of $F(x,y)$, $\arg(F(x,y))$

B.3.3. The amplitude spectrum of a digital image

The amplitude spectrum of an image is the matrix of amplitude values of all frequencies in the Fourier matrix. The amplitude of a certain frequency is the amount to which that frequency contributes to the image. In other words, if there is a periodic structure with a certain frequency in the original image, the amplitude of that frequency will be high. To illustrate this, the images in figure B.3 have a constant phase spectrum, so that the appearance of the pictures only depends on the amplitude spectrum. The amplitude spectra of both images are zero, except for the value of one frequency (and the DC-value for the brightness of the images, which is explained later). For the picture on the left, the non-zero frequency is (3,0), resulting in a periodical structure that repeats itself 3 times over the image. Conversely, on the right side of figure B.3, the non-zero frequency is (5,0). Note that the only difference between the two pictures is the *frequency* of the periodic structure, and that this difference is caused by a non-zero amplitude value of *two different frequencies* in the amplitude spectrum. The amplitudes of both non-zero frequencies are equal. So, a periodic structure with frequency f causes a peak at frequency f in the amplitude spectrum.

A special case is the amplitude of the zero-frequency component, $F(0,0)$. This amplitude value is called the DC-value. If there are no periodic structures in the image, or, in other words, if all pixels in the image have the same value, then all frequency components are zero, except for the DC-value. Dividing the DC-value by the number of pixels in the image gives the average intensity, i.e., brightness, of the image. Therefore, the DC-value can be considered to be the total value of brightness in the image. Both images in figure B.3 have the same DC-value.

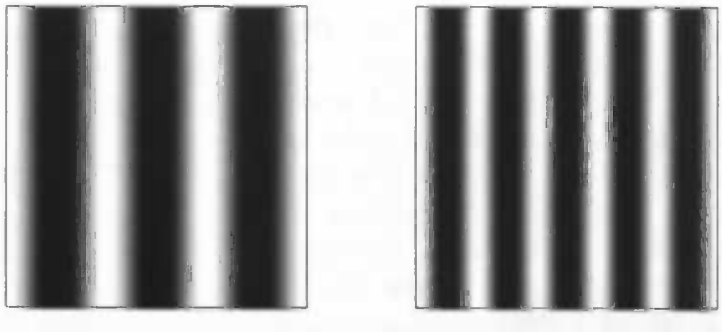

Figure B.3: two images with zero phase spectrum. The image on the left has a non-zero amplitude at frequency = (3,0), the image on the right has a non-zero amplitude at frequency = (5,0). All other values of both amplitude spectra (except for the DC-value, for brightness) are zero.

B.3.4. Approximating the amplitude spectrum of natural images

In general, the low frequency components make up the overall shape of a signal, while the high frequency components are needed to sharpen edges and provide fine detail. This is true for natural images as well: most of the information in natural images is contained in the low frequency components. The amplitude spectrum of a natural image can be approximated by:

(12) $$A = C \cdot f^{-\alpha} \qquad (f > 0)$$

in which A is the amplitude spectrum, C is a scale factor and f the frequency (van der Schaaf & van Hateren 1995). The value of α depends on the ratio of high and low frequencies in the image: if there are more periodical structures of low frequency than of high frequency, α will be higher. The value of C determines the scale of the amplitude spectrum, and can therefore be considered to be a measure of contrast in the image. If we take the natural logarithm of A, equation (12) becomes:

(13) $$\ln A = \ln(f^{-\alpha}) + \ln C = -\alpha \cdot \ln f + \ln C$$

The values of α and C can be computed by making a least square fit trough the log-log plot of the amplitude and frequency of the image Fourier matrix. That is, if we make a least square fit through a plot with $y = \ln A$ and $x = \ln f$, the values of α and C are given by:

(14) $$y = -\alpha \cdot x + \ln C$$

$$\alpha = -\frac{\Delta y}{\Delta x}$$

$$C = e^{y(0)}$$

where $y(0)$ is the intercept of the fit with the x-axis, and $-\frac{\Delta y}{\Delta x}$ is the slope of the fit.

B.3.5. The phase spectrum and its interaction with the amplitude spectrum

The phase spectrum of the image is the matrix with the phase values of all frequencies in the Fourier matrix. In general, the phase spectrum of an image contributes mainly to the spatial structure information, such as edges or corners. For example, if in Fourier space the phase spectrum of a house is replaced by the phase spectrum of a face, the image will show a face in image space. However, the final appearance of an image is the result of a complex interaction between the amplitude spectrum and the phase spectrum.

In figure B.4, two images with a completely random phase spectrum are shown. Both pictures do not really depict anything: a random phase spectrum (without coherence or order), results in visual noise (a picture without coherence). If there is coherence in the phase spectrum, the pixels in image space would have coherence as well, resulting in spatial structures in the image.

However, the two pictures do have different appearances, because their amplitude spectra are different. The picture on the left has a flat amplitude spectrum: all frequencies (except the zero-frequency for brightness) have the same amplitude. The picture on the right has an amplitude spectrum of a natural image, that was created using equation (12). Thus, a random phase spectrum combined with a natural amplitude spectrum results in visual noise with a cloud-like appearance.

In general, the spatial structural information constructing a natural image is largely due to coherence of the phase spectrum, whereas the amplitude spectrum further influences the contrasts of the spatial structures.

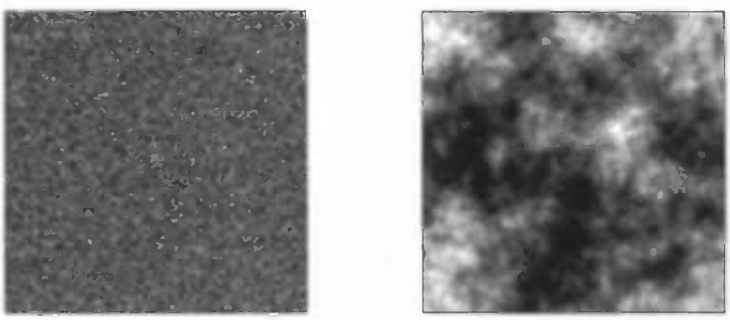

Figure B.4: two images with a random phase spectrum. The image on the left has a flat amplitude spectrum (all frequencies have the same amplitude except for the DC-value), while the image on the right has a natural amplitude spectrum that was created using equation (12).

B.4. Stimulus Development

For the experiment described in this thesis, 50 images were used: 10 house images, 20 fearful face images and 20 neutral face images. For each of these images, a stimulus sequence of 110 pictures with increasing stimulus information had to be created. Since the activity in the brain should only be due to the stimulus information (house or face), the pictures to be created had to meet the following requirements:

1. All stimuli should be of the same size, presented at the same position in the center of the screen, and small enough to be attentively processed by a subject while keeping his/her eyes focused on the screen;
2. There should be no other stimulus information (such as sharp contrast, edges, etc.) on the screen other than that of the face or house;
3. The amount of stimulus information should be quantitatively controlled, and the increase of stimulus information should be equal for all pictures;
4. All other aspects of the stimuli that are not directly inherent to the stimuli themselves, such as brightness and contrast, should be held constant.

The pictures were processed in such a way that they met these requirements, which is described in the next subsections.

B.4.1. Preprocessing

First, the images were preprocessed so that the faces and houses were of the same size and would be presented within the visual focus of 5° (Rainer et al. 2001). To do this, the number of pixels that were within the visual focus of 5°, given the screen resolution and the distance of the eyes to the screen, was calculated. Then the pictures of the faces were scaled in such a way that the entire face, as measured from the hairline to the chin, was 1) equal for each face image and 2) exactly within the 5° visual focus pixel limit, in the centre of the screen. Resizing the faces based on the height of the face ensured that the entire face was within visual focus of 5°, because face width was always smaller than face height. After resizing, all faces were 420 pixels high and between 198 and 261 pixels wide. Houses were rescaled to the same dimensions as the faces, and all pictures were cropped to the same size. For all the pictures, the background was deleted, after which the average color of all faces and houses was computed. This color was then used as the background color for all pictures. The resultant pictures were then further processed using the Fourier transform.

Using Matlab 6.5 (http://www.mathworks.com/products/matlab/), a two-dimensional fast Fourier transform of the images was computed, resulting in 3 Fourier matrices for each image, one for each color Red, Green and Blue. These three Fourier matrices were treated separately until reconstruction of the final image. For each Fourier matrix, the amplitude and phase spectra were computed, which were then manipulated to meet the requirements described at the beginning of the section.

B.4.2. Creating an average amplitude spectrum

As stated before, the amplitude spectrum of a natural image can be approximated by equation (12). For each color of each of the images, the values of α and C were obtained, as described in the previous section. These values were then averaged, resulting in an average α and C for each color. The values of our averaged α were 1.59, 1.52 and 1.41 for Red, Green and Blue respectively. These values are consistent with (Rainer et al. 2001; Reinders et al.

2005). With the average α and C, an approximated average amplitude spectrum was created, by applying equation (12).

In section 2.4.2 it was indicated that the amplitude spectrum is symmetric if the signal is real. Since an image is a two-dimensional signal with only real values, the amplitude spectrum of the image is symmetric in both dimensions. Therefore, only the upper left quadrant of the amplitude spectrum needed to be constructed in this way, and the complete amplitude spectrum was obtained by copying the upper left quadrant symmetrically to the other three quadrants. This averaged amplitude spectrum was used for all images, so that the brightness and contrast were the same for all stimuli.

B.4.3. Controlling the amount of stimulus information: the phase spectrum

The phase spectra of the images were used to control the amount of stimulus information in the picture. First, a random phase spectrum was created, which, combined with the averaged amplitude spectrum, gives rise to an image with a cloud-like appearance, thus providing a form of visual noise while still preserving the characteristics common to natural images. For each of the 110 pictures to be created, the final phase spectrum was obtained by averaging the randomized phase spectrum and the phase spectrum of the original image, such that the first picture had a 100% randomized phase spectrum (i.e. 100% noise) and the last picture had the phase spectrum of the original image (i.e. 100% stimulus information). The amount of stimulus information (i.e. the phase coherence, or the fraction of the original phase spectrum) was increased according to the following exponential function:

$$\text{(15)} \qquad \text{fraction of original phase} = \frac{(e^{0,0033 \cdot p} - 1)}{(e^{0,0033 \cdot (N-1)} - 1)} \qquad p \in [0, N-1]$$

where N is the number of pictures to be created, in this case 110. This function is plotted in figure B.5.

By changing the exponential increase, the approximate moment of pop-out, relative to the duration of the stimulus sequence, can be modified. The value of 0,0033 was determined by pilot experiments, in such a way that the moment of pop-out would be approximately halfway in the sequence, for an optimal timing of the BOLD response.

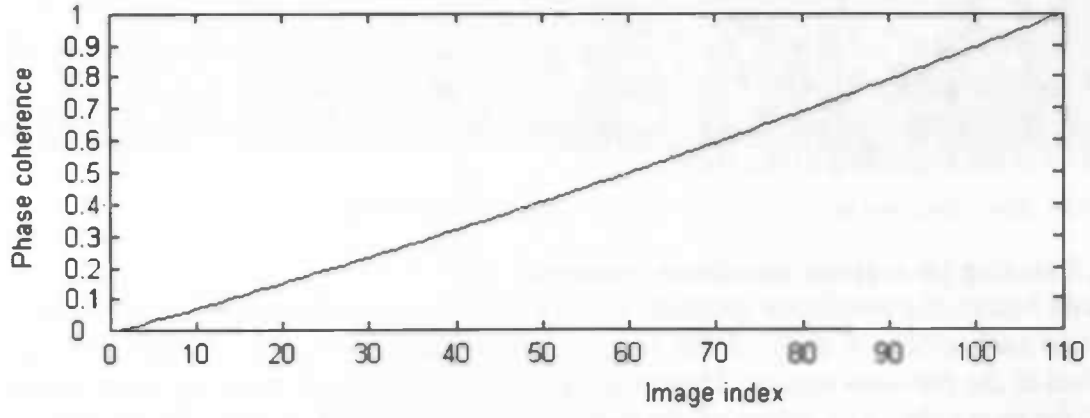

Figure B.5: the increasing phase coherence within a stimulus sequence.

B.4.4. Reconstructing the images

Using the matrices of the manipulated amplitude and phase spectra, the Fourier matrix of each color was constructed. The pictures were reconstructed by applying an inverse Fourier transform on the resultant matrices. In image space, the brightness (the DC-value) of the images was further optimized by shifting all pixel values of all images by the same amount, which was set by visual inspection. Finally, values outside the standard [0, 255] range were clipped to fit this range. That is, values below 0 were set to 0, while values exceeding 255 were set to 255. An example of the set of 110 pictures of one stimulus is shown in figure B.6.

B.4.3. Creating a smooth transition from picture to background

Since the images were smaller than the screen resolution with which they were presented, the edges of the images would cause a sharp contrast with the background. Furthermore, manipulating the images in Fourier space introduced small artifacts in the corners (resulting in white corner-tips, see figure B.6), which could possibly be distracting. For those reasons, the edges of the pictures were smoothed into the background, by presenting a frame of 60 pixel width as a foreground to the images (see also Rainer et al. 2001).

The frame contained both transparent pixels and pixels with the same (grey) color as the background. The number of grey pixels increased linearly over the 60 pixels from the inside to the outside of the frame, resulting in a smooth transition from picture to background. This minimizes any neural activation due to the contrast between the outer edges of the images and the background. The color of the background was equal to the average color of the first and 110th pictures of all stimuli, to further minimize the contrast between images and background. In this way, activation in the brain due to contrasts in the stimuli, other than those from the faces or houses, was prevented.

The frame was constructed in the following way. To create a linear ramp of w pixels, a vector W of length w of linearly increasing values was created, such that the lowest value was 0 and the highest value was 1. Then to create the rectangle depicted in figure B.7, each pixel at position (i, j) in the rectangle was randomly assigned either a grey or a white transparent color, in such a way that for each row j, the percentage of grey pixels was given by:

(16) $$\%\ \text{grey pixels in row } j = (1 - W(j)) \cdot 100\%$$

Figure B.6: the 110 pictures of one stimulus sequence, starting with 100% noise and ending with 100% stimulus information.

Thus, the top row of the rectangle consists only of grey pixels and the last column consists exclusively of transparent pixels, and for each column in between, the percentage of white pixels was linearly increased by $\frac{100}{w-1}$ %. Given that the rectangle is sufficiently wide, this results in an approximately linear ramp of w pixel width. The frame was constructed from four of these rectangles, with rounded corners connecting the sides. The rounded corners were created in the shape of the four quadrants of a circle. In other words, instead of creating the pixels row by row, they were created in circular arcs, where the percentage of grey pixels increased with the radius of the arc (see figure B.8).

The fixation dots that were used to keep attention focused (see chapter 6), were constructed in the same way. In the centre of the fixation dot, all pixels are blue (or red, respectively). The percentage of colored pixels decreases linearly as the distance from the origin increases. In contrast, the number of transparent pixels increases with the distance from the origin, resulting in the fixation dots in figure B.9. Finally, figure B.10 shows some examples of the final pictures that were used in the fMRI experiment.

Figure B.7: a linear ramp of w pixel width.

Figure B.8: the upper right corner of the frame.

Figure B.9: the fixation dots.

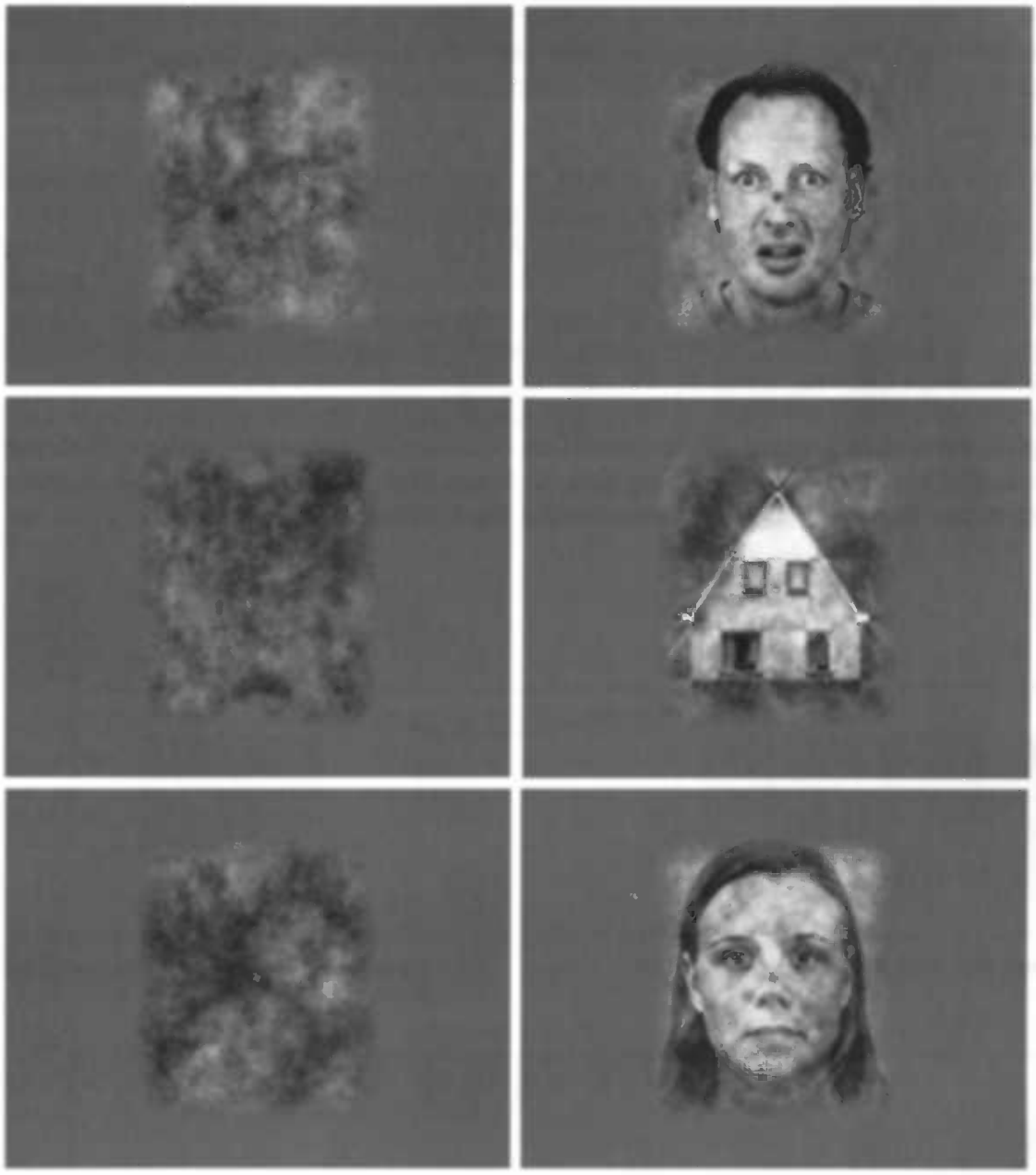

Figure B.10: the first and last pictures (of the series of 110 pictures) of a house, a neutral face and fearful face.

Appendix C: Jittering

C.1. Introduction

In the fMRI experiment (see chapter 6) subjects were to press a button as soon as the stimulus "popped out" from the visual noise. Theoretically, for one (type of) stimulus (e.g. a house), this moment of pop-out within one subject depends only on the amount of stimulus information in the image, and will always be at the same time in the stimulus sequence. In reality, however, the different moments of pop-out of all houses are spread out, or "jittered" over a small interval of time: although they are very close to one another, they are never all at the exact same time. This variation in the moment of pop-out due to intrinsic variation in subjects is called natural or uncontrolled jittering of the moment of pop-out.

In addition to natural jittering, the moment of pop-out can also be jittered artificially, by manipulating the timing of the amount of stimulus information at which the stimulus is recognized. Controlled jittering has several advantages. Firstly, since the moment of pop-out is slightly different for all stimuli in one category, it is less predictable. Therefore, the probability that the subjects' button presses are influenced by timing and expectancy is decreased, which results in more reliable indications of the moment of pop-out. Secondly, jittering of the moment of pop-out (both controlled and uncontrolled) can increase the temporal resolution of the fMRI signal. This will be explained in the next section.

C.2. Jittering

The stimulus recognition (the so-called pop-out) gives rise to a change in the blood oxygenation level in certain areas of the brain, which is measured with fMRI (see chapter 2). A schematic reproduction of this BOLD signal (Blood Oxygenation Level Dependent) is depicted in the top panel of figure C.1. The BOLD signal is measured with every pulse of the fMRI scanner. Thus, if the time between two pulses (the TR) is approximately 1.2 seconds, the BOLD response is sampled every 1.2 seconds, and the temporal resolution of the measured signal is 1/1.2 = 0.83 samples per second. This is shown in the bottom panel of figure C.1. However, the temporal resolution can be increased, by "jittering" the moment of pop-out.

If the moment of pop-out of one stimulus is slightly earlier in the sequence than that of another, the BOLD response is shifted somewhat to the left relative to the scanner pulses. In other words, relative to the BOLD response, the scanner pulses (i.e., the samples of the signal) are shifted to the right. This is shown in the top and middle panel of figure C.2. If we take the average of these two BOLD responses, we get the signal depicted in the bottom panel of figure C.2. The temporal resolution of this average BOLD signal is twice as high, because the two signals were sampled asynchronously. Thus, given that there are multiple stimuli for each

experimental condition, the temporal resolution of the BOLD signal can be increased considerably, by jittering the moment of pop-out relative to the scanner pulses. This was done for our fMRI experiment, by using stimuli with slightly different moments of pop-out.

For each of the total of 50 stimuli, a series 110 pictures were created, such that the first picture was 100% noise, and the last was 100% stimulus information. The set of 50 stimuli was divided into five different stimulus categories, each of which consisted of 10 stimuli (houses, female neutral faces, male neutral faces, female fearful faces and male fearful faces). Each stimulus sequence within a specific category consisted of a different subset of 100 pictures of the 110 pictures that were originally created. For example, of the total of 10 houses, the picture sequence of one house started at picture number 1 and ended at picture number 100, that of another started at picture number 2 and ended at picture 101, and so on, and the sequence of the 10^{th} house started at picture number 10 and ended at picture number 109. This is shown in the top panel of figure C.3.

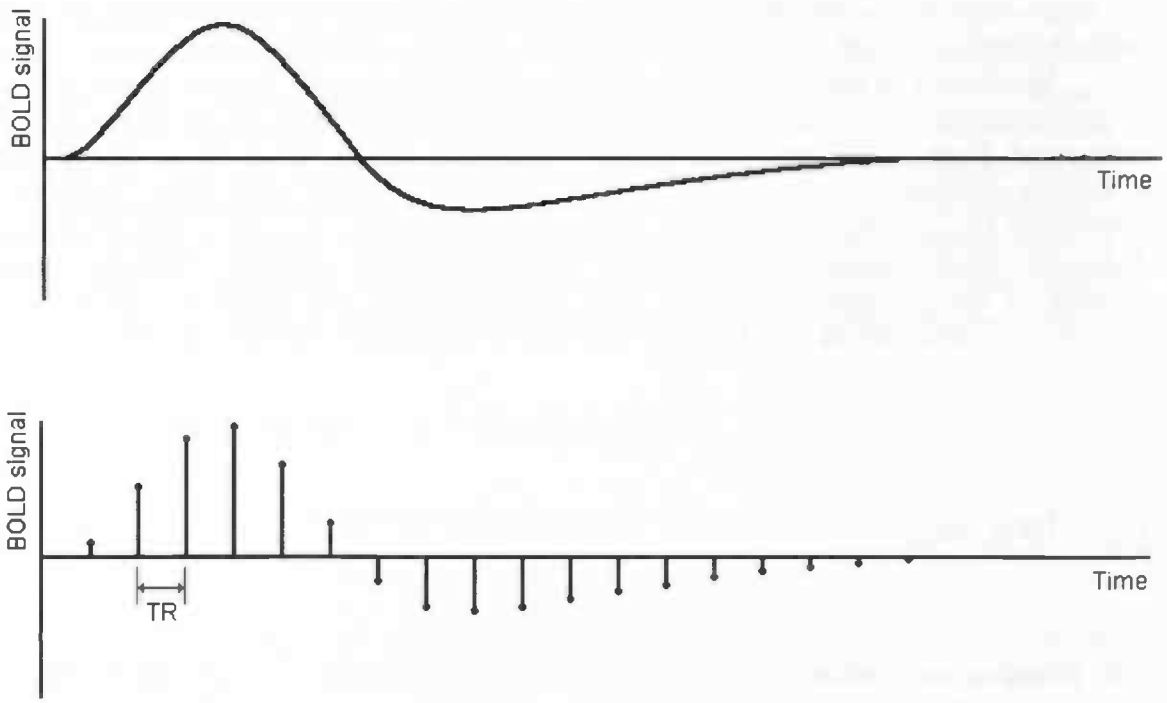

Figure C.1: The (sampled) BOLD response. The top panel depicts the BOLD response, whereas the bottom panel shows the BOLD response as sampled by fMRI with a TR of 1200 ms.

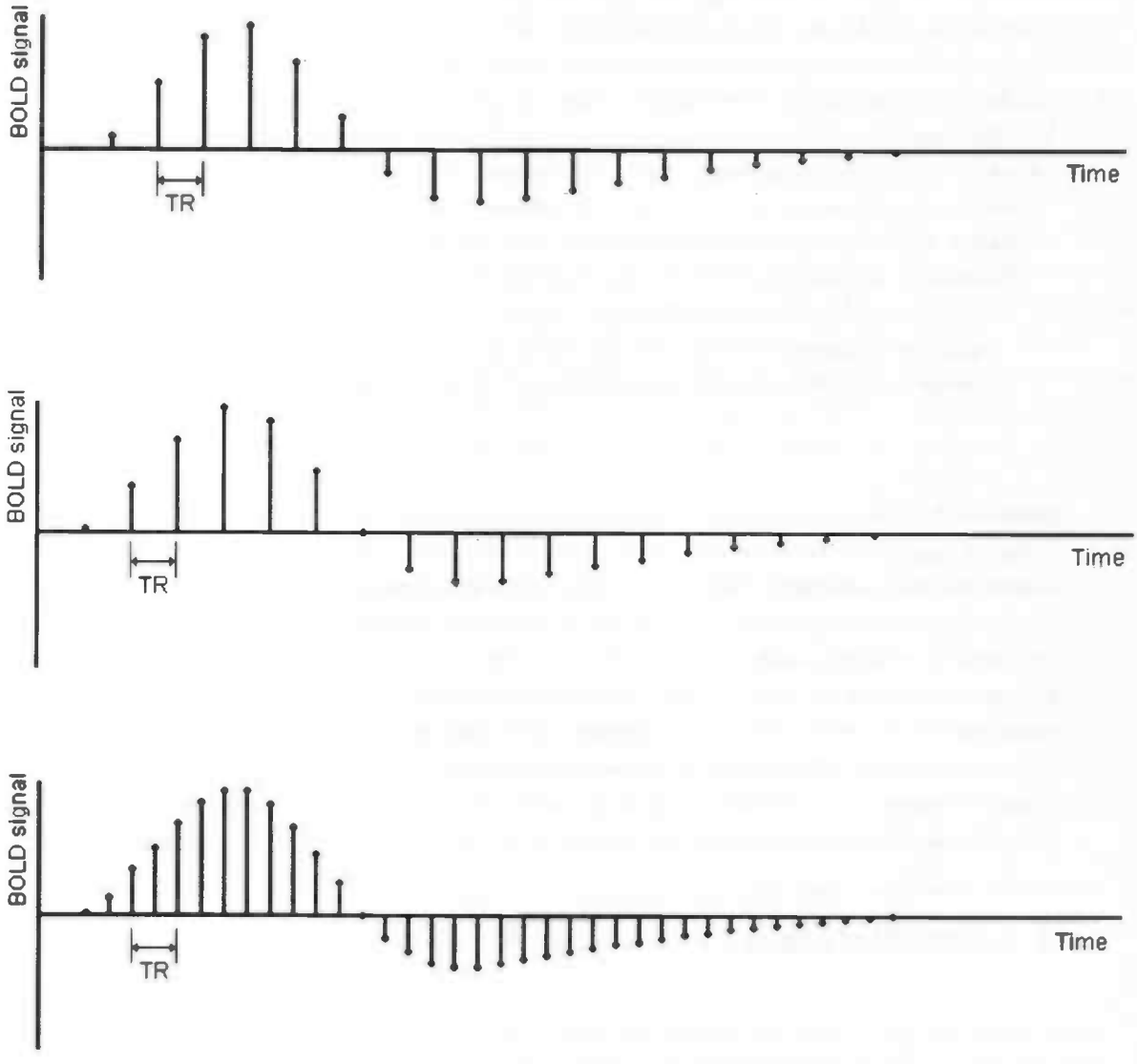

Figure C.2: Three sampled BOLD signals. The top and middle panel show two BOLD responses sampled with the same TR, but the 2nd BOLD response is shifted slightly to the left, compared to the BOLD response in the top panel. The bottom panel shows the BOLD signal when the first two signals are averaged. Note that the effective sampling frequency has doubled, although the TR is still the same.

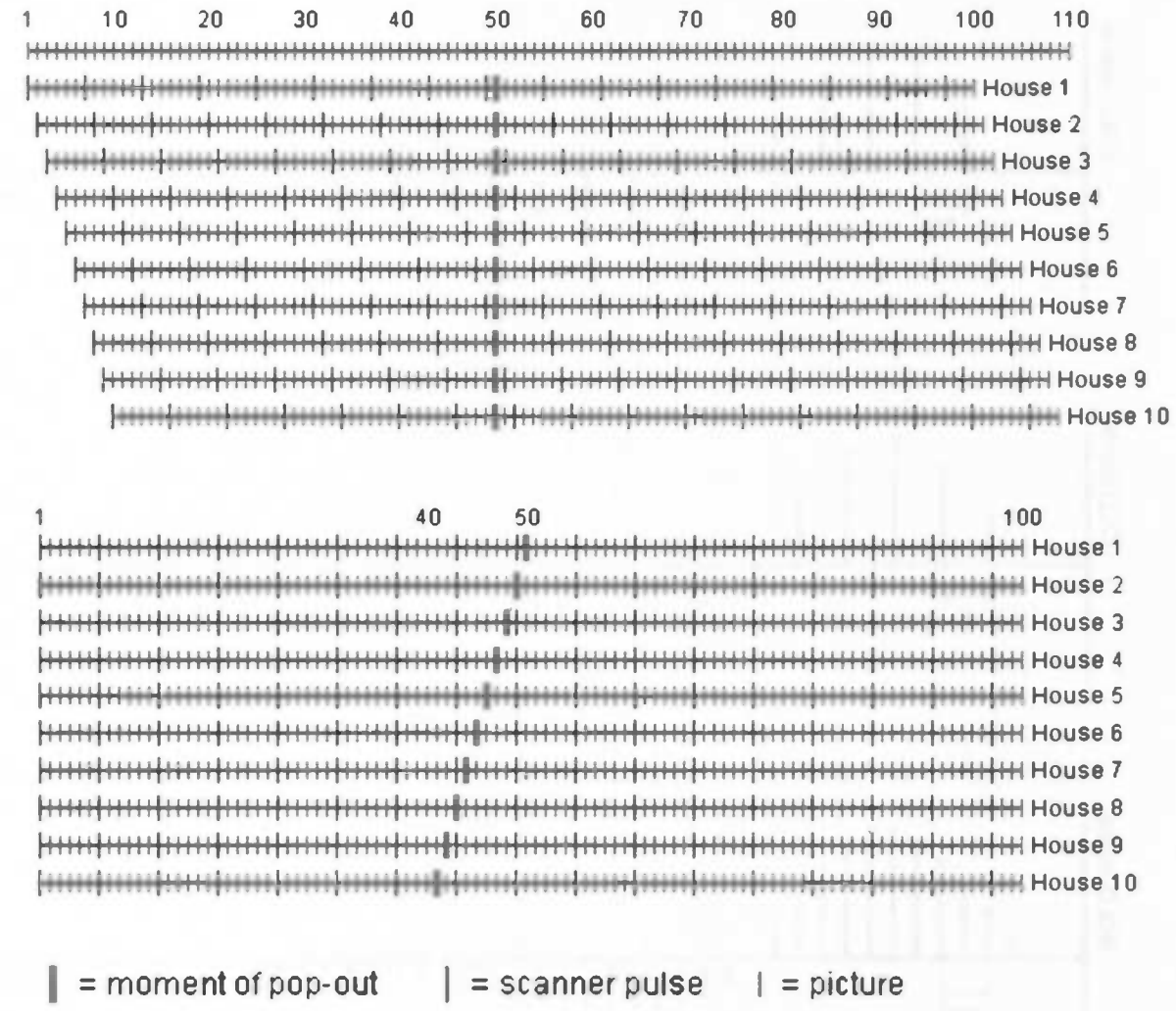

Figure C.3: The ten subsets (100 pictures out of the original 110) in the category houses and their moments of pop-out. With a TR of approximately 1,2 seconds and a picture presentation time of 0,2 seconds, there is a scanner pulse every six pictures. The top panel shows the different subsets, where for each consecutive set, the starting picture is shifted one picture (= 0,2 seconds) to the right. The theoretical moment of pop-out at the 50th picture of the series of 110 pictures. The bottom panel shows that with these different starting pictures, the moment of pop-out (which depends on the amount of stimulus information), is shifted 0,2 seconds to the left.

Theoretically, the amount of stimulus information at the moment of pop-out could be equal for all stimuli in one category (e.g., at the 50th picture in the series of 110 pictures). Given the different starting pictures, the 50th picture in the series of 110 pictures will be at different positions within the subsets of 100 pictures. The moment of pop-out, measured from the starting point of the sequence, will be different for each stimulus within one category. That is, the pop-out is between the 41st and the 50th picture in the sequence of 100 pictures, as we can see in the bottom panel of figure C.3.

In terms of time, the 10 moments of pop-out in one category of stimuli will be in the range of 8,2 to 10 seconds in the total sequence of 20 seconds, with each moment of pop-out 0,2 seconds apart. This means that the timing of the signal samples differs (with 0,2 seconds) for each stimulus sequence. Note that, since there are six intervals of 0,2 seconds in one TR of 1,2 seconds, the last four sampling shifts are redundant. For the first six, the samples of the BOLD response are shifted 0,2 seconds to the right, resulting in six different sampled signals of the same BOLD response. If all ten signals are averaged, the result is a sampled signal of the BOLD response with a sampling rate that is six times as high as the TR of 1,2 seconds (see figure C.4). In other words, the temporal resolution is 6 x 0,83 = 5 samples per second, six times as high as the original temporal resolution. In sum, artificial jittering, in addition to natural jittering, can increase the temporal resolution of the fMRI signal considerably.

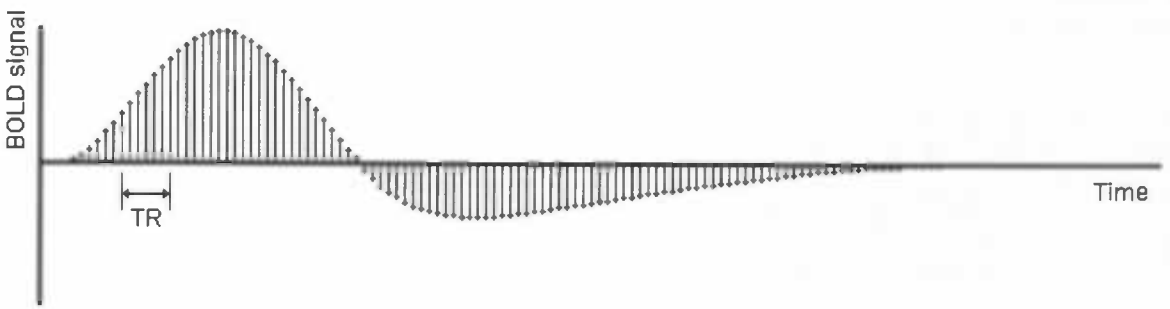

Figure C.4: The BOLD signal as sampled by fMRI, with a sampling rate that is six times as high as the TR.

References cited

Addington, J. & Addington, D. (1998). Facial affect recognition and information processing in schizophrenia and bipolar disorder. *Schizophrenia Research* 32, 171-181.

Adolphs, R., Tranel, D., Damasio, H. & Damasio, A. R. (1994). Impaired recognition of emotion in facial expressions following bilateral damage to the human amygdala. *Nature* 372, 669-672.

Adolphs, R., Tranel, D., Hamann, S., Young, A. W., Calder, A. J., Phelps, E. A., Anderson, A., Lee, G. P. & Damasio, A. R. (1999). Recognition of facial emotion in nine individuals with bilateral amygdala damage. *Neuropsychologia* 37, 1111-1117.

Adolphs, R. & Tranel, D. (2003). Amygdala damage impairs emotion recognition from scenes only when they contain facial expressions. *Neuropsychologia* 41, 1281-1289.

Andrewes, D. (2001). Executive dysfunction. In: Neuropsychology, 85-137. Psychology press, New York.

Bechara, A., Tranel, D., Damasio, H., Adolphs, R., Rockland, C. & Damasio, A. R. (1995). Double dissociation of conditioning and declarative knowledge relative to the amygdala and hippocampus in humans. *Science* 269, 1115-1118.

Blanchard, J. J. & Panzarella, C. (1998). Affect and social functioning in schizophrenia. In: Handbook of social functioning in schizophrenia, 181-196. Allyn & Bacon, Needham Heights.

Bordi, F. & LeDoux, J. E. (1994a). Response properties of single units in areas of rat auditory thalamus that project to the amygdala I. Acoustic discharge patterns and frequency receptive fields. *Experimental Brain Research* 98, 261-274.

Bordi, F. & LeDoux, J. E. (1994b). Response properties of single units in areas of rat auditory thalamus that project to the amygdala II. Cells receiving convergent auditory and somatosensory inputs and cells antidromically activated by amygdala stimulation. *Experimental Brain Research* 98, 275-286.

Breiter, H. C., Etcoff, N. L., Whalen, P. J., Kennedy, W. A., Rauch, S. L., Buckner, R. L., Strauss, M. M., Hyman, S. E. & Rosen, B. R. (1996). Response and habituation of the human amygdala during visual processing of facial expression. *Neuron* 17, 875-887.

Brigham, E. O. (1974). The fast fourier transform. Prentice-Hall, Inc., New Jersey.

Buxton, R. B. (2002). Introduction to functional magnetic resonance imaging principles & techniques. Cambridge University Press, Cambridge.

Calder, A. J., Young, A. W., Rowland, D., Perrett, D. I., Hodges, J. R. & Etcoff, N. L. (1996). Facial emotion recognition after bilateral amygdala damage: Differentially severe impairment of fear. *Cognitive Neuropsychology* 13, 699-745.

Campeau, S. & Davis, M. (1995a). Involvement of the central nucleus and basolateral complex of the amygdala in fear conditioning measured with fear-potentiated startle in rats trained concurrently with auditory and visual conditioned stimuli. *Journal of Neuroscience* 15, 2301-2311.

Campeau, S. & Davis, M. (1995b). Involvement of subcortical and cortical afferents to the lateral nucleus of the amygdala in fear conditioning measured with fear-potentiated startle in rats trained concurrently with auditory and visual conditioned stimuli. *Journal of Neuroscience* 15, 2312-2327.

Davis, M. (1992). The role of the amygdala in fear and anxiety. *Annual Review of Neuroscience* 15, 353-375.

Edwards, J., Jackson, H. J. & Pattison, P. E. (2002). Emotion recognition via facial expression and affective prosody in schizophrenia: A methodological review. *Clinical Psychological Review* 22, 789-832.

Ekman, P., Friesen, W. V. & Ellsworth, P. (1972). Emotion in the human face. Pergamon Press Inc., New York.

Ekman, P. & Friesen, W. V. (1975). Unmasking the face. Prentice-Hall, Inc., New Jersey.

Ekman, P. & Friesen, W. V. (1976). Pictures of facial affect. Palo Alto, Consulting Psychologist Press.

Epstein, R. & Kanwisher, N. (1998). A cortical representation of the local visual environment. *Nature* 392, 598-601.

Epstein, R., Harris, A., Stanley, D. & Kanwisher, N. (1999). The parahippocampal place area: Recognition, navigation, or encoding. *Neuron* 23, 115-125.

Esteves, F., Dimberg, U. & Öhman, A. (1994a). Automatically elicited fear: Conditioned skin conductance responses to masked facial expressions. *Cognition and Emotion* 8, 393-413.

Esteves, F., Parra, C., Dimberg, U. & Öhman, A. (1994b). Nonconscious associative learning: Pavlovian conditioning of skin conductance responses to masked fear-relevant facial stimuli. *31*, 375-385.

Exner, C., Boucsein, K., Degner, D., Irle, E. & Weniger, G. (2004). Impaired emotional learning and reduced amygdala size in schizophrenia: a 3-month follow-up. *Schizophrenia Research* 71, 493-503.

Friston, K. J., Ashburner, J., Frith, C. D., Poline, J.-B., Heather, J. D. & Frackowiak, R. S. J. (1995). Spatial Registration and Normalization of Images. *Human Brain Mapping* 2, 165-189.

Gegenfurtner, K. R. & Rieger, J. (2000). Sensory and cognitive contributions of color to the recognition of natural scenes. *Current Biology* 10, 805–808.

Goosens, K. I. & Maren, S. (2001). Contextual and auditory fear conditioning are mediated by the lateral, basal and central amygdaloid nuclei in rats. *Learning & Memory* 8, 148-155.

Grill-Spector, K. (2003). The neural basis of object perception. *Current Opinion in Neurobiology* 13, 159-166.

Gur, R. E., Turetsky, B. I., Cowell, P. E., Finkelman, C., Maany, V., Grossman, R. I., Arnold, S. E., Bilker, W. B. & Gur, R. C. (2000). Temporolimbic volume reductions in schizophrenia. *Archives of General Psychiatry* 57, 769-775.

Gur, R. E., McGrath, C., Chan, R. M., Schroeder, L., Turner, T., Turetsky, B. I., Kohler, C. G., Alsop, D., Maldjian, J., Ragland, J. D. & Gur, R. C. (2002). An fMRI study of facial emotion processing in patients with schizophrenia. *American Journal of Psychiatry* 159, 1992-1999.

Hofer, E., Doby, D., Anderer, P. & Dantendorfer, K. (2001). Impaired conditional discrimination learning in schizophrenia. *Schizophrenia Research* 51, 127-136.

Hooker, C. & Park, S. (2002). Emotion processing and its relationship to social functioning in schizophrenia patients. *Psychiatry Research* 112, 41-50.

Hulshoff Pol, H. E., Schnack, H. G., Mandl, R. C. W., van Haren, N. E. M., Koning, H., Collins, D. L., Evans, A. C. & Kahn, R. S. (2001). Focal gray matter density changes in schizophrenia. *Archives of General Psychiatry* 58, 1118-1125.

Ihnen, G. H., Penn, D. L., Corrigan, P. W. & Martin, J. (1998). Social perception and social skill in schizophrenia. *Psychiatry Research* 80, 275-286.

Kanwisher, N., McDermott, J. & Chun, M. M. (1997). The fusiform face area: A module in human extrastriate cortex specialized for face perception. *The Journal of Neuroscience* 17, 4302-4311.

Kanwisher, N., Stanley, D. & Harris, A. (1999). The fusiform face area is selective for faces not animals. *NeuroReport* 10, 183-187.

Kee, K. S., Kern, R. S. & Green, M. F. (1998). Perception of emotion and neurocognitive functioning in schizophrenia: what's the link? *Psychiatry Research* 81, 57-65.

Kerr, S. L. & Neale, M. L. (1993). Emotion perception in schizophrenia: Specific deficit or further evidence of generalized poor performance? *Journal of Abnormal Psychology* 102, 312-318.

Klüver, H. & Bucy, P. C. (1937). "Psychic blindness" and other symptoms following bilateral temporal lobectomy in rhesus monkeys. *American Journal of Physiology* 119, 352-353.

Klüver, H. & Bucy, P. C. (1938). An analysis of certain effects of bilateral temporal lobectomy in the rhesus monkey with special reference to "Psychic Blindness". *Journal of Psychology* 5, 33-54.

Knight, D. C., Nguyen, H. T. & Bandettini, P. A. (2005). The role of the human amygdala in the production of conditioned fear responses. *NeuroImage* 26, 1193-1200.

Kohler, C. G., Bilker, W., Hagendoorn, M., Gur, R. E. & Gur, R. C. (2000). Emotion recognition deficit in schizophrenia: Association with symptomatology and cognition. *Society of Biological Psychiatry* 48, 127-136.

Kosmidis, M. H., Breier, A. & Fantie, B. D. (1999). Avoidance learning in schizophrenia: a dissociation between the effects of aversive and non-aversive stimuli. *Schizophrenia Research* 38, 51-59.

Kucharska-Pietura, K., Shaw, P., Russel, T., Phillips, M. L. & David, A. S. (2003). Amygdala volume abnormalities in chronic schizophrenia. *European Neuropsychopharmacology* 13, S353.

LaBar, K. S., LeDoux, J. E., Spencer, D. D. & Phelps, E. A. (1995). Impaired fear conditioning following unilateral temporal lobectomy in humans. *Journal of Neuroscience* 15, 6846-6855.

LaBar, K. S., Gatenby, J. C., Gore, J. C., LeDoux, J. E. & Phelps, E. A. (1998). Human amygdala activation during conditioned fear acquisition and extinction: A mixed-trial fMRI study. *Neuron* 20, 937-945.

LeDoux, J. E. (1990). Topographic organization of neurons in the acoustic thalamus that project to the amygdala. *Journal of Neuroscience* 10, 1043-1054.

LeDoux, J. E., Cicchetti, P., Xagoraris, A. & Romanski, L. M. (1990). The lateral amygdaloid nucleus: Sensory interface of the amygdala in fear conditioning. *Journal of Neuroscience* 10, 1062-1069.

LeDoux, J. E. (1995). Emotion: Clues from the brain. *Annual Review of Psychology* 46, 209-235.

LeDoux, J. E. (2000). Emotion: Circuits in the brain. *Annual Review of Neuroscience* 23, 155-184.

LeDoux, J. E. (2003). The emotional brain, fear and the amygdala. *Cellular and Molecular Neurobiology* 23, 727-738.

Lewis, S. F. & Garver, D. L. (1995). Treatment and diagnostic subtype in facial affect recognition in schizophrenia. *Journal of Psychiatry Research* 29, 5-11.

Linke, R., De Lima, A. D., Schwegler, H. & Pape, H. C. (1999). Direct synaptic connections of axons from superior colliculus with identified thalamo-amygdaloid projection neurons in the rat: possible substrates of a subcortical visual pathway to the amygdala. *Journal of Comparative Neurology* 403, 158-170.

Lundqvist, D., Flykt, A. & Öhman, A. (1998). The Karolinska Directed Emotional Faces. Stockholm, Karolinska Institute.

Mandal, M. K., Pandey, R. & Prasad, A. B. (1998). Facial expressions of emotions and schizophrenia: a review. *Schizophrenia Bulletin* 24, 399-412.

Maren, S. & Fanselow, M. S. (1996). The amygdala and fear conditioning: Has the nut been cracked? *Neuron* 16, 237-240.

Maren, S. (2001). Neurobiology of Pavlovian fear conditioning. *Annual Review of Neuroscience* 24, 897-931.

Mathalon, D. H., Heinks, T. & Ford, J. M. (2004). Selective attention in schizophrenia: sparing and loss of executive control. *American Journal of Psychiatry* 161, 872-881.

Morris, J. S., Frith, C. D., Perrett, D. I., Rowland, D., Young, A. W., Calder, A. J. & Dolan, R. J. (1996). A differential neural response in the human amygdala to fearful and happy facial expressions. *Nature* 383, 812-815.

Morris, J. S., Friston, K. J., Büchel, C., Frith, C. D., Young, A. W., Calder, A. J. & Dolan, R. J. (1998). A neuromodulatory role for the human amygdala in processing emotional facial expressions. *Brain* 121, 47-57.

Morris, J. S., Öhman, A. & Dolan, R. J. (1999). A subcortical pathway to the right amygdala mediating "unseen" fear. *Proceedings of the National Academy of Sciences of the United States of America* 96, 1680-1685.

Morris, J. S., Buchel, C. & Dolan, R. J. (2001). Parallel neural responses in amygdala subregions and sensory cortex during implicit fear conditioning. *NeuroImage* 13, 1044-1052.

Mueser, K. T., Doonan, R., Penn, D. L., Blanchard, J. J., Bellack, A. S., Nishith, P. & DeLeon, J. (1996). Emotion recognition and social competence in chronic schizophrenia. *Journal of Abnormal Psychology* 105, 271-275.

Narr, K. L., Thompsom, P. M., Sharma, T., Moussai, J., Blanton, R., Anvar, B., Edris, A., Krupp, R., Rayman, J., Khaledy, M. & Toga, A. W. (2001). Three-dimensional mapping of temporo-limbic regions and the lateral ventricles in schizophrenia gender effects. *Biological Psychiatry* 50, 84-97.

Pavlov, I. P. (1927/1960). Conditioned reflexes. Dover Publications, Inc., New York.

Penn, D. L., Spaulding, W., Reed, D. & Sullivan, M. (1996). The relationship of social cognition to ward behavior in chronic schizophrenia. *Schizophrenia Research* 20, 327-335.

Penn, D. L., Ritchie, M., Cassisi, J., Combs, D. R., Francis, J., Morris, S. & Townsend, M. (2000). Emotion recognition in schizophrenia: Further Investigation of generalized versus specific deficit models. *Journal of Abnormal Psychology* 109, 512-516.

Phelps, E. A., O'Connor, K. J., Gatenby, J. C., Gore, J. C., Grillon, C. & Davis, M. (2001). Activation of the left amygdala to a cognitive representation of fear. *Nature Neuroscience* 4, 437-441.

Phillips, M. L., Williams, L., Senior, C., Bullmore, E. T., Brammer, M. J., Andrew, C., Williams, S. C. R. & David, A. S. (1999). A differential neural response to threatening and non-threatening negative facial expressions in paranoid and non-paranoid schizophrenics. *Psychiatry Research* 92, 11-31.

Rainer, G., Augath, M., Trinath, T. & Logothetis, N. K. (2001). Nonmonotonic noise tuning of BOLD fMRI signal to natural images in the visual cortex of the anesthetized monkey. *Current Biology* 11, 846-854.

Regan, M. & Howard, R. (1995). Fear conditioning, preparedness, and the contingent negative variation. *Psychophysiology* 32, 208-214.

Reinders, A. A. T. S., den Boer, J. A. & Büchel, C. (2004). The robustness of perception. In: From methods to meaning in functioning neuroimaging, 95-114. Bibliotheek der RuG, Groningen.

Reinders, A. A. T. S., den Boer, J. A. & Büchel, C. (2005). The robustness of perception. *European Journal of Neuroscience* 22, 524-530.

Rogan, M. T., Stäubli, U. V. & LeDoux, J. E. (1997). Fear conditioning induces associative long-term in the amygdala. *Nature* 390, 604-607.

Sachs, G., Steger-Wuchse, D., Kryspin-Exner, I., Gur, R. C. & Katschnig, H. (2004). Facial recognition deficits and cognition in schizophrenia. *Schizophrenia Research* 68, 27-35.

Sanfilipo, M., Lafargue, T., Rusinek, H., Arena, L., Loneragan, C., Lautin, A., Feiner, D., Rotrosen, J. & Wolkin, A. (2000). Volumetric measure of the frontal and temporal lobe regions in schizophrenia. *Archives of General Psychiatry* 57, 471-480.

Sato, W., Kubota, Y., Okada, T., Murai, T., Yoshikawa, S. & Sengoku, A. (2002). Seeing happy emotion in fearful and angry faces: Qualitative analysis of facial expression recognition in a bilateral amygdala-damaged patient. *Cortex* 38, 727-742.

Schneider, F., Gur, R. C., Gur, R. E. & Shtasel, D. L. (1995). Emotional processing in schizophrenia: Neurobehavioral probes in relation to psychopathology. *Schizophrenia Research* 17, 67-75.

Shaw, R. J., Dong, M., Lim, K. O., Faustman, W. O., Pouget, E. R. & Alpert, M. (1999). The relationship between affect expression and affect recognition in schizophrenia. *Schizophrenia Research* 37, 245-250.

Sigmundsson, T., Suckling, J., Maier, M., Williams, S. C. R., Bullmore, E. T., Greenwood, K. E., Fukuda, R., Ron, M. A. & Toone, B. K. (2001). Structural abnormalities in frontal, temporal and limbic regions and interconnecting white matter tracts in schizophrenic patients with prominent negative symptoms. *American Journal of Psychiatry* 158, 234-243.

Silver, H. & Shlomo, N. (2001). Perception of facial emotions in chronic schizophrenia does not correlate with negative symptoms but correlates with cognitive and motor dysfunction. *Schizophrenia Research* 52, 265-273.

Steel, R. M., Whalley, H. C., Miller, P., Best, J. J. K., Johnstone, E. C. & Lawrie, S. M. (2002). Structural MRI of the brain in presumed carriers of genes for schizophrenia, their affected and unaffected siblings. *Journal of Neurology, Neurosurgery and Psychiatry* 72, 455-458.

Steeves, J. K. E., Humphrey, G. K., Culham, J. C., Menon, R. S., Milner, A. D. & Goodale, M. A. (2004). Contribution of color and texture information to scene classification in a patient with visual form agnosia. *Journal of Cognitive Neuroscience* 16(6), 955-965.

Takahashi, H., Koeda, M., Oda, K., Matsuda, T., Matsushima, E., Matsuura, M., Asai, K. & Okubo, Y. (2004). An fMRI study of differential neural response to affective pictures in schizophrenia. *NeuroImage* 22, 1247-1254.

Talairach, J. & Tournoux, P. (1988). Co-Planar Stereotaxic Atlas of the Human Brain. Thieme Medical Publishers, Inc, New York.

van der Schaaf, A. & van Hateren, J. H. (1995). Modelling the power spectra of natural images: Statistics and information. *Vision Research* 36, 2759-2770.

Vuilleumier, P., Armony, J. L., Driver, J. & Dolan, R. J. (2003). Distinct spatial frequency sensitivities for processing faces and emotional expressions. *Nature Neuroscience* 6, 624-631.

Weiskranz, L. (1956). Behavioral changes associated with ablation of the amygdaloid complex in monkeys. *Journal of Comparative Physiological Psychology* 49, 381-391.

Whalen, P. J., Rauch, S. L., Etcoff, N. L., McInerney, S. C., Lee, M. B. & Jenike, M. A. (1998). Masked presentations of emotional expressions modulate amygdala activity without explicit knowledge. *Journal of Neuroscience* 18, 411-418.

Wible, C. G., Anderson, J., Shenton, M. E., Kricun, A., Hirayasu, Y., Tanaka, S., Levitt, J. J., O'Donnel, B. F., Kikinis, R., Jolesz, F. A. & McCarley, R. W. (2001). Prefrontal cortex, negative symptoms, and schizophrenia: an MRI study. *Psychiatry Research* 108, 65-78.

Wong, P. S., Shevrin, H. & Williams, W. J. (1994). Conscious and nonconscious processes: An ERP index of an anticipatory response in a conditioning paradigm using visually masked stimuli. *Psychophysiology* 31, 87-101.

Wright, I. C., Rabe-Hesketh, S., Woodruff, P. W. R., David, A. S., Murray, R. M. & Bullmore, E. T. (2000). Meta-Analysis of Regional Brain Volumes in Schizophrenia. *American Journal of Psychiatry* 157, 16-25.

Yip, A. W. & Sinha, P. (2002). Contribution of color to face recognition. *Perception* 31, 995-1003.

Young, A. W., Hellawell, D. J., van de Wal, C. & Johnson, M. (1996). Facial expression processing after amygdalotomy. *Neuropsychologia* 34, 31-39.

Zakzanis, K. K., Poulin, P., Hansen, K. T. & Jolic, D. (2000). Searching the schizophrenic brain for temporal lobe deficits: a systematic review and meta-analysis. *Psychological Medicine* 30, 491-504.